Stability Augmentation of Two-Wheeled Robots on Pedestrian Terrain

Zareena Kausar

A Thesis Submitted in Partial Fulfilment of

The Requirements for the Degree of

DOCTOR OF PHILOSOPHY

Department of Mechanical Engineering

The University of Auckland

New Zealand

September 2014

To my Daughters

Abstract

Wheeled robots, which are expected to be a beneficial and revolutionary mechanism for the next generation robotic systems, have gained worldwide attention from research communities. In this dissertation, statically unstable two-wheeled Robots (TWRs) are studied on pedestrian terrain. The pedestrian terrain includes flat horizontal footpaths, ramps and uneven terrain, for example, bumps. The primary issue faced by statically unstable two-wheeled robots on these terrains is the instability due to only one contact point of the robot wheel to the ground, which reduces normal force and the wheel motion or any kind of tiny disturbance that causes the robot body to fall. Thus, stability augmentation and performance enhancement of TWRs on the ramps and bumps, a major control challenge faced by the TWR users and researchers, requires control design along with the stability analysis of the closed-loop TWR system and dynamics modelling.

In this thesis a linear, a semi-nonlinear and a nonlinear control scheme for statically unstable TWRs is proposed for the motion on horizontal, inclined and uneven terrain scenario considering the availability of feedback of the system states. The main issues that are analysed in depth in this research are the effects of terrain inclination on stability and performance of the TWRs, the dynamics of TWR motion on horizontal, inclined and uneven terrain, control synthesising, stability and the stability region of closed-loop dynamics of TWRs. Furthermore, the equations of motion in three scenarios have been derived using the Lagrangian method, which is a new contribution to the statically unstable TWRs. The performance analysis of transient response has been carried out with simple PD and LQR controllers. The LQR is utilised, later, as a baseline controller and the Gain-Scheduled (GS) controller is designed based on the assumption that the wheel-terrain contact angle is known. The control is implemented for non-horizontal, inclined and uneven, terrain.

Another novel controller proposed and synthesized in this dissertation is the Control Lyapunov Function Based Controller (LFBC) for motion of TWRs on all the three terrain, which is a new contribution to the TWRs. The proposed CLF based control schemes aim to perform control authority robustly with guaranteed asymptotic stability and with a wider stability region to enhance the performance and to augment the stability of TWRs on pedestrian terrain. It is proved through simulations that GS control is a good choice for inclined terrain, compared to the linear optimal controller, the LFBC is proven to be an

optimal choice to solve the non-linear control problems of TWR on pedestrian terrain to augment their stability.

Another contribution of this research is in the field of control implementation on a physical real time two-wheeled robot. Real time implementation is presented with many challenges in terms of reliability and accuracy of information from sensors in measuring the states and the wheel-terrain contact angle. The novel and simple terrain inclination measuring scheme based on wheel encoders is proposed, which detects the absolute position of the wheel whilst a wheel-terrain contact angle is determined online from known function of the terrain. By applying controllers at different speeds of the TWR the effectiveness and reliability of the proposed scheme is proved.

All the proposed algorithms have been investigated through simulations as well as real time implementation under different initial conditions to validate the significance and effectiveness of them for the performance regulation and velocity tracking.

Acknowledgements

For his expert guidance, provision and encouragement throughout this research work, I would like to express my sincere gratitude to Dr. Karl Stol, my supervisor. Dr. Stol's hard work and enthusiasm was the greatest motivation I could ask for throughout this research study. The Dynamics and Control Research group Dr. Stol established at the University of Auckland provided me with the valuable research experience I could use to extend my knowledge further.

For his devotion to the project during the entire period I would also like to thank my co-supervisor, Dr. Nitish Patel. Due to the inter disciplinary nature of this project, it is important to thank Associate Prof Dr. Bruce McDonald at the Robotics Lab and to acknowledge his valuable experience and ideas that have helped customise and shape this project.

The Two Wheeled Robotic Research group that I worked with, especially Daniel Jones, Ronald Chan, Jeremie and Leron, have also helped greatly with my research providing interesting discussions for me to benefit from. Thanks also go to my office mate Elisabeth for providing me with benefiting interactions and my group mate, Oliver, for going out of his way to help me.

Many thanks go to the Dynamics and Control laboratory technicians, Rob Earl and Saraath, who helped throughout this research in fabricating and improving the mechanical and electronic hardware. Thanks also to the IT staff, especially Barry Fullerton and Craig Barton, they deserve special thanks for their support.

Thanks go to my spouse for pushing me towards my goal and likewise I am forever indebted to my daughters for their unlimited motivation throughout my PhD study period for their encouragement to never give up and for their patience in supporting me.

Lastly, I must take this opportunity to express all my love and appreciation towards my mother who has never once stopped praying for my success and it is entirely due to her inspiration and endless support that I have managed to complete this thesis.

Table of Contents

List of Figures

List of Tables

Chapter 1. Introduction

The use of robotic manipulators has a long history in industrial automation and the trend to utilize robots is increasing as mobile robots [1, 2] are used in entertainment, industrial, medical, military and space and transport applications. In the near future, mobile robots will be used in every aspect of our life. They have been applied as autonomous robots in the area of exploration in recent years. An important area is the exploration in robot application in rough [3, 4] and/or uneven [5] terrain environment. Much research has been dedicated to the design and motion control of mobile robots in rough terrain. This research study which focuses on one of the mobile robots called the two-wheeled robot (TWR), investigates the modelling and control aspect of the two-wheeled robots on pedestrian terrain.

This chapter provides background knowledge on issues relating to this research, and begins with the definition, classifications and development background of two-wheeled robots. An overview is provided of the modelling and control methods used for two-wheeled robots including a study of mathematical models and various regulating techniques as they apply to two-wheeled robots. State-of-the-art regarding modelling and control strategies of two-wheeled robots is stated. The chapter ends with an overview of this thesis as well as the objective and motivation for the study.

1.1. Background

Mobile robots can freely navigate and manoeuvre in virtually any environment. Different types of configurations exist for mobile robots. They are legged robots, wheeled robots and a few hybrid robots. The legged robots are to imitate motions of a human being while a hybrid robot is one which has both wheels and legs. The early decade (1990-2000) of robotics contributed towards the mechanical design, control [6], stability [7] and other problems of legged robots [8-16]. Later, wheeled mobile robots became part of the active research in the field of robotics. A wheeled robot is generally recognized by the number of wheels it has. There exist single [17], two [18], three [19], four [20] and six [21] wheeled mobile robots. A Three Wheeled robot shown in Figure 1.1(c) is statically stable [22] while Four Wheeled Mobile Robots, Figure 1.1(d), are car-like high speed robots [23]. These robots, if the active suspension is combined with a steerable wheel mechanism, introduce great complexity. The tip over (longitudinal fall) and Rollover (side/lateral fall) problems are reported to be a few of

the obstacles these vehicles encounter on rough terrain and slopes. A Six-Wheeled Mobile Robot Figure 1.1(e), is mostly preferred for rough terrain [21] like "Mars Rover" [24] due to its terrain adaptability.

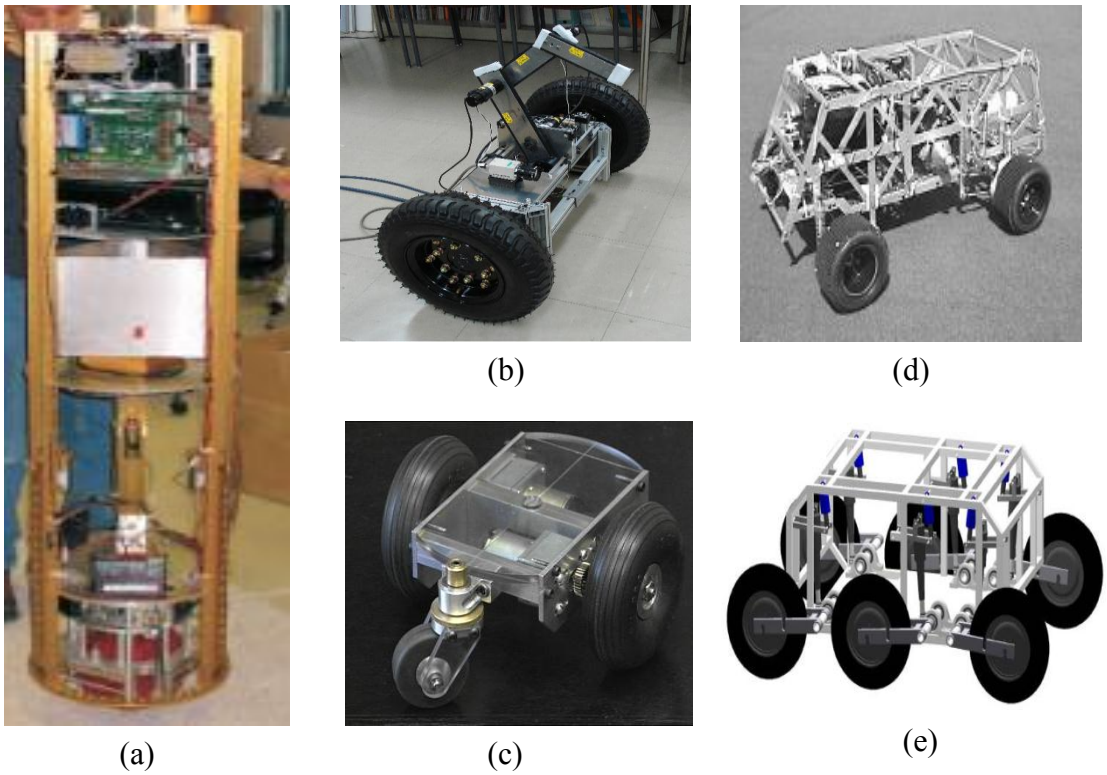

Figure 1-1: Wheeled Mobile Robots: (a) Single-wheeled [17] (b) Two-wheeled [25] (c) Three-wheeled [20] (d) Four-wheeled [21] (e) Six-wheeled [21].

Three or higher number of wheels driven mobile robots mechanisms have mechanistic faults such that they are unable to take a short turn or casters are wedged or trapped in the bumps. Due to a large turning radius, six wheel driven robots are difficult for use at tight turns. Therefore during the last decade the research, at the industrial, and hobby level, due to their many advantages, efforts to develop the Two Wheeled Mobile Robot have increased dramatically.

Two-Wheeled Mobile Robots, Figure 1-1 (b) provide significant advantages over multi-wheel as they have good dynamic stability, high manoeuvrability, recovery from fall and insensitivity to attitude disturbances [26]. They have a smaller footprint, less interfering and a high load-carrying capacity. Consequently these mobile robots have a big advantage in terms of mobility, since they do not have casters and can take a short turn quickly. Although the

configuration of a two-wheeled mobile robot is statistically unstable this is avoided by stabilization control [27, 28] which is constructed by the simplification of its complex model [29].

TWRs have applications as entertainment [30] and transport robots [31] for their flexible actions and easiness to control. Another potential application is as a high-speed lunar vehicle [32], where the absence of aerodynamic disturbances and low gravity would permit efficient and high-speed mobility. The applications such as guard robots and care robots require a fewer number of wheels [33] to get less footprint and short turn capability . Here a TWR becomes a good choice. TWR has a disadvantage of less terrain adaptation ability. Therefore in order to achieve effective locomotion of TWR on a sloped or uneven terrain, suitable control algorithms are required. An overview of the achievements in the field of TWRs is documented in the following sections by studying the TWR state-of-art, classification, mathematical models and control techniques in a pedestrian environment which includes footpaths, ramps and bumps.

1.2. Two-Wheeled Robots

A large number of two wheeled robots are noticed in the literature. One of those is the commercial two-wheeled vehicle named Segway. Different versions of Segway include PT, RMP and PUMA. Segway RMP [34] is available for research purposes. PT [31] is used as personal vehicle and PUMA [35] for public use. A chronological development of two wheeled mobile robots is described in following sub-section.

1.2.1. Development of two-wheeled robots

Research on two-wheeled robots began in 1986 with an introduction of the parallel bicycle robot, Figure 1-3 (a), by Kazuo Yamafuji [36]. After a decade, SEGWAY [37] unveiled the two-wheeled personal transporter, Figure 1-3 (b), providing a breakthrough towards worldwide development of both commercial and research two-wheeled platforms. A few of these are named JOE (a mobile inverted pendulum) [38]; Quasimoro (a quasi-holonomic mobile robotproposed at McGill University's Centre for Intelligent Machines) [39, 40]; nBot [41]; uBot (a dynamically balancing two-wheeled platform) [42]; T-WIP robots [1] (Figure 1-4 (a)); Hitachi's Emiew [43, 44] (Figure 1-4 (b & c)). To achieve quasiholonomy, the mass centre of the robot is placed on the vertical plane equidistant from the two mid-planes of the wheels.

A pleasure vehicle "gyrauto," was introduced in Europe in 1935 [45]. Designed by Ernest Fraquelli, a young Italian engineer, the gyrauto (Figure 1.2a) could not replace the conventional cars. At the University of Michigan's Mobile Robotics Lab, a GuideCane was invented in 1981 as a robotic guide dog, Figure 1-2 (b), for the blind [46]. However, mobile robots require drive motors and battery power for driving and are too heavy to be lifted up by a user, making it impossible to negotiate stairs or steps. Later, Kazuo Yamafuji, Professor at the University of Electro-Communications in Tokyo, built the first two wheeled inverted pendulum for research purpose in 1986 [47], however, was not able to continue this work.

Cye (Figure 1-2c) is a two-wheeled differential drive robot balanced on its two wheels by placing the centre of gravity (C.o.G) below the wheel axel [48]. Another TWR with C.o.G below the wheel axel, the scout (Figure 1-2d), was developed by the Centre for Distributed Robotics at The University of Minnesota in 2000 for surveillance purposes [49]. An nBot [41] (Figure 1-3c), C.o.G above the wheel axel, was featured as NASA's Cool Robot of the Week in May 2003 due to its features developed step by step during a period from 2001-2007. uBot [42] is a research platform developed and modelled as an inverted pendulum to solve the control problem. The model and control was implemented in real time on T-WIP Robot [1].

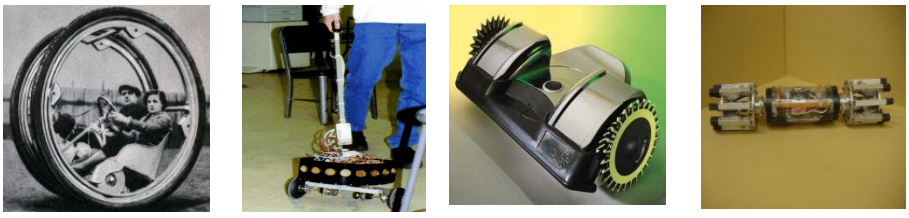

(a) (b) (c) (d)

Figure 1-2: (a) Gyrauto [45], (b) Guidecane[45] , (c) Cye[47, 48], (d)Scout [49].

(a) (b) (c) (d)

Figure 1-3: (a) Inverted Pendulum [36] (b) Segway HT [31] (c) nBot [41] (d) JOE [38]

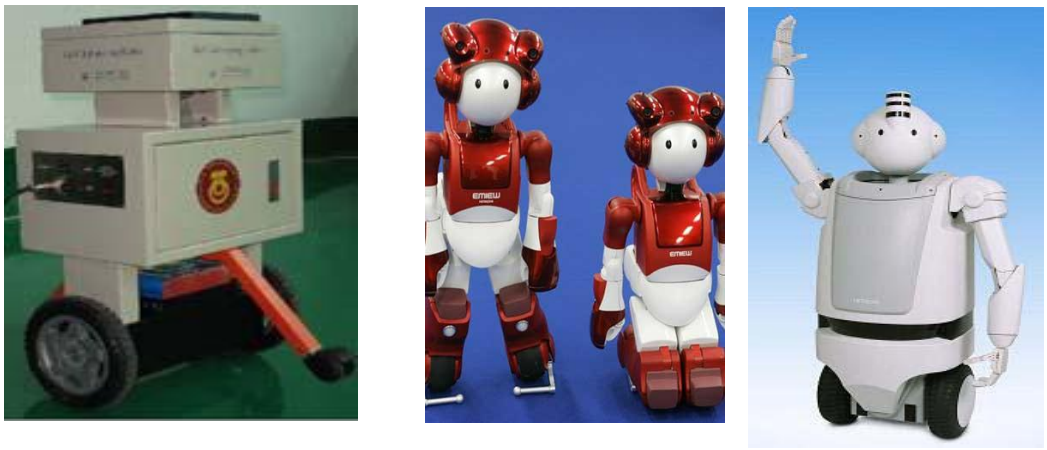

(a) (b) (c)

Figure 1-4: (a) T-WIP [1], (b) Hitachi Emiew1 [44], (c) Hitachi Emiew 2 [43] .

Many other similar systems reported by D.P. Anderson [41] include BBot a balancing robot by Brody Radford inspired by nBot and JOE, LegWay, BaliBot built by Bill and Mark Sherman, GyroBot a gyroscopically stabilized robot, Equibot, crunch, Spider by Francisco Lobo de la Garza, ichibot, Balance-bot by a graduate of M.I.T., ballybots based around the excellent eyebot a robot controller and Blind Man, a fuzzy logic-based two wheel balancer.

A feature common to these TWR platforms is that they are constituted of two parts: two wheels connected in parallel through an axle and a body which lies on and around the axle. The robot body rotates about the wheel axis. Differences between these robots are: *first*, a way of sensing the orientation of the robot body with respect to the vertical axis, for example, Quasimoro [39] uses a cost-effective inclinometer, while JOE [38] uses a rate gyro; *second*, the location of C.o.G relative to the line joining wheels centre, for example, C.o.G of Quasimoro is placed below, while for JOE it is placed above; *third*, the type of controllers used, for example, linear controllers are used by [50-54] while nonlinear control algorithms are proposed by [55-60]. The linear controller quickly degrades the accuracy as the speed increases. This is because linear control neglects the nonlinear forces associated with the motion of the robot. These forces include coriolis and centrifugal forces which vary as the square of the speed [61]**.** In the case of nonlinear feedback control these forces are taken into account to overcome the problem [62].

1.2.2. Definitions and Classification

Based on the literature survey presented in section 1.2.1, a classification of two-wheeled robots and their definitions are described in this section. A two-wheeled mobile robot is defined as "a robot which uses two wheels for the propulsion and has an Intermediate Body (IB) with all the rest of the parts of the system". The IB is "the central body of the robot which carries axle and robot accessories including sensors, electronics and actuators".

The two-wheeled robots are classified (Figure 1-5) as two-serial-wheeled and two-parallel-wheeled mobile robots. If two wheels are arranged in series with IB in longitudinal direction the robot is called Two-serial-wheeled Mobile Robot (TSWMR), for example, bicycles and motorcycles. If the wheels are arranged in parallel with an IB in longitudinal direction, it is named Two-parallel-wheeled Mobile Robot (TPWMR). A two-parallel-wheeled mobile robot is further divided into two categories: statically stable and statically unstable. A statically stable TPWMR is defined as: "A TWR with centre of mass (c.o.m) of the IB lying at or below the axis of rotation of the wheels". Similarly: "A TWR with centre of mass (c.o.m) of the IB lying above the axis of rotation of the wheels is statically unstable TWR".

A statically unstable TWR [63] always requires an active stabilization of its IB. For an active stabilization several sensor subsystems are used to give a feedback of states like position and velocity of the robot. A rate gyro [64], five gyros and two tilt sensors [65], a rate gyro and two orthogonal accelerometers [41] are the sensors employed for statically unstable TWRs. A classification of the statically stable TWRs is derived based on type of IB stabilization employed [32]. This includes statically stable TWRs: without any stabilization of the IB; with passive mechanical stabilization and with active stabilization of the IB. Examples of robots belonging to the category of statically stable TWR which have no stabilization of the IB are Cye[48] and Gyrauto [44]. As only two points of the robot touch the ground, the IB has a tendency to rock back and forth [66].

To cope with this problem, robot designers have adopted several mechanical solutions which stabilize the IB, such as a long handle attached to the robot manoeuvred by the user [67] and a sliding supporting point [68]. A problem of too much weight on the mechanical stabilizer increases traction losses. This also causes tip over while manoeuvring up/downhill. To avoid the problems encountered with this category, a few robot designers have developed an active

stabilization of the IB. With reference to the latter, several sensor subsystems have been used for such stabilization.

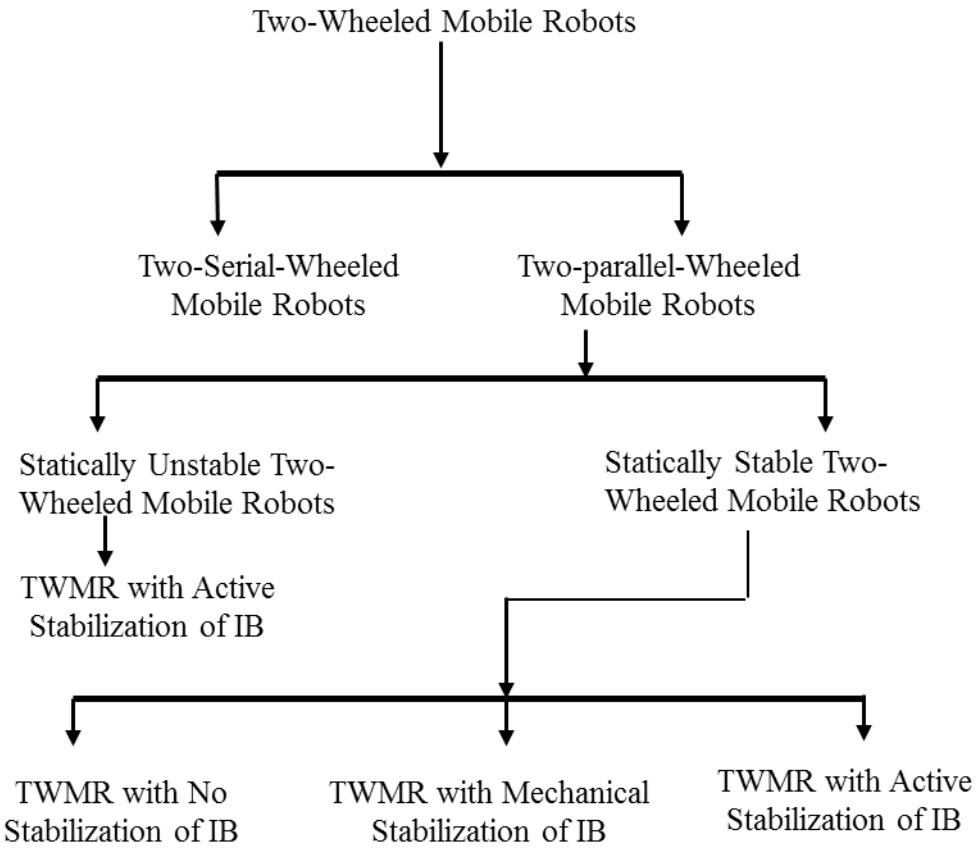

Figure 1-5: Classification of two-wheeled mobile robots

1.3. Modelling of Two-Wheeled Robots

Even though the wheeled mobile robots are well suited for operation on relatively smooth, flat, and rigid floors, they are also studied for inclined terrain [69]. The performance of a controller depends upon which dynamic model of the system is used. A statically unstable TWR resembles an inverted pendulum placed on two wheels. The system has three degrees of freedom in a 3D plane, during its motion on a flat horizontal terrain. Two-wheeled robots are modelled with assumptions of no slip between wheel & ground and wheels remain in contact with the ground surface.

The simplest model is for straight-line 1-dimensional motion [70] which has yaw considered [71] or yaw not considered [38, 55, 72-77]. Most of the models involve two degrees of freedom which includes four states, that is two states for each degree: longitudinal displacement and pitch of the IB. Instead three states are modelled omitting longitudinal position as this does not affect the robot dynamics [71, 74]. The resulting non-linear model is complex. Addition of yaw motion adds to complexity which is accounted for by using inertia tensor of the IB [78] or simplified by decoupling [79-82]. A few of these researchers developed their own 2D model for the system to design a controller.

The dynamic models of the TWR system have been developed using Newton's Laws [38], [83], Lagrangian method [62, 77, 78] and Kane's method [33, 84]. All these models have been developed for a flat and smooth horizontal terrain. For outdoor as well as some indoor applications of TWRs, however, mobile robots have to face more challenges including uneven, sloped or rough terrain. When the TWR traverses on an uneven terrain, the dynamic disturbance forces are generated at wheel-terrain contact point due to a change in contact force or a change in terrain slope. It is therefore necessary to include these effects in the dynamic model of the TWR system.

1.4. Control of Two-Wheeled Robots

The posture stability of the IB is a primary issue of a TWR. During motion the location of the centre of mass of the TWR changes, due to the inertial accelerations. An instability event occurs in this situation. If the robot is traversing an uneven terrain the instability becomes worse. A suitable controller, therefore, is required to solve the problem. A TWR utilizes trajectory tracking and states regulation for manoeuvring on horizontal, inclined and uneven terrain. In this section existing approaches for controller designed or used for the TWR are reviewed for its motion on a horizontal, inclined and uneven terrain.

1.4.1. Control of TWR on horizontal terrain

One of the main control purposes of the TWR is stability control, since the TWR is an inherently statistically unstable under-actuated system [85]. The control schemes that are used to stabilize TWRs are generally regarded as trajectory tracking or self-balancing and velocity tracking controllers. The self-balancing and velocity tracking control is important for the robot utilization for any application, especially in a pedestrian environment where human traffic is present. The velocity tracking with self-balancing control scheme may help in

providing smooth running or walking or stationing of the robot. It may also help to avoid accidents.

The self-balancing control of conventional two wheeled robots such as SEGWAY [37] works on the basis of proportional-derivative (PD) control law with large actuation torque values. These values produce a large overshoot in presence of high payloads [86]. Due to advantages of the optimal linear controller, a FSFBC is implemented on a TWR. Since FSFBC has been designed on the linear approximation of the nonlinear TWR dynamics and was implemented on nonlinear TWR dynamics, the performance of the overall design cannot be guaranteed. A nonlinear controller is, therefore, proposed in order to ensure the stability of the TWR with a large stability region, namely, a novel control Lyapunov function based control scheme for stability control and velocity tracking. The novelty of the proposed control scheme is that it allows the TWR's stability and velocity to be controlled with guaranteed stability. This control enables a large region of stability to be able to be computed.

The vertical position of the IB is an unstable equilibrium point. In addition, the rotation of the IB of a two wheeled robot is powered by the torque applied by the motion of the wheels on horizontal terrain which displays a highly nonlinear behaviour that presents a control problem. The control problem has been approached via various methodologies. The control methods used for TWRs, available in literature, are Proportional Integral Derivative (PID) [83, 87] and Linear Quadratic Regulator (LQR) [51, 52, 87, 88]. In Grasser et al. [89] two decoupled state-space controllers were presented. A pole placement controller has been proposed by Nawawi et al. [90]. The control approaches mentioned above are not suitable as they are non-robust with respect to un-modelled dynamic uncertainties. A linear quadratic regulator (LQR) has been designed [91] to avoid this problem. Since the presence of nonlinearities in the system limit the control authority and leads to limit cycles or even instability, nonlinear controllers were suggested. These nonlinear control schemes have been Fuzzy adaptive [74], neural network controls [92, 93], feedback linearization [94] and Sliding mode with back-stepping [95] controllers. They were designed to improve the stability control capability of TWRs. Even though these nonlinear controllers improve the performance of the stability control, the issue of stability region and guaranteed stability still need to be addressed, with regard to TWRs.

The methods used to determine the stability region for nonlinear systems are generally categorized as Lyapunov function methods [96-104] and non Lyapunov function methods

[105-111]. The Lyapunov function methods are high-up in the literature [98, 112-115]. They require a Lyapunov function which represents the system. The methods proposed in the literature for the construction of Lyapunov function were based on the conventional [116, 117] and numerical [118, 119] approach. A constructive method is used in this work to develop a control Lyapunov function (CLF). This approach utilizes the technique of added integration, presented by Lozano [120]. An advantage of this method is to add new states in the present CLF to construct a new CLF.

A CLF based nonlinear controller (LFBC) has been proposed by *Jankovic et al.*[121]. LFBC provides or exhibits all the advantages of baseline controller and guarantees the stability by utilizing a control Lyapunov function. This chapter presents a novel control Lyapunov function for a two wheeled robot's motion on a flat, smooth and horizontal terrain as well as a design for a controller for stability control and velocity tracking of TWRs. This follows the evaluation of the BLC and LFBC laws for the stability and velocity control of TWR in simulation. Simulations for comparison of BLC and LFBC were performed. The contribution of this chapter includes the design of a linear and a nonlinear control scheme that allows the TWR stability and velocity to be controlled with guaranteed stability in order to compute the stability region.

1.4.2. Control of TWR on inclined terrain

Figure 1-6: A ramped footpath

For outdoor applications, mobile robots face challenges like a sloped terrain. A sloped terrain is experienced as ramps on pedestrian footpaths (Figure 1-6) and roads in hilly areas, industrial floor and shops. Whereas wheeled mobile robots are suitable for use on a flat, rigid and smooth terrain [122]. They are not suitable on non-flat terrain due to their under actuation and tip over characteristics [69]. Two-Wheeled Mobile Robots (TWMRs) provide an advantage over multi-wheel robots, as for example, they can balance at any slope whilst maintaining their centre of mass above wheel-terrain contact point. They can, in this way, overcome the tip over problem using a suitable control strategy [123]. Control of unstable equilibrium point and the robot velocity tracking on flat horizontal terrain has been presented [123] for different applications. The linear as well as nonlinear control schemes [85] have been designed and implemented. The nonlinear algorithms improved the

performance of the stability control. An issue related to the stability region and guaranteed stability for TWR on a horizontal terrain has been addressed by Kausar Z [124].

As an inclined terrain dynamically constrains the wheel's motion, the resulting behaviour of IB, requires further investigation. A limited number of studies related to the effect of terrain inclination and stabilization control of TWR have been reported upon in the literature. Stabilization control on horizontal terrain has been studied implementing a large number of control algorithms. Effects of ramp have been evaluated relative to parameters of bipedal robot [125] to study passive dynamic gait. Still, the question as to the way in which the terrain inclination affects performance and stability region of two wheeled robots and how to control these effects to stabilize the robot on inclined terrain remain unanswered. Also, control of the velocity of the robot, directly related to the tangential force at the wheel-terrain contact point, has not been studied.

The objective of this study has been to investigate the effect of terrain inclination angle on stabilization of TWR and develop a control scheme that works to minimize these effects. A linear FSFB controller was designed for horizontal terrain. The controller was implemented in simulations on the nonlinear dynamic model of the TWR. The performance of a closed loop system for stabilization and velocity tracking was evaluated on horizontal terrain. The same controller was implemented for stabilization and velocity tracking on an inclined terrain. The effects were quantified through comparison of performance and stability region. A Gain-Scheduled (GS) controller was developed to compensate for the effect of inclination. Nonlinear Dynamic system equations were simplified and normalized to keep the nonlinear controller design simple. A feedback linearization controller was designed. Finally, a nonlinear controller (LFBC) was developed using a control Lyapunov function. This controller increases the stability region and guarantees the stability of the closed loop system.

The contributions of this work include the first quantification of the effects of terrain inclination. Two novel controllers were also developed for TWR motion on inclined terrain. The GS controller was based on the gain updates according to the terrain inclination angle. An LFBC was developed on the basis of a control Lyapunov function which acts to represent the energy of the system.

The chapter begins with an evaluation of the effects of terrain inclination. Next the researcher describes the GS control of the robot based on optimized FSFB controller gains scheduled based on the value of wheel-terrain contact angle. After that an LFBC nonlinear control algorithm is presented which is followed by a stability analysis and computation of

the stability region. The results of the simulation are presented next and finally the chapter ends with the discussion and conclusion sections.

1.4.3. Control of TWR on uneven terrain

The initial prototypes of two wheeled robots, such as SEGWAY, work on horizontal terrain on the basis of linear control [35]. The problem with them is that they are not capable of moving on uneven terrain with linear control. The uneven terrain is experienced as bumps on roads or on pedestrian footpaths (Figure 1-7) and rough paths in hilly areas. On industrial floor and shops, small bumps are observed where cables, passing through on the floor, are covered with a bridge. In fields or undeveloped footpaths the mud rocks cause unevenness in the terrain. Wheeled mobile robots are thought to be suitable for use on a smooth horizontal terrain. The objective of the study in this chapter was to design an appropriate control approach to turn TWMRs into robots suitable for use on uneven terrain.

Figure 1-7: A bump along a footpath

Although an extensive bibliography has dealt with the control of wheeled robots, the control on uneven terrain still requires attention. Stabilization problem of the wheeled mobile robots on uneven terrain has often been overlooked. In the existing literature most of the wheeled robots are assumed to be moving on horizontal terrain. The main difference between motion on horizontal and uneven terrain is that in case of uneven terrain the potential energy is important to be considered. This appears in the equations of motion with some terms related to the effect of gravity. Karl and Steven [4] proposed traction control of four wheeled robots in rough terrain considering skid steered wheeled robot on uneven terrain. Chakraborthy and Ghosal [126] first attempted to control the motion of three wheeled robot on an uneven terrain followed by Choi *et al*. [127]. Both of them proposed a variable length axle for slip free motion on uneven terrain without considering the gravity and inertial loads. Danielle *et al.* [128] considered the control of two wheeled robot moving on inclined plane. Even though they presented the control without imposing any restriction on the IB, the control has been designed for statically stable TWR. Even though the two wheeled robots have stabilization problem they do not have tip over stability problem on uneven or sloped terrain unlike three or four wheeled vehicles. Therefore, one of the aims of this thesis is to present a control

scheme for the stabilization of TWRs moving on uneven terrain which guarantees the stability.

1.5. Research Motivation

Although the motivation for this research has come from several sources, it mostly derives from the widespread application of TWRs in research, service robotics and transportation. Even though much effort has been dedicated to the research of TWRs, there are still many open areas to be studied. Furthermore, as current dynamic modelling and control of TWRs apply many unrealistic assumptions and are limited to only a few real scenarios, this leaves plenty of room for improvement.

A second motivation arose from the nature of the terrain a TWR has to move on, for example, ramps and bumps. We have learnt from the previous section that in most dynamic models the terrain is assumed to be flat and horizontal, which limits its application in pedestrian walkways and on factory ramps. The application of TWR as an assistive device or vehicle for the mobility-challenged also demands that the vehicle is capable of moving on ramps without losing balance. Therefore, the dynamic modelling and control of TWRs on inclined terrain is believed to be necessary, in order to provide a more realistic and augment application of TWRs. Nasrallah [128] recommended a sliding mode controller for a statistically stable two wheeled mobile robot on inclined terrain. In this thesis, we aim to model and control TWRs with motion on an inclined terrain for statistically unstable TWRs.

Moreover, a bump induces dynamic disturbance which causes loss in wheel traction and stability. A way to resolve this problem which has been suggested for six wheeled mobile robot [21] and three wheeled mobile robot [127] is to change the configuration of the robot. Reconfiguration has limitation to support gravity loading for high inclination of the IB and inertial loading at high speed that may cause slipping. A control on uneven terrain has not been properly addressed for TWRs. The spirit of the Gain-Scheduled (GS) controller [129] represents an important approach to control the systems with variable disturbance based on the use of scheduling variable. This provides a method for determining the controller gains at variable terrain angles. It has been shown recently that the GS method is effective in solving wheeled robot stability problems on bumps [85]. This leads to our belief that the utilization of the GS controller should be effective in regulating the equilibrium position of the IB in the presence of the disturbance caused by an uneven terrain. A dynamic model which considers the rate of variation of wheel-terrain contact angle is required to implement the controller on

uneven terrain in simulations. We attempt to derive the model and implement the GS controller in this work.

It is also necessary for us to further consider the stability region of the closed loop TWR system because the stability region is an important metric responsible for the applications of a TWR on inclined and uneven terrain. Stability region is defined as: "an envelope of the initial condition of a state from which it returns back to its equilibrium position". So far, there are very few attempts in the literature and as the existing approaches have not been fully applied on TWRs this makes the design unrealistic. Hence, we are required to quantify the stability region along with the performance of the controller for a class of TWRs which are statistically unstable.

An additional motivation arose from the successful implementation of the control Lyapunov Function Based Control (LFBC) that overcomes the stability and the stability region problem for nonlinear systems. Due to the use of a Lyapunov function, which is not determined using any one standard method the controller design for nonlinear systems continues to be an open problem. One of the most common approaches is to linearize the system with respect to an operating point, and use linear control theory to design a controller. This approach is successful when the operating point of the system is restricted to a certain region. When a wide range operation of the system is required, however, the method may fail. The Lyapunov theory enables us to utilize a Lyapunov function for a highly coupled nonlinear system to construct a control law that guarantees the stability and computes the stability region. Recent studies show that a constructive method [130] can be used to synthesize the control law for a highly coupled nonlinear system.

The final and outlying motivation has been that many control algorithms have been implemented in simulations rather than on real systems. Existence of a commercial two wheeled transporter (SEGWAY) [31] inspired to think that the control algorithm can be applied to develop an autonomous TWR. However, the practical implementation of online controller parameter tuning has been proven to be extremely complex as it has certain risks. However xPC target, a very powerful and efficient toolbox in MATLAB has been available for hardware-in-the-loop implementation which solves the problem. Some examples have been developed to implement the controllers in real time and this research attempts to implement the controllers on horizontal, inclined and uneven terrain.

1.6. Thesis Contribution

In this research study, the focus is on the control of statistically unstable two-parallel-wheeled mobile robots, not the statistically stable TWRs. Therefore, the design objectives involve the performance and stability of a TWR having c.o.m. below the axle. More precisely, it will address the problem of modelling and control of statistically unstable TWR while manoeuvring in pedestrian environment which includes motion of the TWR on horizontal, inclined and uneven terrain.

Our general objective in this research is to develop a TWR that is capable of manoeuvring autonomously on a variety of terrain keeping itself balanced, based on known terrain inclination and rate of change of inclinations, with decisions established on states feedback through sensors. Moreover, it is our conviction that although strategies have to be adapted to the specific application area, it is possible to develop a general methodology from the foundations of the system dynamics and control theory and of the robotics.

The focus of the thesis is to establish novel methodologies for control on horizontal, inclined and uneven terrain, dynamic analysis and performance quantification for a class of wheeled robots with differential drive and statically unstable behaviour. Our methodology is incorporated in three respects. First, this relies on a theoretic description of the system and environment at in the place that sensors and actuators are deployed and thus it is general and covers specific applications as particular cases. Second, it endeavours to optimize system related characteristics such as stability and performance. Third, it pertains to the real system to provide confidence that the theories are worthwhile and useful in real life.

In this work, we first model the dynamics which includes effects of terrain parameters, that is, wheel-terrain contact angle, rate of change of terrain inclination and acceleration produced by terrain unevenness, for motion of TWRs on both inclined and uneven terrain by using Lagrangian method. Based on this model, dynamic analysis and control design problems are considered respectively. It should be noted that for systems with parameter-varying exo-variable, it is difficult to analyse regulation of equilibrium states based on a single gain because the stated variation depends not only on the current input it also depends on the disturbance input due to non-horizontal terrain. In this work we introduce scheduling of controller gains with respect to the wheel-terrain contact angle. This GS state feedback controller is designed so that both stability and a prescribed velocity tracking performance for the closed-loop TWR are achieved. In parallel, stability region, state regulation, and the velocity tracking problems have also been studied for nonlinear TWR using nonlinear

Lyapunov function based controllers. The Lyapunov function based controller is synthesized for TWR motion on three terrains. To derive the LFBC nonlinear control law, the developed dynamic model is normalized and partial feedback linearized to get an affine form of the model. A control Lyapunov function is proposed. Based on the derivative of the control Lyapunov function a control law is deduced. The stability region is computed and the constraints of the LFBC are presented.

Three controllers; Baseline, GS and LFBC are tested in simulations to demonstrate the effectiveness, limits and advantages of the proposed methodologies. Finally, the controllers are implemented on a real time TWR platform, developed in the dynamics and control lab of the University of Auckland to validate the effectiveness of the proposed design methodologies in this thesis. The simulation results show and the experimental results validate that the proposed design methodologies can achieve the stability requirement, velocity tracking or the prescribed performance index.

1.7. Thesis Outline

The contents of the thesis are as follows. Chapter 2 describes the dynamic model of TWRs investigated in this thesis. The equations of motion are derived for TWR motion on uneven terrain and they are reduced for the inclined terrain. The reduced equations for a TWR on horizontal terrain are verified in comparison to the existing models and their experimental validation is presented.

Chapter 3 provides a basis of the control theory implemented and presents synthesizing of the control laws. A baseline controller, Linear quadratic regulator, synthesis is described. The design of a gain scheduled (GS) controller is detailed. Based on the Lyapunov method a novel methodology for designing a nonlinear controller for TWRs that stabilizes this class of two-wheeled robots is proposed. The existence of such a controller guarantees the asymptotic stability and computes the stability region. The performance of the controller is tuneable using gains introduced in controller synthesizing. This chapter also explains the performance indices to be used for performance quantification of the controllers for TWRs.

Chapter 4 presents the design and implementation of two control algorithms: Baseline controller and LFBC on TWR motion on a horizontal terrain. Sufficient conditions to the design of such a controller have been derived. As the scheduling variable is not changing on a horizontal terrain, therefore, GS controller is not designed or presented in this chapter. The

performance of the controllers is evaluated in simulations in different scenarios. A comparison of the performance of both of the controllers is given to show the advantages of the nonlinear controller over the linear controller.

In Chapter 5, control design for the stability of a TWR on inclined terrains is introduced. Three controllers (BL, GS and LFBC) are implemented. The GS controller is designed by scheduling the linear gains calculated at different wheel-terrain contact angles, a scheduling variable. The gains are linearly interpolated for intermediate situations. The performance is presented through simulation results to show the effectiveness of the designed controllers.

In Chapter 6, we apply the same formulation of the GS controller, used in Chapter 5, for TWRs motion on uneven terrain. As a result of such an implementation, the simulation results propose a discrepancy in the stability region. To achieve an enhanced stability region the nonlinear controller designed in chapter 3 is implemented and the simulation results show an augmentation in stability irrespective of the terrain-induced effects.

Chapter 7 details an overview of the experimental setup, that is, a TWR platform developed in the dynamics and control lab of the University of Auckland for research purposes. The details of the tests designed to verify the controller performance are described. The experimental results for BL and GS controllers are presented to show the effectiveness of the linear and semi nonlinear control algorithms on horizontal, inclined and uneven terrain. An implementation of the nonlinear LFBC algorithm is given for a horizontal terrain. The results for experiments on inclined and uneven terrain to verify nonlinear controller are not included in the thesis due to insufficient time. The research is continued and these results will be presented in another work report.

In Chapter 8, concluding remarks and suggestions for future research work are discussed to enhance the capabilities of the developed TWR system. This research had produced publications in international journals and peer reviewed international conferences (Listed on last page of this thesis). Certain sections of this thesis, are therefore, based on these published work.

Chapter 2. Modelling of Two-Wheeled Robots

Modelling of two wheeled mobile robots is an important task in order to design the control algorithms. The main objective of this model is to simulate the real robot dynamics including environmental disturbances, control input and sensor outputs. This chapter presents the kinematic and dynamic modelling of the two wheeled robot moving on horizontal and non-horizontal terrain. The TWR was pondered as an inverted pendulum in order to derive the dynamic and kinematic model of two wheeled robots. The equilibrium position of the IB relative to wheel-terrain contact angle was derived from equations of motion. It is necessary to derive the equilibrium position so that the controller is able to regulate that desired equilibrium IB. A complete set of governing equations of the mobile two wheeled robot is derived on horizontal, inclined and uneven terrain. After linearizing these equations, a linearized as well as state space model is presented. The developed models are then verified comparing them with other available models that have been previously validated through simulations. The dynamic models developed in this chapter will be used for the design of linear and nonlinear controllers in later chapters.

2.1. Modelling of the TWR on uneven terrain

Consider the two wheeled mobile robot as shown in Figure 2-1, which consists of two parts: an IB and the base. The base of the TWR is comprised of two driving wheels which are driven independently by two DC servomotors and are joined through the motor carrying plates. The IB consists of the rest of the robot parts placed on or around the motor carrying plates. The IB of the TWR was modelled as an inverted pendulum attached to a two-wheeled platform. The centre of the mass of each wheel was assumed to be at the centre of the wheel, while the centre of the mass of the IB was assumed to be above the axle joining the two wheel centres.

Assumptions

In order to model the dynamics of a TWR, the following assumptions have been made to simplify the modelling process:

i. The motion of the robot is restricted in x-z direction, a longitudinal plane;
ii. Two bodies, the IB and the base are assumed to be rigid bodies;

iii. The mass of each wheel, *m*, was alleged to be located at the centre of the wheel having a radius *r;*

iv. The mass of the IB, *M* was located at a distance *l* from the axle joining two wheels;

v. The wheels rotate at an angle Ø and no slippage occurs between wheels and the ground;

vi. Each wheel remains in contact with the ground at a single point;

vii. A differential drive was assumed such that motors apply total torque (*T*) on the wheels, to navigate the robot a horizontal distance *x* along the x-plane;

viii. The IB rotates from the vertical, denoted by pitch angle, θ;

ix. The mass moment of inertia for the IB and wheels (including gearbox and transmission) were known and denoted as *Ip* and *I*, respectively. These moments of inertias are about the respective centres of masses and were calculated using real time data extracted from the experiments performed on the TWR [131];

x. The wheel terrain contact angle α is used to define the characteristic of uneven terrain and is assumed to be known. All terrain are assumed flat and smooth;

xi. The pitch was assumed to be changing at an angular rate, $\dot{\theta}$. The linear displacement of the wheel-ground contact point along x-axis is *x*.

The dynamics of the robot is modelled using the Lagrangian method.

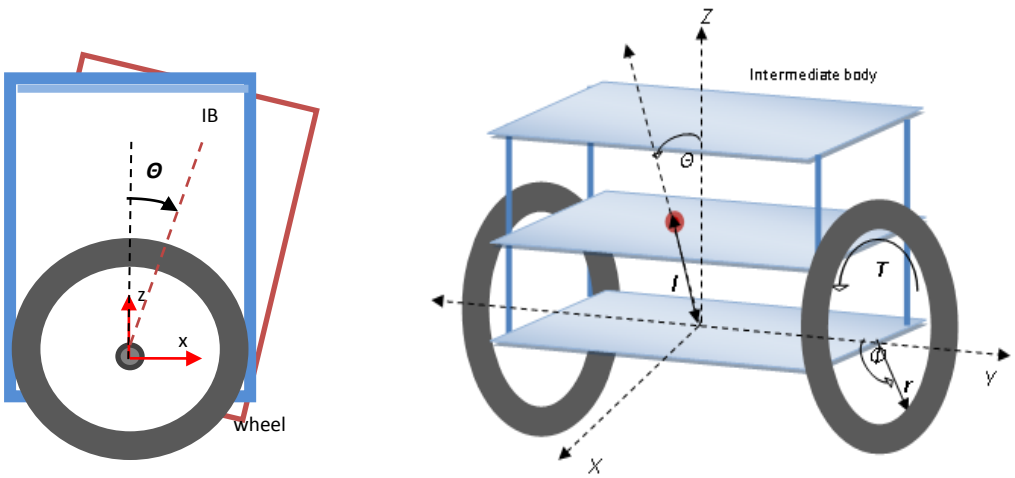

Figure 2-1: Views of schematic of the TWR (Left: Side view; Right: Front view)

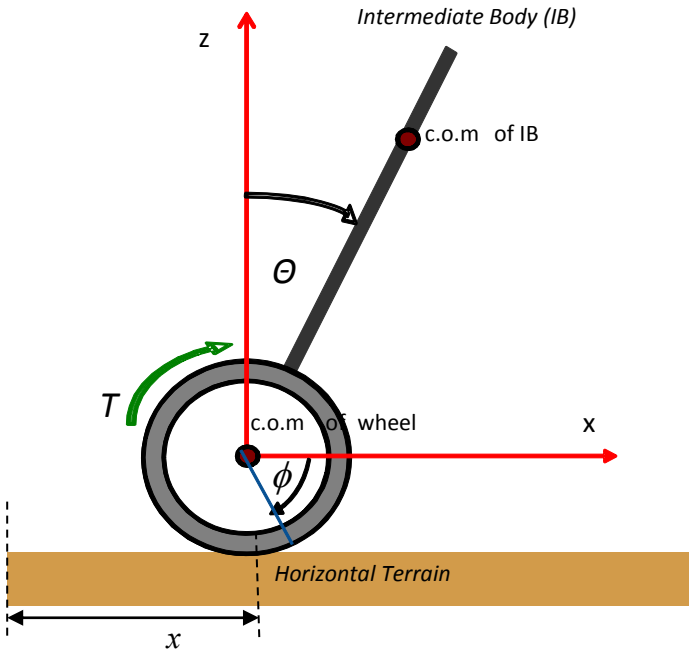

(a) Schematics of the TWR on a horizontal terrain.

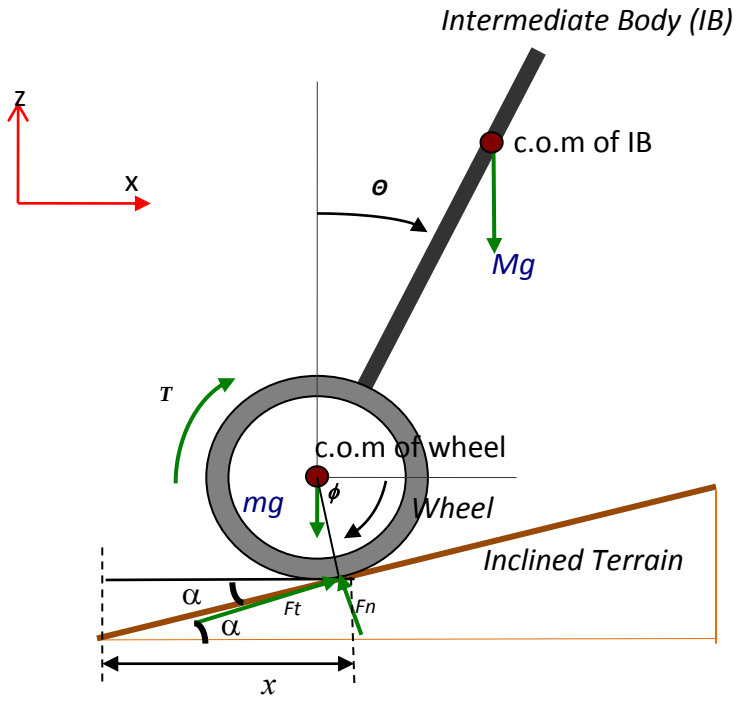

(b) Schematics of the TWR on an inclined terrain.

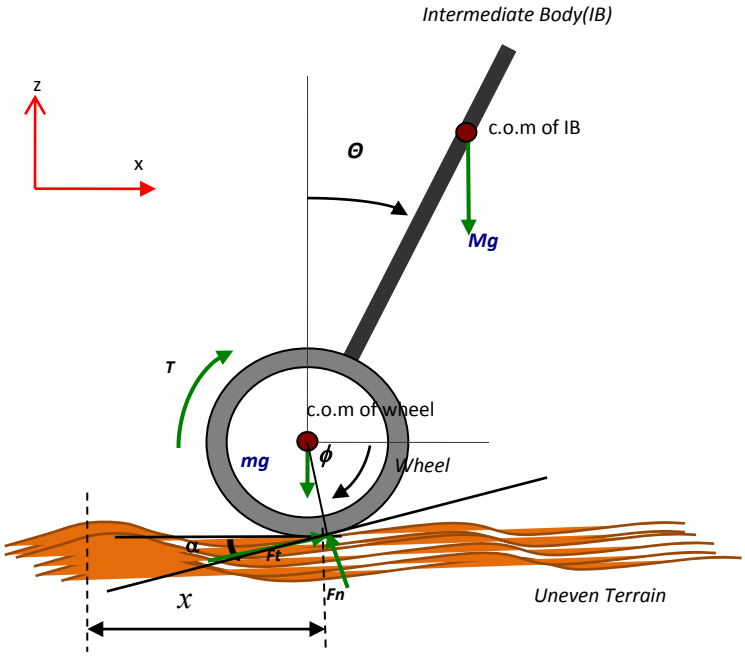

(c) Schematics of the TWR on an inclined terrain.

Figure 2-2: Schematics of the TWR on different terrain.

2.2. Kinematics of the TWR

The kinematics of the TWR is essential to calculate the position, velocity and acceleration of the IB and the wheel without considering the torque that causes this motion. The relationship between motion and the associated torque is studied in the next section as the robot dynamics. A schematic diagram of the TWR on uneven terrain is shown in Figure 2-3 in which c is a wheel-terrain contact point, w is the wheel center and p is at the point where the center of mass of the pendulum lies. The position, velocity and the acceleration vectors at these corresponding points are described hereunder.

Position Vectors

$$\boldsymbol{C} = \begin{bmatrix} x \\ z \end{bmatrix} ;$$

$$\boldsymbol{W} = \begin{bmatrix} x - r\sin(\alpha) \\ z + r\cos(\alpha) \end{bmatrix};$$

$$\boldsymbol{P} = \begin{bmatrix} x - r\sin(\alpha) + l\sin(\theta) \\ z + r\cos(\alpha) + lco\,s(\theta) \end{bmatrix};$$

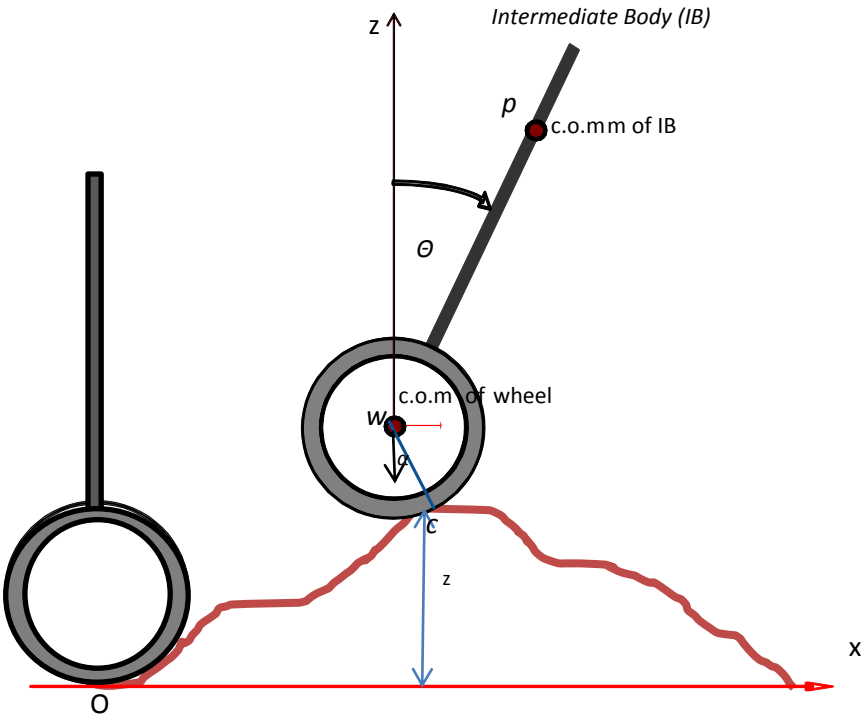

Figure 2-3: Schematics of points: wheel-terrain contact point, wheel centre and IB c.o.m

Velocity Vectors

$$\boldsymbol{V_c} = [\dot{x} \quad \dot{z}]^T$$

$$\boldsymbol{V_w} = [\dot{x} - r\cos(\alpha)\dot{\alpha} \quad \dot{z} - r\sin(\alpha)\dot{\alpha}]^T$$

$$\boldsymbol{V_p} = [\dot{x} - r\cos(\alpha)\dot{\alpha} + l\cos(\theta)\,\dot{\theta} \quad \dot{z} - r\sin(\alpha)\dot{\alpha} - l\,\dot{\sin}(\theta)\dot{\theta}]^T$$

Acceleration Vectors

$$\boldsymbol{a_c} = [\ddot{x} \quad \ddot{z}]^T$$

$$\boldsymbol{a_w} = \begin{bmatrix} \ddot{x} + r\sin(\alpha)\dot{\alpha}^2 - r\cos(\alpha)\ddot{\alpha} \\ \ddot{z} - r\cos(\alpha)\dot{\alpha}^2 - r\sin(\alpha)\,\ddot{\alpha} \end{bmatrix};$$

$$\boldsymbol{a_p} = \begin{bmatrix} \ddot{x} + r\sin(\alpha)\dot{\alpha}^2 - r\cos(\alpha)\ddot{\alpha} + l\cos(\theta)\,\ddot{\theta} - l\sin(\theta)\,\dot{\theta}^2 \\ \ddot{z} - r\cos(\alpha)\dot{\alpha}^2 - r\sin(\alpha)\,\ddot{\alpha} - l\sin(\theta)\,\ddot{\theta} - l\cos(\theta)\,\dot{\theta}^2 \end{bmatrix};$$

2.3. Dynamics of the TWR

Schematics of a TWR is shown at different terrain in Figure 2-2. The dynamic equations are deduced based on the Lagrange equation. The Lagrange function is:

$$L(\theta, \dot{\theta}) = K(\theta, \dot{\theta}) - P(\theta, \dot{\theta}) \quad (2.1)$$

Where,

L = Lagrange operator;

K = Total kinetic energy of the system;

P = General potential energy of the system;

θ = Generalized coordinate of the system;

The equation of motion is formulated expressing the Lagrange equation in partial derivative of Lagrange operator with respect to the generalized coordinates:

$$\frac{d}{dt}\left(\frac{\partial L}{\partial(\dot{\theta}_i)}\right) - \frac{\partial L}{\partial \theta_i} = T \quad (2.2)$$

In (2.2): i = 1, 2, 3, …..n. f_i is external force along the generalized direction or constraint energy. The generalized coordinates in the TWR system, shown in Figure 2-2, are x and θ.

2.3.1. Total kinetic energy of the TWR

According to the selected coordinates x and θ, the total kinetic energy of the two wheeled robot on an uneven terrain can be expressed as:

$$K_{total} = K_{IB} + K_{wheel} \quad (2.3)$$

As the wheels have rotational as well as translational kinetic energy, the total kinetic energy of wheels is as follows:

$$K_{wheel} = \frac{1}{2} m V_w^2 + \frac{1}{2} I \dot{\phi}^2 \quad (2.4)$$

The kinetic energy of the IB is:

$$K_{IB} = \frac{1}{2} M V_p^2 + \frac{1}{2} I_p \dot{\theta}^2 \quad (2.5)$$

The total kinetic energy of the TWR is obtained combining (2.4) and (2.5) into (2.3) as:

$$K_{total} = K_{IB} + K_{wheel} = \frac{1}{2}[m V_w^2 + I\dot{\phi}^2 + M V_p^2 + I_p \dot{\theta}^2]$$

Simplifying after substitution of expressions of V_w^2 and V_p^2 :

$$K = \frac{1}{2}(m+M)\dot{x}^2 + \frac{1}{2}(m+M)\dot{z}^2 + \frac{1}{2}(m+M)r^2\dot{\alpha}^2 + \frac{1}{2}\left(Ml^2 + I_p\right)\dot{\theta}^2 - (m+M)r\sin(\alpha)\,\dot{\alpha}\dot{z} - (m+M)r\cos(\alpha)\,\dot{\alpha}\dot{x} - Ml\sin(\theta)\,\dot{\theta}\dot{z} + Ml\cos(\theta)\dot{\theta}\dot{x} - Mlr\cos(\theta-\alpha)\,\dot{\alpha}\dot{\theta} + I\dot{\phi}^2 \quad (2.6)$$

2.3.2. General potential energy of the TWR

When wheels of TWR are on uneven terrain potential energy is of robot's base has not. The general potential energy of flexible humanoid robot researched includes two parts in this paper:

$$P_{total} = P_{IB} + P_{wheel} \quad (2.7)$$

Potential energy of wheel, $P_w = mg(z + r\cos\alpha) = mgz + mgr\cos(\alpha)$

Potential Energy of the IB, $P_{IB} = Mg(z + r\cos(\alpha) + l\cos(\theta)) = Mgz + Mgr\cos(\alpha) + Mgl\cos(\theta)$

$$P_{total} = P_{IB} + P_{wheel} = (m+M)gz + (m+M)g\,r\cos(\alpha) + Mgl\cos(\theta) \quad (2.8)$$

2.3.3. Generalized coordinates

The generalized coordinates of the TWR system, considered for the development of equations for its dynamics are as follows: the angular position of the wheel (∅), pitch (θ) and pitch rate ($\dot{\theta}$). These may be used as states of the system at some later stage.

2.3.4. Dynamic equations of the TWR on uneven terrain

The Lagrange function for the TWR is: $L\left(\dot{x},\theta,\dot{\theta}\right) = K(\dot{x},\theta) - P\left(\dot{x},\theta,\dot{\theta}\right)$. If we consider θ as a generalized coordinate then we get (2.2), where *T* is the generalized moment which causes change in the generalized coordinate, θ. Now,

$$\frac{\partial L}{\partial\dot{\theta}} = \left(Ml^2 + I_p\right)\dot{\theta} - Ml\sin(\theta)\,\dot{z} + Ml\cos(\theta)\,\dot{x} - Mlr\cos(\theta-\alpha)\,\dot{\alpha}$$

$$\frac{d}{dt}\left(\frac{\partial L}{\partial\dot{\theta}}\right) = [\left(Ml^2 + I_p\right)\ddot{\theta} - Ml\sin(\theta)\,\ddot{z} - Ml\cos(\theta)\,\dot{\theta}\dot{z} + Ml\cos(\theta)\,\ddot{x} - Ml\sin(\theta)\,\dot{\theta}\dot{x} + Mlr\sin(\theta-\alpha)\dot{\theta}\dot{\alpha} + Mlr\sin(\theta+\alpha)\dot{\alpha}^2 - Mlr\cos(\theta-\alpha)\ddot{\alpha}]$$

$$\boldsymbol{\frac{\partial L}{\partial\theta}} = -Ml\cos(\theta)\,\dot{\theta}\dot{z} - Ml\sin(\theta)\,\dot{\theta}\dot{x} + Mlr\sin(\theta-\alpha)\dot{\theta}\dot{\alpha} + Mgl\sin(\theta)$$

Substitution above expressions of $\frac{d}{dt}\left(\frac{\partial L}{\partial\dot{\theta}}\right)$ and $\boldsymbol{\frac{\partial L}{\partial\theta}}$ in Lagrange equation (2.2) gives:

$$T = Ml\sin(\theta)\,\ddot{z} - Ml\cos(\theta)\,\ddot{x} - \left(Ml^2 + I_p\right) - Mlr\sin(\theta+\alpha)\dot{\alpha}^2 + Mlr\cos(\theta-\alpha)\ddot{\alpha} + Mgl\sin(\theta) \tag{2.9}$$

When no slip condition is assumed, the position of contact point on the wheel is the same as on the ground. This position can be defined as wheel rotation angle, $\emptyset$. Let generalized coordinates is $\emptyset$ then equation of motion can be written as follows:

$$T - f_t r = \frac{d}{dt}\left(\frac{\partial L}{\partial \dot{\emptyset}}\right) - \frac{\partial L}{\partial \emptyset} \tag{2.10}$$

$$\frac{\partial L}{\partial \dot{\emptyset}} = I\dot{\emptyset}$$

$$\frac{d}{dt}\left(\frac{\partial L}{\partial \dot{\emptyset}}\right) = I\ddot{\emptyset}$$

$$\frac{\partial L}{\partial \emptyset} = 0$$

$$T - f_t r = I\ddot{\emptyset} \tag{2.11}$$

Therefore,

$$f_t = -(m+M)\sin(\alpha)\,\ddot{z} + (m+M)\cos(\alpha)\ddot{x} + ml\cos(\theta+\alpha)\ddot{\theta} - ml\sin(\theta-\alpha)\dot{\theta}^2 - (m+M)g\sin(\alpha) - (m+M)r\cos(2\alpha)\,\ddot{\alpha} + (m+M)r\sin(2\alpha)\dot{\alpha}^2$$

This results in second equation of motion:

$$T = (m+M)r\cos(\alpha)\ddot{x} - (m+M)\,\mathrm{r}\sin(\alpha)\,\ddot{z} + Mlr\cos(\theta+\alpha)\ddot{\theta} + (m+M)r^2\cos(2\alpha)\,\ddot{\alpha} + (m+M)r^2\sin(2\alpha)\dot{\alpha}^2 - Mlr\sin(\theta-\alpha)\dot{\theta}^2 - (m+M)gr\sin(\alpha) + I\ddot{\emptyset} \tag{2.12}$$

The equations of motion representing the dynamics of the two wheeled robot with kinematic constraint of no-slip and moving on an uneven terrain are, therefore written as given in (2.13) and (2.14),

$$(Ml\,sin\theta)\,\ddot{z} - (Ml\,cos\theta)\,\ddot{x} - \left(Ml^2 + I_p\right)\ddot{\theta} + Mgl\,sin\theta + Mlr\,cos(\theta-\alpha)\,\ddot{\alpha} - Mlr\,sin(\theta+\alpha)\dot{\alpha}^2 = 0 \tag{2.13}$$

$$[r\,(M+m)\,cos\,\alpha]\,\ddot{x} - [r\,(M+m)\,sin\,\alpha]\,\ddot{z} - r\,(m+M)g\,sin(\alpha) + [Mlr\,cos(\theta+\alpha)]\ddot{\theta} - [Mlr\,sin(\theta-\alpha)]\dot{\theta}^2 + [r^2\,(M+m)\,cos(2\alpha)]\,\ddot{\alpha} + [r^2\,(M+m)\,sin(2\alpha)]\,\dot{\alpha}^2 + I\ddot{\emptyset} = T \tag{2.14}$$

(2.13) and (2.14) are equations of motion of the TWR motion on an uneven terrain but these may be used for all terrain for which the terrain inclination is known.

2.4. Dynamic model of the TWR on inclined terrain

The equations of motion representing the dynamics of the two wheeled robot with kinematic constraint of no-slip and moving on an inclined terrain are, as given in (2.15) and (2.16),

$$(Ml\,sin\theta)\,\ddot{z} - (Ml\,cos\theta)\,\ddot{x} - \left(Ml^2 + I_p\right)\ddot{\theta} + Mgl\,sin\theta + = 0 \tag{2.15}$$

$$[r\,(M+m)\,cos\,\alpha]\,\ddot{x} - [r\,(M+m)\,sin\,\alpha]\,\ddot{z} - r\,(m+M)g\,sin(\alpha) + [Mlr\,cos(\theta+\alpha)]\ddot{\theta} - [Mlr\,sin(\theta-\alpha)]\dot{\theta}^2 + I\ddot{\emptyset} = T \tag{2.16}$$

2.5. Dynamic model of the TWR on horizontal terrain

The equations of motion representing the dynamics of the two wheeled robot with kinematic constraint of no-slip and moving on a horizontal terrain are, as given in (2.17) and (2.18):

$$(Ml\,sin\theta)\,\ddot{z} - (Ml\,cos\theta)\,\ddot{x} - \left(Ml^2 + I_p\right)\ddot{\theta} + Mgl\,sin\theta = 0 \tag{2.17}$$

$$[r\,(M+m)]\,\ddot{x} + [Mlr\,cos(\theta)]\ddot{\theta} - [Mlr\,sin(\theta)]\dot{\theta}^2 + I\ddot{\emptyset} = T \tag{2.18}$$

2.6. Equilibrium position of the IB

The pitch equilibrium is updated as a function of wheel-terrain contact angle, α, as shown in Figure 2-5. The pitch equilibrium is mathematically computed as (2.19) and shown graphically in Figure2-6.

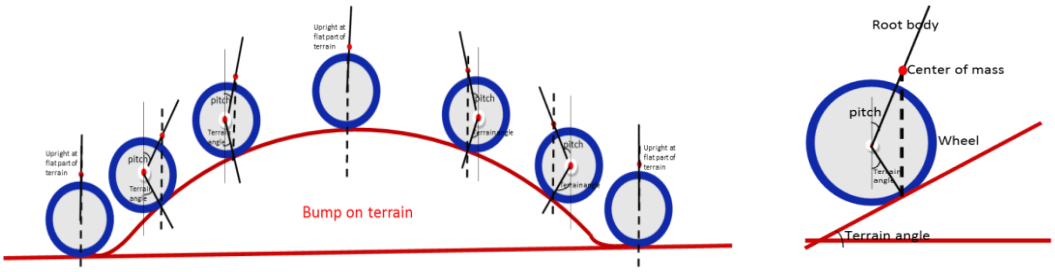

Figure 2-4: Equilibrium pitch as a function of wheel-terrain contact point.

$$\theta_e = sin^{-1}\left[-\frac{(M+m)r}{Ml}.\sin\alpha\right] \tag{2.19}$$

This relationship is developed for the steady state of each operating condition. The equilibrium states of linear speed and pitch rate are assumed to be zero in this control design.

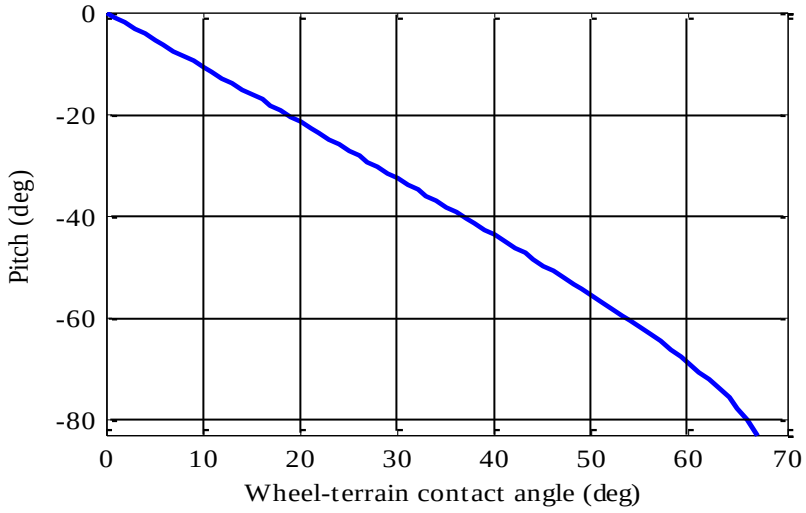

Figure 2-5: Relationship between equilibrium pitch and wheel-terrain contact angle

2.7. Linearized model of the TWR

A TWR system is a highly nonlinear system. Therefore to design a FSFB controller the dynamic equations are required to be linearized. The dynamic model (2.13) & (2.14) is linearized with regard to the upright position of a TWR. The upright equilibrium position represents a zero pitch angle and pitch rate. The linearization is performed applying standard method of Taylor expansion around equilibrium neighbourhood, using MATLAB. The resulting equations of motion are rearranged in the linear state space form of (2.20).

$$\dot{\boldsymbol{X}} = A\boldsymbol{X} + B\boldsymbol{u} \tag{2.20}$$

The matrices A **,** a system matri**x,** and B**,** a control input matrix, consist of coefficients of inertia and input terms respectively. $\boldsymbol{u}$ is an input vector and $\boldsymbol{X}$ is a state vector. The state vector consists of velocity, pitch and pitch rate. As the robot position control is not our main objective, the state of robot position has been omitted from the set of possible states. A state vector, used for gain evaluation instead, includes an integral of speed error as follows:

$$\boldsymbol{X} = \left[\int \dot{x} - v_{ref}\, dt \quad \dot{x} \quad \theta \quad \dot{\theta}\right]^T$$

This additional state has been used to track the speed of the robot and compensate for the mass imbalance.

2.8. State space model of the TWR

The resulting state space model is given in (2.21).

$$\begin{bmatrix} \dot{x} - v_{ref} \\ \ddot{x} \\ \dot{\theta} \\ \ddot{\theta} \end{bmatrix} = \begin{bmatrix} 0 & 1 & 0 & 0 \\ 0 & 0 & -\frac{c^2 g}{ab-c^2} & 0 \\ 0 & 0 & 0 & 1 \\ 0 & 0 & \frac{g(cM_0 r + Mll)}{ab-c^2} & 0 \end{bmatrix} \begin{bmatrix} \int \dot{x} - v_{ref}\, dt \\ \dot{x} \\ \theta \\ \dot{\theta} \end{bmatrix} + \begin{bmatrix} 0 \\ \frac{c(l+\dot{r})+I_p r}{ab-c^2} \\ 0 \\ -\frac{c+b}{ab-c^2} \end{bmatrix} [T] \qquad (2.21)$$

In (2.21), $a = Ml^2 + I_p$; $b = M_0 r^2 + I$; $c = Mlr$; $M_0 = M + m$; $g =$ acceleration due to gravity ; and $v_{ref} =$ desired speed. r, M, l, I *and* I_p are physical parameters of the robot as defined in Table 2-1. The system matrices are defined as:

$$\boldsymbol{A} = \begin{bmatrix} 0 & 1 & 0 & 0 \\ 0 & 0 & -\frac{c^2 g}{ab-c^2} & 0 \\ 0 & 0 & 0 & 1 \\ 0 & 0 & \frac{g(cM_0 r + Mll)}{ab-c^2} & 0 \end{bmatrix}, \ \boldsymbol{B} = \begin{bmatrix} 0 \\ \frac{c(l+\dot{r})+I_p r}{ab-c^2} \\ 0 \\ -\frac{c+b}{ab-c^2} \end{bmatrix}, \boldsymbol{C} = [\boldsymbol{0}], \ \boldsymbol{D} = [\boldsymbol{0}], \quad \boldsymbol{u} = [\boldsymbol{T}]$$

The system matrices are evaluated using parameter values of a physical TWR as listed in Table 2.1. The same physical TWR system will be used for experimental results in following chapters.

2.9. Uneven Terrain Model

Let the uneven terrain be defined as a function of terrain height, $z = f(x)$. The variation and rate of variation of the terrain are computed as shown in the Figure 2-6 below.

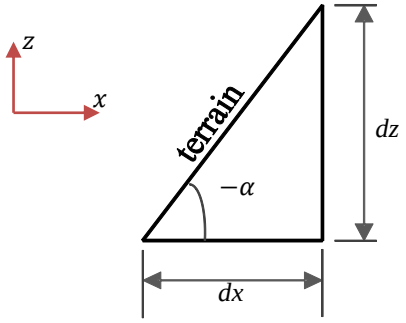

Figure 2-6: Terrain definition

$$\dot{z} = \frac{\partial f}{dt} = \frac{df}{dx}.\frac{dx}{dt} = f'\dot{x} \tag{2.22}$$

$$\ddot{z} = f'\ddot{x} + \dot{x}^2 f'' \tag{2.23}$$

$$f' = \frac{dz}{dx} = -\tan\alpha \quad ; \quad f'' = \frac{\dot{\alpha}}{\cos^2\alpha} \tag{2.24}$$

$$\ddot{\emptyset} = \frac{\ddot{x}}{r} \tag{2.25}$$

Substituting (2.23) - (2.25) in (2.13) and (2.14):

$$[Ml(-\tan\alpha.sin\theta - \cos\theta)]\ddot{x} - \left(Ml^2 + I_p\right)\ddot{\theta} + (Ml\,sin\theta)\,\frac{\dot{\alpha}}{(\cos\alpha)^2}.\dot{x}^2 + Mgl\,sin\theta + Mlr\,cos(\theta-\alpha)\,\ddot{\alpha} - Mlr\,sin(\theta+\alpha)\dot{\alpha}^2 = 0 \tag{2.26}$$

and

$$\left[\frac{r\,(M+m)}{\cos\alpha} + \frac{I}{r}\right]\ddot{x} - [r\,(M+m)\,sin\,\alpha]\,\frac{\dot{\alpha}}{(\cos\alpha)^2}.\dot{x}^2 - r\,(m+M)g\,sin(\alpha) + Mlr\left[\ddot{\theta}.cos(\theta+\alpha) - \dot{\theta}^2.sin(\theta-\alpha)\right] + r^2\,(M+m)[\ddot{\alpha}.cos(2\alpha) + \dot{\alpha}^2.sin(2\alpha)] = T \tag{2.27}$$

(2.26) and (2.27) are the equations of motion of the TWR written in terms of wheel-terrain contact angle. Wheel-terrain contact angle is the parameter we are using for measurement of terrain inclination and uneveness.

2.10. Nonlinear E.O.M for Simulation

The manipulation of the above equations (2.26) and (2.27) reveal into the following:

$$\ddot{x} = \frac{1}{h}\left[h_1 T + h_2\dot{x}^2 + h_3\dot{\theta}^2 + h_4 g + h_5\dot{\alpha}^2 + h_6\ddot{\alpha}\right] \tag{2.28}$$

$$\ddot{\theta} = \frac{1}{h}\left[h_7 T + h_8\dot{x}^2 + h_9\dot{\theta}^2 + h_{10} g + h_{11}\dot{\alpha}^2 + h_{12}\ddot{\alpha}\right] \tag{2.29}$$

$h_1, h_2, h_3, h_4, h_5, h_6, h_7, h_8, h_9, h_{10}, h_{11}, h_{12}$ are given in appendix-A for three types of terrain.

2.11. Model verification and validation for the TWR

Verification of a model intends to ensure that the model is built and implemented correctly and it does what it is expected to do. In this section the model is verified through comparison of the model with one being developed using another technique. Later, the model outputs are examined under a variety of settings of input parameters. The aim is to conclude how reasonable the model is and how correctly the model parameters are represented. If the model output shows a significant difference, either it should be possible to explain the difference

from a more detailed knowledge of the system, or the possibility of a modelling error should be investigated. A test for torque is performed with variations in wheel-terrain contact angle shown in Figure 2-7. This verifies the model on inclined terrain. Another graph plots torque variation with variations in pitch angle which also verifies the model and to show reliability and repeatability.

A variation in different parameters, shown in Figure 2-8 verifies the model considers the terrain variations and this could be compensated later. Input-output relations: at different input torques the outputs which are theta and xd are simulated to confirm their variation with torque change shown in Figure 2-9. To validate the model the PD controller is implemented in simulation as well as in experiments. The experimental setup is described in chapter 7. Tests show (Figure 2-10) the same performance in simulation and experiments which confirms the good agreement between the dynamic model and real time TWR.

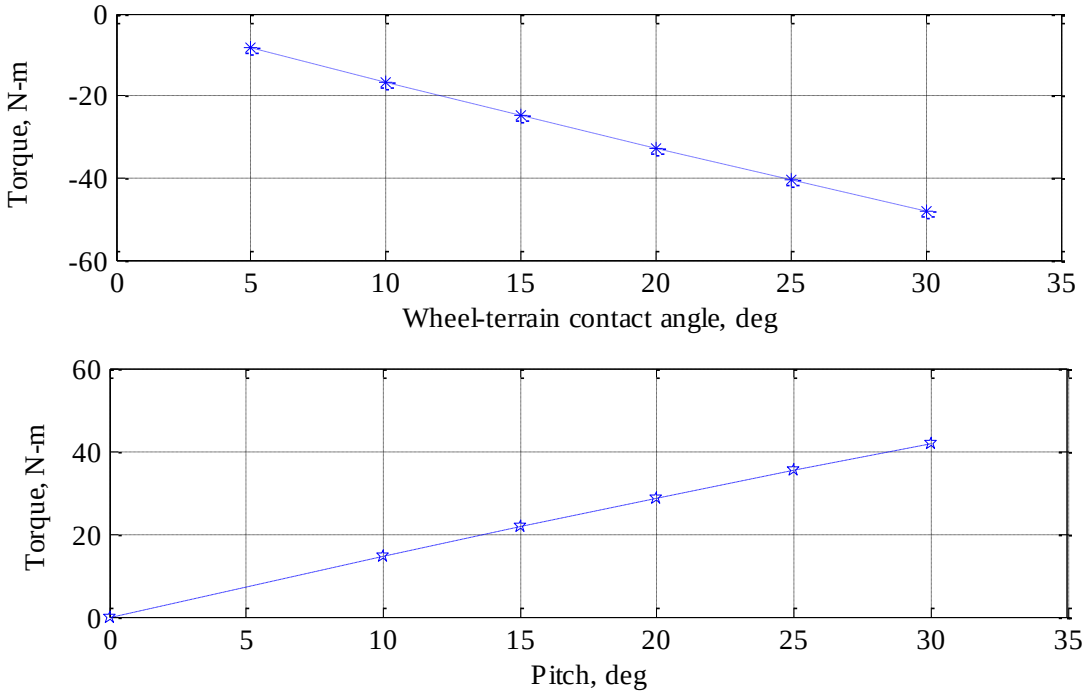

Figure 2-7: Torque variations with variations in wheel-terrain contact angle to verify the model on inclined terrain and with variations in pitch angle to verify model on horizontal terrain.

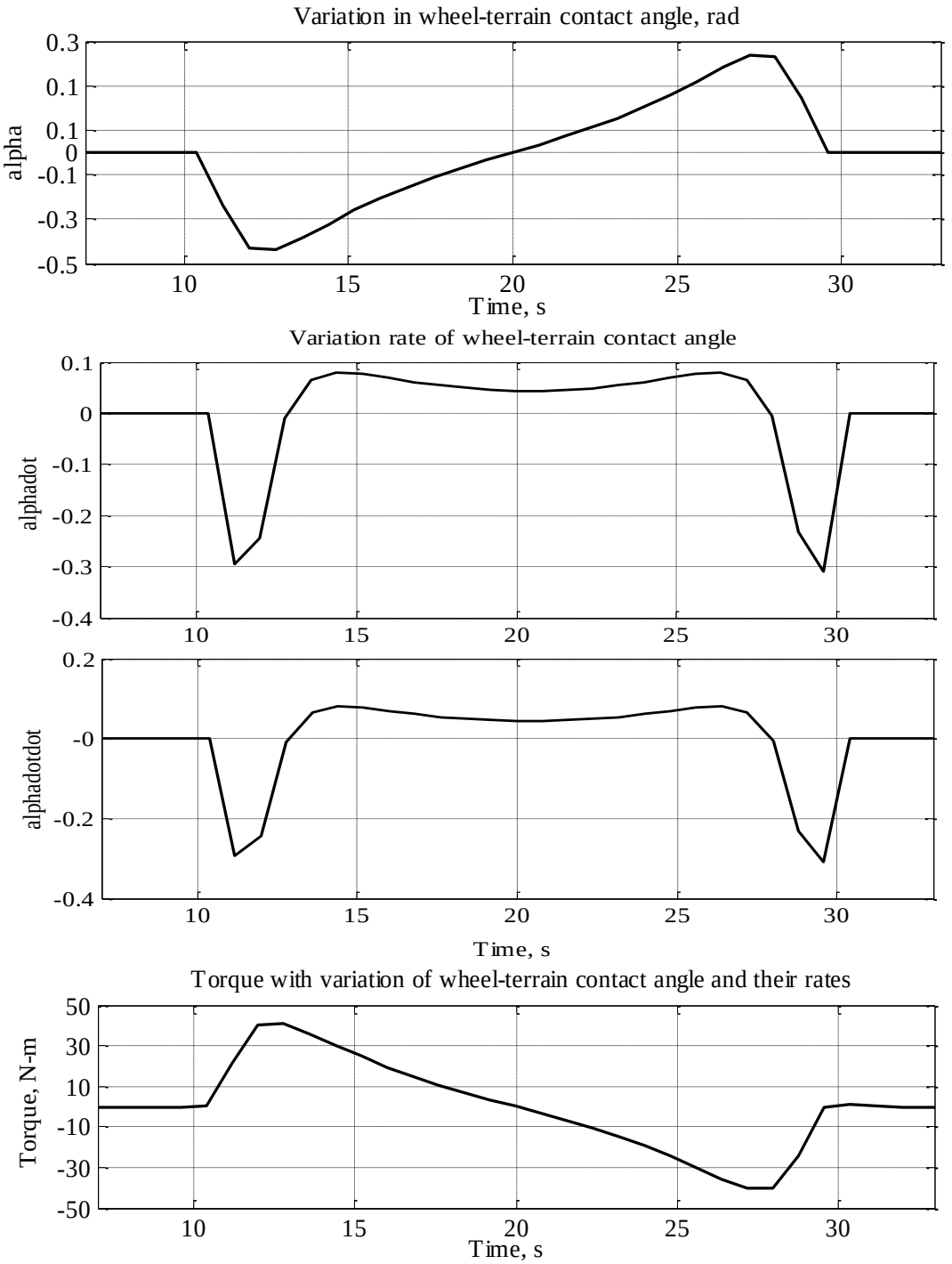

Figure 2-8: Variation of torque with variations in wheel-terrain contact angle, terrain variation rate and acceleration of angle variations.

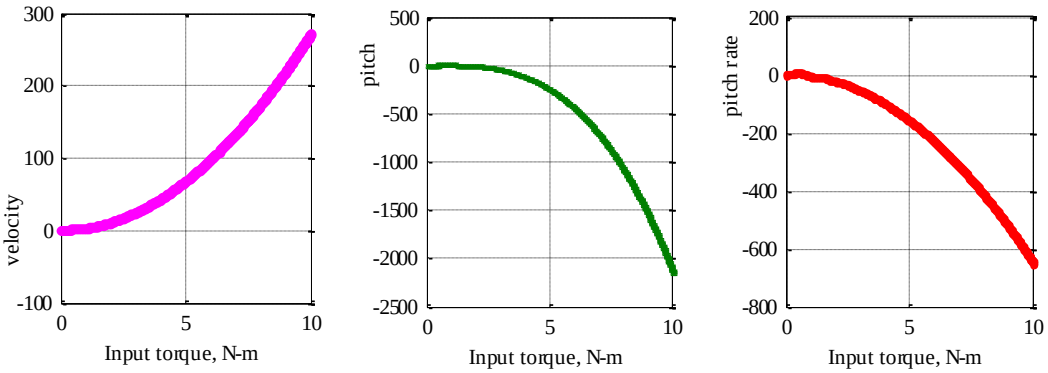

Figure 2-9: The parameter variations verify the input output relationship.

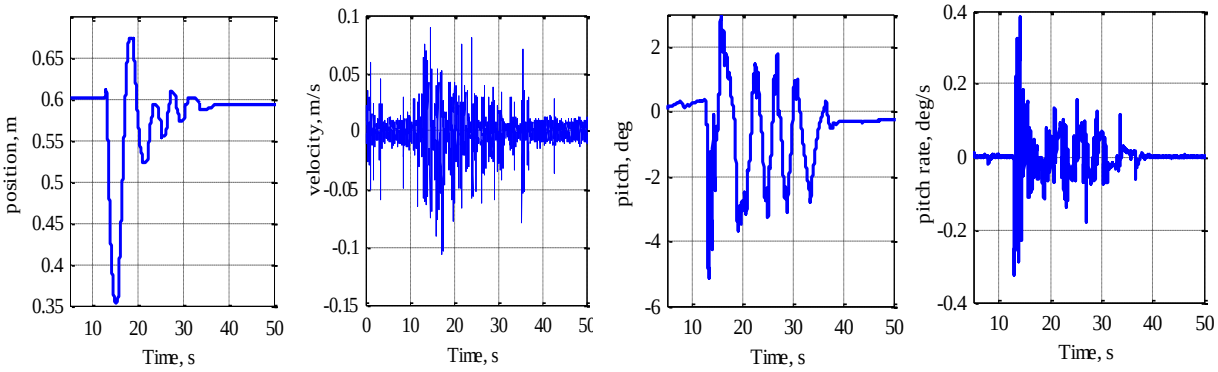

Figure 2-10: Response of PD control of the TWR, used to validate the system model.

Table 2-1: Parameters of the two wheeled robot for simulations.

Name	**Symbol**	**Value**	**Unit**
Intermediate Body:			
Mass of IB	M	43.0	Kg
Mass moment of inertia of IB	I_p	0.56	Kg.m^2
Distance of center of mass of IB from wheel axle	l	0.024	m
Wheels:			
Mass of each wheel	M	2.77	Kg
Mass moment of inertia of each wheel	I	0.0891	Kg.m^2
Radius of each wheel	r	0.196	m
Motors for wheels:			
Torque constant of motor	K_t	0.1911	*Nm/A*
Friction constant of motor	K_f	0.0292	*Nm/rad.s*
Current demand limits	-	± 5	*Amp*

Chapter 3. Controllers Methodologies/Synthesis for the Two-Wheeled Robot

The objective of control synthesis in this study is to regulate the balance of the intermediate body of a TWR (pitch), pitch rate and track the desired robot velocity on horizontal, inclined and uneven terrain. Such a control is important for a variety of applications of TWRs on different terrain. This chapter presents the development of controller synthesis of three controllers: Baseline controller; Gain Scheduled controller and Lyapunov function based controller. The procedure is described to carry out the stability analysis of closed loop TWR system for each controller. This stability analysis shows to what extent the controller can be used with stable output. Stability analysis determines how close the system is to instability and how much margin there is when disturbances are present and when the gain is adjusted. The region of attraction of a closed loop system is important to be known as it gives information about the boundary of the initial states of the system from where the system can come back to the equilibrium states. The stability region is not unique with any controller and parameter. But for one controller and one fixed set of values of parameters, the stability regions are comparable. We shall use region of attraction to compare three controllers designed for TWR in later chapters. At the end of this chapter some performance evaluation criterion are presented.

3.1. Baseline Controller Design

The control approaches designed for two wheeled mobile robot's application on flat horizontal terrain have been to balance the robots and track their desired velocity. To achieve this goal a few of linear and nonlinear controllers have been implemented. In order to show advantage or disadvantage of new designed controllers for TWRs we need to choose a baseline controller. It is not clear which controller we can use for this purpose. A comparative study [87] showed that amongst linear controllers, designed for balancing the IB, a Full State Feed Back (FSFB) controller with Linear Quadratic Regulator (LQR) gain optimization gives promising results. The results have been compared with regards to overshoot and rise time of the transient response of the system. However, to minimize the steady state error of the IB position, the addition of reference velocity tracking is necessary [52]. In this research, a FSFB state space controller is selected as a baseline controller. This type of controller

assumes all states are known through sensors and are fed back. The gain matrix of the controller is determined using LQR.

The simulation results will clearly be comparable to the experimental results at a later stage of this research.

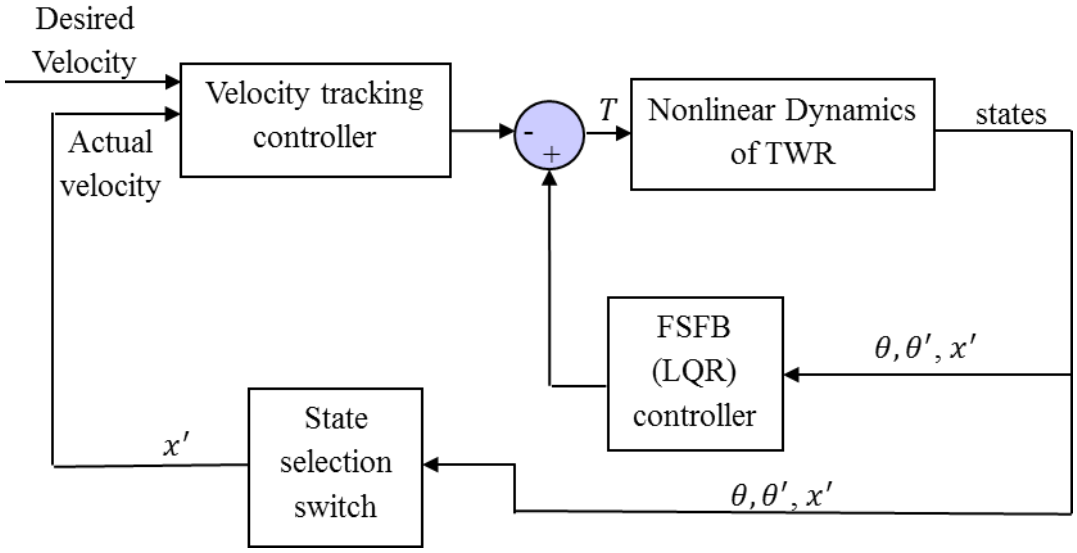

Figure 3-1: Baseline controller - block diagram

A block diagram of the closed loop control system is shown in Figure 3-1. This implements a control law (3.1):

$$u = -K_x \boldsymbol{X} - K_r e_r \tag{3.1}$$

In this control law K_x is the FSFB gain matrix, K_r is the speed reference tracking gain and e_r is an error between the desired and the measured linear speed of the wheel. The controller gains are tuned using linear quadratic regulator (LQR). The linear quadratic regulator concludes closed loop pole locations which are the best pole locations satisfying a given performance. LQR method uses an optimal cost function to decide the controller gains which minimizes a performance index. In general, it is desired to have maximum state regulation so that the system states are driven strongly to equilibrium [Franklin's book]. But this high regulation of states requires high control effort. LQR provides a trade-off between state regulation and control effort. The LQR optimal cost function is given as (3.2):

$$\boldsymbol{J} = \int_0^\infty (\boldsymbol{x^T} Q\, \boldsymbol{x} + R\boldsymbol{u}^2) dt \tag{3.2}$$

The Q matrix contains weighted values for each state. These values are assigned according to the importance and the level of each state regulation. A higher weighting indicates a higher level of regulation. The R, input weighting, matrix controls the amount of effort each actuator contributes to the stabilization of the system. The cost function (3.2) is minimized such that the gain matrix K is :

$$K = R^{-1}B^{T}P \text{ .}$$

B is system matrix of the state space model (2.21). P is determined finding the solution of the Riccati equation (3.3):

$$A^{T}P + PA - PBR^{-1}B^{T}P + Q = 0 \tag{3.3}$$

The state weighting matrix Q and input weighting matrix R for LQR which fulfil the control objective is selected and the controller is implemented on nonlinear dynamics of TWR in simulation in next chapter.

Stability analysis of linear dynamic systems is a well-studied subject [28] in comparison to the nonlinear systems [29-30]. The former approach for stability analysis was therefore adopted for TWRs in this study. The nonlinear robot system was linearized about the upright equilibrium position and the eigenvalues of control matrix of the robot system were analyzed.

3.2. Gain Scheduled Controller Design

Gain Scheduled controller employs well understood and powerful linear design tools on difficult nonlinear problems. In gain scheduled controller the performance specifications are formulated in linear terms which enable a controller to respond rapidly to changes in the operating conditions. On an uneven terrain, the wheel terrain contact angle varies as a function of displacement. This variation changes the operating conditions. In addition, the requirements on the control also changes with the change of operating conditions, hence a Gain Scheduled controller is proposed due to a potential of gain scheduling to incorporate linear robust control methodologies into nonlinear control design. The gain scheduled controller designed here is based on the fundamental assumption that the values of the scheduling variable are known on-line by the controller. The lack of information related to the scheduling variable may lead to a failure in achieving the desired specifications.

3.2.1. Controller Synthesis

Gain scheduled controller design follows the guidelines of LQR. That is, the design is formulated as a problem of minimisation of the given states: pitch, pitch rate and velocity.

Therefore, the problem formulation consists in measuring the state variables, pitch, pitch rate and the robot velocity respectively. Then, suitable weighting functions are selected in such a way that the minimisation of the cost function ensures the attainment of the control objectives. Once the problem is formulated, the LQR controller is obtained by solving an optimisation problem.

The Wheel-terrain contact angle is the scheduling variable assumed to be measured on line. In order to select the operating points the range of allowable wheel-terrain contact angle needs to be known. The range of allowable wheel-terrain contact angle on an uneven surface is based on the geometry of a robot IB and its clearance from the flat terrain surface (H). The maximum permitted inclination angle of terrain is computed using (3.4).

$$\alpha \leq \tan^{-1} \frac{H}{W} \tag{3.4}$$

where, $W =$ width of IB at base as shown in Figure 3-2. This range is divided into equal step size, 4 degrees, of discrete operating conditions. For each operating condition, a linearized model is extracted and controller gains are then determined by tuning the weighting matrices of LQR for the system running on respective operating condition. Other operating conditions are scheduled or interpolated linearly from known data of controller gains, resulting in a global compensator. A block diagram of GS controller is given in Figure 3-3.

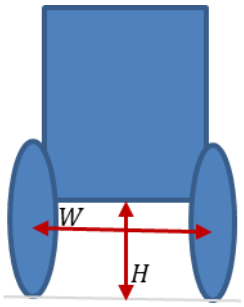

Figure 3-2: Illustration of clearance and width of a TWR.

3.2.2. Stability Analysis

Since the local designs at each operating point are based on linear approximations to the TWR system, the stability and performance can be guaranteed on each operating point. The overall gain scheduled system may not have these properties as the actual TWR system is nonlinear. To carry over these properties of robustness and performance to full GS we need to keep slow changes in scheduling variable and ensure that the scheduling variable captures nonlinearities of the plant. This will be concluded from computer simulations using MATLAB to check the stability of the gain-scheduled system considering the variation range and the variation rate of the time-varying parameter.

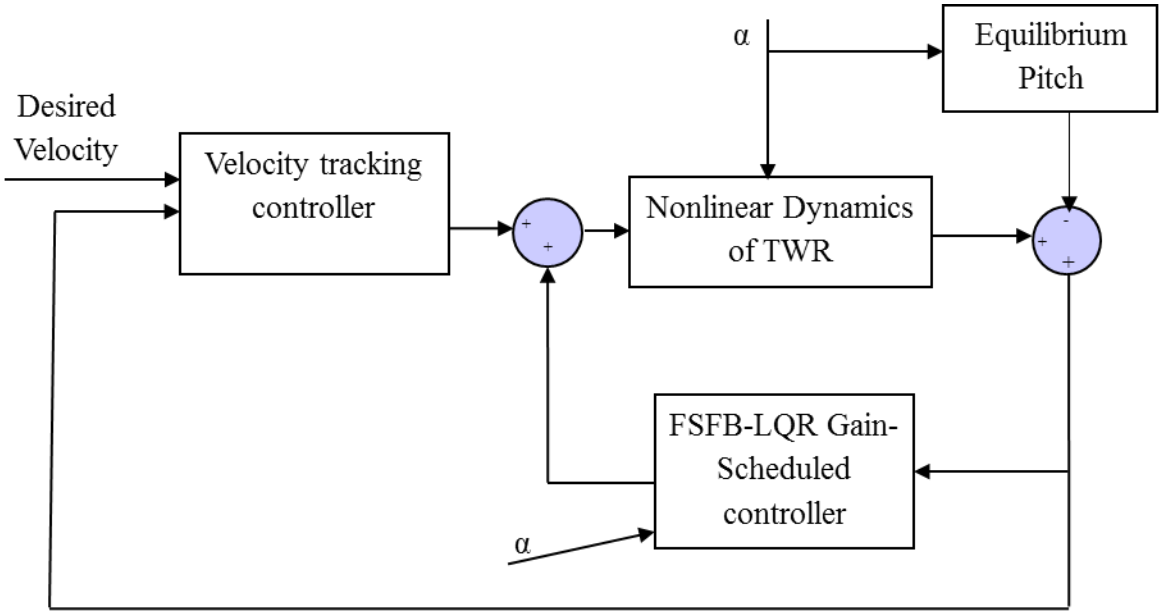

Figure 3-3: Gain scheduled controller - block diagram

3.2.3. Stability Region

The regions of the envelope of operating conditions, for which these controllers assure stability and desired performance of the local closed-loop systems, will be determined. The controller selection procedure has the advantage of simplicity in defining the controller family. This comes down to the definition of regions for which the members of the set of controllers are valid. However, discontinuities may appear in the control output or in the controller coefficients due to the switching speed which may result in chattering behaviour.

3.3. Lyapunov Function Based Controller Design

The dynamic models used for linear control design are only linearized approximations to the nonlinear plant. If these models are not an accurate reflection of the actual plant, then performance of the overall design cannot be guaranteed. This can be addressed in appropriate selection of the scheduled variable. This also depends on scheduling algorithm. The scheduling of controller gains is such that good performance may be expected for any fixed interpolated operating condition. A gain scheduling remains an *ad hoc* methodology because the gains were calculated selecting the weight matrix by hit and trial. Moreover, the robustness, performance, or even stability properties of a global gain scheduled controller are not addressed explicitly in the design process.

There is another important issue in linear controller design that involves the robustness and performance of the closed-loop system in the presence of disturbance or uncertainty. The

neglected plant dynamics or inaccurate knowledge of the value of physical parameters causes poor performance. A Lyapunov-based technique is therefore recommended (Apkarian & Gahinet 1995) to guarantee the stability and increased stability region. In this section of the chapter a Lyapunov function based controller design is presented in context to the background of stability for two wheeled robots.

3.3.1. Stability Background

Knowing the Lyapunov function of a system, we will be able to prove the asymptotic stability of the system (add equation numbers from modelling chapter) by checking the semi algebraic conditions on the closed loop dynamics. However, we will first explicitly define all of the terminology and prove the conditions that will later exploit to synthesise the Lyapunov function based controller.

3.3.2. Definitions

Definition 1 (Stability) *The system ($\dot{\boldsymbol{X}} = f(\boldsymbol{X})$) is stable about $\boldsymbol{X} = 0$ if for every $\in > 0$ there exists $\delta_{\in} > 0$ such that if $\|\boldsymbol{X}(0)\| < \delta_{\in}$, then $\|\boldsymbol{X}(0)\| < \in$ for all $t > 0$.*

Definition 2 (Asymptotic Stability) *The system ($\dot{\boldsymbol{X}} = f(\boldsymbol{X})$) is asymptotically stable about $\boldsymbol{X} = 0$ if it is stable about $\boldsymbol{X} = 0$ and, additionally, there exists $r > 0$ such that if $\|X(0)\| < r$, then as $t \to \infty, \boldsymbol{X}(t) \to 0$. Furthermore, if asymptotic stability does not hold for all initial states then the equilibrium point of system is called locally asymptotically stable.*

Definition 2 (Stability Region) *A set of all initial states of the system ($\dot{\boldsymbol{X}} = f(\boldsymbol{X})$) is called a stability region if the system trajectories starting from states within the ball converge to the origin.*

Definition 4 (Positive Definite Functions) *A scalar function $V(\boldsymbol{x})$ is defined as a positive definite function if it is continuous, has the property $V(0) = 0$ and in a ball of states $V(\boldsymbol{X}) > 0$ for all $\boldsymbol{X} \neq 0$.*

Definition 5 (Negative Definite Functions) *A function $V(\boldsymbol{x})$ is defined as a negative definite function if it is continuous, has the property $V(0) = 0$ and in a ball of states $V(\boldsymbol{x}) < 0$ for all $\boldsymbol{x} \neq 0$.*

Definition 7 (Lyapunov Functions) *A scalar function $V(\boldsymbol{x})$ defined on a region that is continuous, positive definite $V(\boldsymbol{x}) > 0$ for all $x \neq 0$, and has continuous first order partial derivative at every point of the region. The derivative of $V(\boldsymbol{x})$ with respect to the system $\dot{\boldsymbol{X}} = f(\boldsymbol{X})$ is defined as the dot product $V'(\boldsymbol{x}) = \nabla V(\boldsymbol{x}).f(\boldsymbol{x})$.*

Definition 6 (Control Lyapunov Functions) *A function for the system ($\dot{\boldsymbol{X}} = f(\boldsymbol{X})$) is called a control Lyapunov function $V(\boldsymbol{x})$ if for every fixed $\boldsymbol{x} \neq 0$ there exists a value v for the control such that $\nabla V(\boldsymbol{x}).f(\boldsymbol{x}, v) < 0$ or the derivative of the function can be made negative definite by the choice of control values.*

3.3.3. Theorems

We can state and prove the standard Lyapunov theorem for asymptotic stability with the above definitions.

Theorem 3.3 (Lyapunov) *The system ($\dot{\boldsymbol{X}} = f(\boldsymbol{X})$) is asymptotically stable about its equilibrium point if there exists a positive definite function $V(\boldsymbol{x}): \mathbb{R}^n \to \mathbb{R}$ such that $\dot{V}$ is negative definite.*

Remark 1 *If the system ($\dot{\boldsymbol{X}} = f(\boldsymbol{X})$) has equilibrium points away from $\boldsymbol{x}(\boldsymbol{t}) = 0$, then the system cannot be globally asymptotically stable.*

Theorem 3.4 (LaSall's Invariant Set Theorem) *Consider the system ($\dot{\boldsymbol{X}} = f(\boldsymbol{X})$), with $f(\boldsymbol{x})$ continuous, having V(**x**) (a scalar function) with continuous first partial derivatives, and that*

- *for some $r > 0$, the region Ω defined by $V(\boldsymbol{x}) < r$ is bounded*
- *$\dot{V}(\boldsymbol{x}) \leq 0$ for all x in Ω.*

Let **R** *be the set of all points within Ω where $\dot{V}(x) = 0$, and* **M** *be the largest invariant set in* **R**. *Then, every solution $\boldsymbol{x}(t)$ originating in Ω tends to* **M** *as $t \to \infty$.*

3.3.4. Selection of Lyapunov Function

The challenge of selecting a 'good' Lyapunov function is related to the maximization of the stability region where the negativity of the derivative of Lyapunov function is ensured. In order to select a 'good' Lyapunov function we shall estimate the stability region of the closed loop dynamics of a statically unstable TWMR for a controller. Stability region tells how far away from the equilibrium point a controller would be able to stabilize the system at different initial conditions of the system states. The Lyapunov direct method is used for the evaluation of stability region. The direct method of Lyapunov has been considered as clean and short method but for some systems it is not straight forward to find a Lyapunov function. Various methods proposed in literature for the construction of Lyapunov function are based on conventional [116, 117] and numerical [118, 119] approaches. For a complex system, excessive computer memory is required to implement conventional method. Numerical methods, therefore, have been applied in many applications [104, 132, 133] to avoid

computational problems. To devise a Lyapunov function for TWRs two Lyapunov function candidates have been considered to select one that gives less conservative stability region.

Quadratic Function

The quadratic Lyapunov function is expressed as (3.5)

$$\boldsymbol{V}(\boldsymbol{X}) = \boldsymbol{X}^T P \boldsymbol{X} \tag{3.5}$$

In (3.5) $\boldsymbol{X}$ is a state vector and P is a symmetrically scalar matrix. According to Lyapunov, indirect method the set of equations (3.6) must be satisfied for a system to be stable.

$$\left.\begin{aligned} V(X) &= X^T P X > 0 \\ \dot{V}(X) &= X^T P \dot{X} + \dot{X}^T P X = X^T (PJ + J^T P) X \\ &= -X^T Q X < 0 \\ -Q &= PJ + J^T P \\ Q^T &= Q \end{aligned}\right\} \tag{3.6}$$

A positive definite matrix Q is selected as an identity matrix and then solved the Lyapunov equation $PJ + J^T P = -I$ for P. The quadratic Lyapunov function established using P would be a positive definite scalar differentiable function as the evaluated P is a positive definite matrix. Using the quadratic formula given in (3.5) the Lyapunov function generated for the TWR motion on a horizontal terrain is is (3.7)

$$\begin{aligned} V_q(\boldsymbol{X}, \dot{\boldsymbol{X}}) = {} & 19.85\, x_1^2 + 0.70\, x_2^2 + 0.976\, x_3^2 + 7.735\, x_4^2 + 2(-0.5 x_1 x_2 - 0.686\, x_1 x_3 + \\ & 0.534\, x_1 x_4 + 0.534 x_3 x_2 - 1.39\, x_4 x_2 - 0.5 x_3 x_4) \end{aligned} \tag{3.7}$$

$\boldsymbol{X} = [x_1,\ x_2,\ x_3\ ,\ x_4]^T$ is the state vector of the system. The state x_1 is displacement error, x_2 is linear speed of robot, x_3 is pitch, and x_4 is pitch rate. The derivative of Lyapunov function is (3.8)

$$\begin{aligned} \dot{V}_q(\boldsymbol{X}, \dot{\boldsymbol{X}}) = {} & -(x_1 - 1.4 x_2 + 1.07 x_3 + 2.78 x_4)\ddot{x} - (2.78 x_2 + x_3 - 15.47 x_4 - 1.07 x_1)\ddot{\theta} - \\ & {x_2}^2 - {x_4}^2 + 39.7\, x_1 x_2 + 1.95\, x_3 x_4 - 1.37\, x_1 x_4 - 1.37\, x_2 x_3 \end{aligned} \tag{3.8}$$

All the states in (3.7) & (3.8) are function of control input and $\ddot{x}$ and $\ddot{\theta}$ are function of control input and states x_3 &x_4.

Energy Function

The Energy Lyapunov function is developed taking sum of kinetic and potential energies.

$$V_e = \left(\frac{1}{2} {x_2}^2 \left(m + \frac{I}{r^2}\right)\right) + \left(\frac{1}{2} {x_4}^2 \left(Ml^2 + I_p\right) + \frac{1}{2} M {x_2}^2 + Ml \cos(x_3)\, x_2 x_4\right)$$

The values of $m, M, l, r, I\ and\ I_p$ are given in Table 2.1. Using these parameter values and substituting $\boldsymbol{X} = [x_1,\ x_2,\ x_3\ ,\ x_4]^T$ the Lyapunov function candidate is expressed as below:

$$V_e(\boldsymbol{X}, \dot{\boldsymbol{X}}) = 26.5893\, {x_2}^2 + 0.2924\, {x_4}^2 + 1.032\, x_2 x_4 \cos(x_3) \quad (3.9)$$

The derivative of Energy Lyapunov Function is:

$$\dot{V}_e(\boldsymbol{X}, \dot{\boldsymbol{X}}) = [53.18x_2 + 1.03x_4 \cos(x_3)]\ddot{x} + [0.58x_4 + 1.03x_2 \cos(x_3)]\ddot{\theta} - x_2 {x_4}^2 \sin(x_3) \quad (3.10)$$

Stability region

The stability can be concluded without knowing the solutions of the system governing equations but simply looking at the values of Lyapunov functions and their derivative at different initial conditions. $V_e(\boldsymbol{X}, \dot{\boldsymbol{X}})$ or $V_q(\boldsymbol{X}, \dot{\boldsymbol{X}})$ represent energy of the TWR. This energy corresponds to the wheel and IB rotation that need to be stabilized. To assure stabilization, the functions $V_q(\boldsymbol{X}, \dot{\boldsymbol{X}})$ or $V_e(\boldsymbol{X}, \dot{\boldsymbol{X}})$ decreases along the closed loop system solution while satisfying the controller performance i.e. $V(\boldsymbol{X}(t), \dot{\boldsymbol{X}}(t))$ tend to be some constant value as $t \to \infty$ [134]. Similarly, $\dot{V}_e(\boldsymbol{X}, \dot{\boldsymbol{X}})$ or $\dot{V}_q(\boldsymbol{X}, \dot{\boldsymbol{X}})$ has to be negative along the closed loop system solution. As the function $V(\boldsymbol{X}, \dot{\boldsymbol{X}})$ was differentiable, the value of derivative of the function tend to zero as $t \to \infty$.

In order to determine the stability region and compare the results for different Lyapunov functions simulations were run using *MATLAB* and *Simulink*. The non-linear equations of motion are solved using the MATLAB ode45 solver. This solver integrates ODE's with specified initial conditions and variable step size. The proposition of Lyapunov direct method was considered to determine the stability region using Lyapunov function.

Since the problem is four dimensional, it is difficult to plot stability region for four states on a single plot. The initial conditions for two of the states, therefore, were considered at the time assuming remaining two states to have zero initial condition. The simulations for each of the given set of initial conditions were run for 5 seconds. The stability criterion was that the IB of TWMR is stabilized within 5 seconds with zero steady state error and with minimum possible overshoot. As the equations represent the dynamics of a statically unstable TWMR system, the stability region obtained from solving these equations has been considered the true region of attraction.

In order to verify the results based on numerical simulations, the stability regions were determined experimentally. The controller was implemented in real time using Simulink and xPC target toolboxes of MATLAB. The experiments were run as hardware-in-loop architecture. The experiments were run by operating the TWR at different sets of initial conditions of the states. The first test was run with zero initial condition of states i.e. the

platform was standing upright at origin. Then the platform operated at different initial pitch angles, 0 to 30^o, and observed whether the platform comes back to its initial position and stands upright, the stable state. The second test was started same as first but when the platform started moving at certain speed a step disturbance in pitch was given ensuring the platform was at origin with IB not rotating. At different speeds of platform disturbance up to 30^o was imparted to IB to test the stability of platform. The tests were repeated for variable initial pitch rates too. The next set of experiments was completed with the platform moving at different speeds initially and having IB rotating at different rates for each speed.

The plots in Figure 3-4 represent the variation of Lyapunov functions and derivative of Lyapunov functions of TWMR at a certain specific set of initial conditions. The set of initial conditions used in this representative plot consisted of Pitch rate (x_4) = 0; Linear displacement (x_1) = 0; Linear velocity (x_2) = 0; Pitch (x_3) = 30 degrees. Energy Lyapunov function resulted with smaller initial value as compared to the initial value of quadratic Lyapunov function. Lyapunov function represents physically the energy thus this result means that the same task has been realized with smaller energy consumption for Energy Lyapunov function as compared to very large initial energy consumption for Quadratic Lyapunov function. The function also tends to zero faster and with slightly smaller oscillations for Energy Lyapunov function in comparison with Quadratic Lyapunov function.

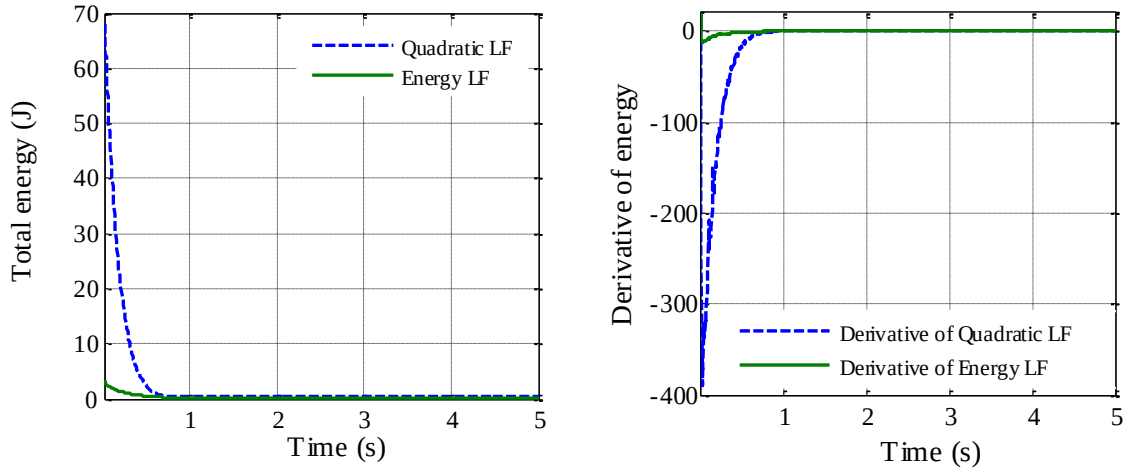

(a) (b)

Figure 3-4: Comparison of (a) Lyapunov functions (b) derivatives of Lyapunov functions

The simulation results of stability regions, projected to x1~x2 phase plane with x3=x4=0 , x3~x4 phase plane with x1=x2=0, x2~x3 phase plane with x1=x4=0 and x2~x4 phase plane with x1=x3=0, as well as the experimental results are plotted as shown in Figure 3-5. The

regions of stability have been plotted along the simulated stability regions as shaded areas. Figure 3-5(a) shows the estimates of stability region for pitch and speed using the Lyapunov functions and ordinary differential equation solver. Figure 3-5(b) shows three estimates of stability regions for pitch and pitch rate. Figure 3-5(c) shows three estimates of stability regions for pitch rate and speed. Figure 3-5(d) shows three estimates of stability regions for speed and displacement.

Conclusion

The stability region boundaries resulted from the Energy Lyapunov function and Quadratic Lyapunov function are compared to the true stability region. The true stability region is the one obtained solving the dynamic equations of motion of the TWR. The larger stability region resulted is from the Energy Lyapunov function. The experimental region of stability of the TWR is wider than the one resulted from Quadratic Lyapunov function but is within the boundary of stability region determined using Energy Lyapunov function.

In simulations, therefore, the Energy Lyapunov function resulted to be a 'good' Lyapunov function, less conservative and closer to the true stability region for TWRs. Although the experimental results do not give the full region of stability due to practical constraints on robot parameter variations and ignorance of noise and delay in sensors, the present results still confirm the outcome of simulation results. In conclusion, the Energy Lyapunov function will be used for comparison of the performance of different controllers proposed for the robot and to visualize its safe region of operation. The proposed Lyapunov function will also provide the infrastructure for design of Lyapunov-based nonlinear robust controllers.

3.3.5. Controller Synthesis

A control algorithm based on Lyapunov theory is synthesized in this section to ensure the local asymptotic stability with large computable stability region. In order to synthesize Lyapunov based controller the system equations are transformed into an affine form that is

$$\dot{\boldsymbol{X}} = \boldsymbol{f}(\boldsymbol{X}) + \boldsymbol{g}(\boldsymbol{X})\boldsymbol{u}. \tag{3.11}$$

The affine form of equations makes the controller design easy. In order to transform the TWR system equations in the affine form, normalization and partial feedback linearization is proposed in this study. In the following part of this chapter, the equations of motion of the TWR (2.26 & 2.27) are simplified, partially feedback linearized and controller synthesized

for the robot motion on an uneven terrain. The controller will be flexible enough to use for inclined and horizontal terrain.

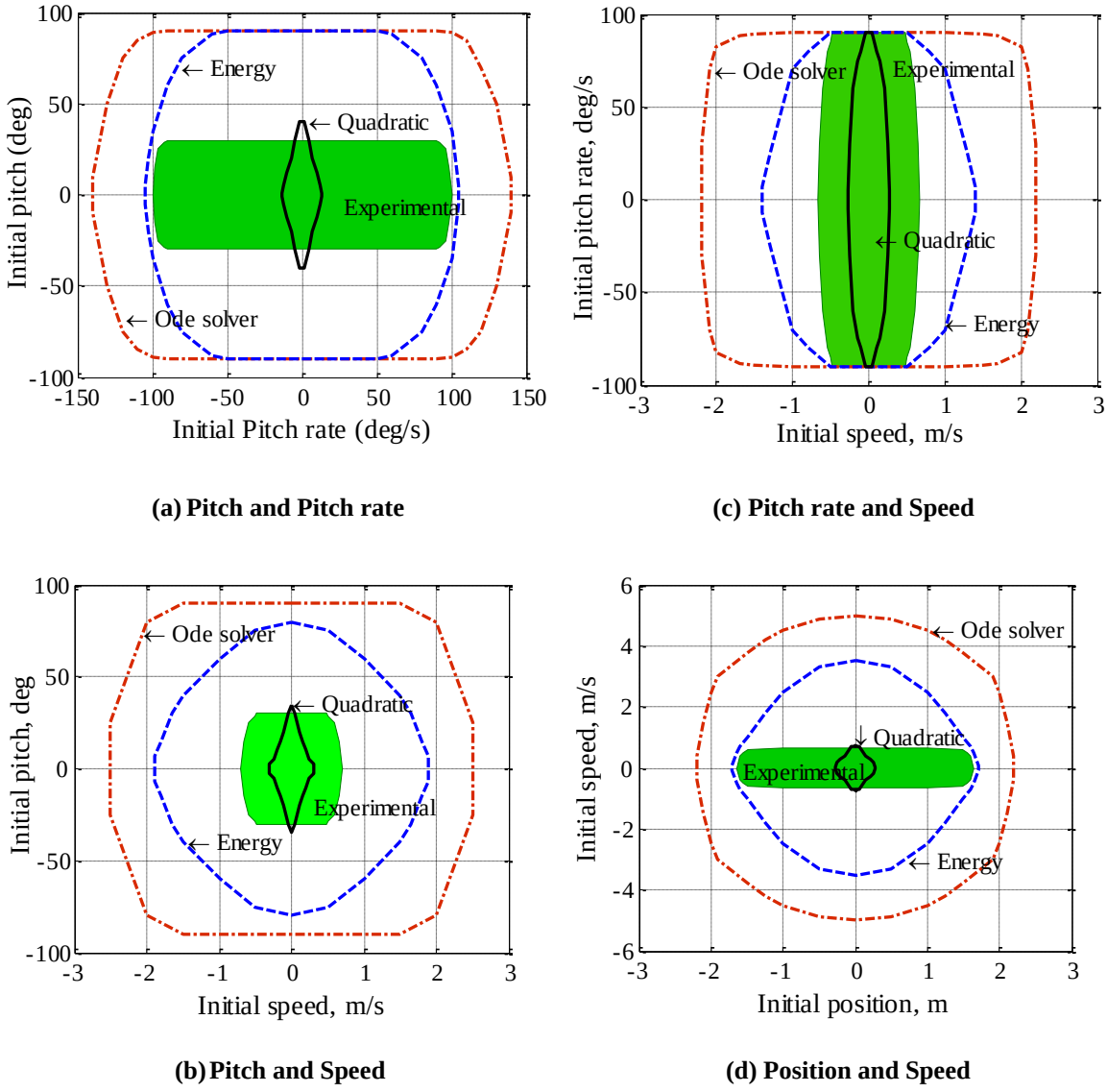

(a) Pitch and Pitch rate

(c) Pitch rate and Speed

(b) Pitch and Speed

(d) Position and Speed

Figure 3-5: Stability regions of initial states of a TWMR based on ode solver, quadratic Lyapunov function, Energy based Lyapunov function techniques and experimental results.

Dynamic model for robot motion on uneven terrain

The equations of motion representing the dynamics of the two wheeled robot with kinematic constraint of no-slip and moving on an uneven terrain are given in chapter 2 as (2.26) and (2.27). These are the equations of motion of the TWR written in terms of wheel-terrain contact

angle. Wheel-terrain contact angle is the parameter we are using for measurement of terrain inclination and uneveness.

Model simplification

Equations (2.26) and (2.27) are simplified and normalized following the approach used in [15]. To achieve normalization, the following scaling transformations are introduced:

$$q = \frac{x}{l}\ ; \qquad \dot{x} = l\dot{q}; \qquad \ddot{x} = l\ddot{q}; \qquad \delta = \frac{m}{M}\ ; \qquad a_1 = \frac{I_p}{Ml^2}\ ; \qquad a_2 = \frac{I}{Mr^2}$$

Substitution of normalizing factors gives:

$$A_1\ddot{q} + (1 + a_1)\ddot{\theta} - \sin\theta - \partial\cos(\theta - \alpha)\ddot{\alpha} + \partial\sin(\theta + \alpha)\dot{\alpha}^2 \ - l_1 \sin\theta \frac{\dot{\alpha}\,\dot{q}^2}{(\cos\alpha)^2} = 0 \quad (3.12)$$

$$A_2\ddot{q} + \cos(\theta + \alpha)\,\ddot{\theta} - (1 + \delta)\sin\alpha \ - l_1\,(1 + \delta)\ \sin\alpha \frac{\dot{\alpha}\,\dot{q}^2}{(\cos\alpha)^2} - \sin(\theta - \alpha)\dot{\theta}^2 +$$
$$\partial\,(1 + \delta)[\cos(2\alpha)\ddot{\alpha} + \sin(2\alpha)\,\dot{\alpha}^2] = u \quad (3.13)$$

where, $\partial = \frac{r}{l}$; $A_1 = \sin\theta\tan\alpha + \cos\theta$; $A_2 = \frac{1+\delta}{\cos\alpha} + a_2$; $u = \frac{T}{Mlr}$.

Partial feedback linearization of the model

The above simplified equations still have strong inertial coupling and the outputs (pitch and displacement) are collocated with the input u making input/output linearization difficult. The simplified system is therefore partially feedback linearized. We manipulate the equation (3.12) to solve for $\ddot{\theta}$ and substitute the result in equation (3.13). Using some standard calculus we have written the new control variable, u.

A general set of equations can be written in the form, following [135] :

$$M_{11}\ddot{q_1} + M_{12}\ddot{q_2} + h_1 + \emptyset_1 = 0 \quad (3.14)$$

$$M_{21}\ddot{q_1} + M_{22}\ddot{q_2} + h_2 + \emptyset_2 = \mathbf{T} \quad (3.15)$$

where,

$q_1 = \theta;$ $q_2 = q\ ;$ $M_{11}\ ,\ M_{12}\ ,\ M_{21}\ ,\ M_{22}$ are inertia matrix terms,

$h_1\ , h_2$ are the centrifugal or coriolis accelerations, and

$\emptyset_1$, $\emptyset_2$ are gravitational terms.

This form of equations resembles to the TWR system. In TWR systems the elements of the inertia, coriolis and gravitational matrices are:

$$M_{11} = 1 + a_1$$

$$M_{12} = A_1 = \sin\theta \tan\alpha + \cos\theta$$

$$M_{21} = \cos(\theta + \alpha)$$

$$M_{22} = A_2 = \frac{1+\delta}{\cos\alpha} + a_2$$

$$\mathbf{T} = \mathrm{u}$$

$$\emptyset_1 = -\sin\theta$$

$$\emptyset_2 = -(1+\delta)\sin\alpha$$

$$h_1 = -\partial\cos(\theta-\alpha)\ddot{\alpha} + \partial\sin(\theta+\alpha)\dot{\alpha}^2 - l_1 \sin\theta \frac{\dot{\alpha}\,\dot{q}^2}{(\cos\alpha)^2}$$

$$h_2 = -l_1(1+\delta)\sin\alpha \frac{\dot{\alpha}\,\dot{q}^2}{(\cos\alpha)^2} - \sin(\theta-\alpha)\dot{\theta}^2 + \partial(1+\delta)[\cos(2\alpha)\ddot{\alpha} + \sin(2\alpha)\dot{\alpha}^2]$$

We can write the new input, u [135] as:

$$u = \overline{M_{22}}v + \overline{h_2} + \overline{\emptyset_2}$$

Where,

$$\overline{M_{22}} = M_{22} - \frac{M_{12}.M_{21}}{M_{11}}$$

$$\overline{h_2} = h_2 - \frac{M_{21}}{M_{11}}h_1$$

$$\overline{\emptyset_2} = \emptyset_2 - \frac{M_{21}}{M_{11}}\emptyset_1$$

For the TWR:

$$\overline{M_{22}} = A_2 - \frac{A_1.\cos(\theta+\alpha)}{1+a_1}$$

$$\overline{h_2} = -l_1(1+\delta)\sin\alpha \frac{\dot{\alpha}\,\dot{q}^2}{(\cos\alpha)^2} - \sin(\theta-\alpha)\dot{\theta}^2 + \partial(1+\delta)[\cos(2\alpha)\ddot{\alpha} + \sin(2\alpha)\dot{\alpha}^2] -$$
$$\frac{\cos(\theta+\alpha)}{1+a_1}\left[-\partial\cos(\theta-\alpha)\ddot{\alpha} + \partial\sin(\theta+\alpha)\dot{\alpha}^2 - l_1\sin\theta\frac{\dot{\alpha}\,\dot{q}^2}{(\cos\alpha)^2}\right]$$

$$\overline{\emptyset_2} = -(1+\delta)\sin\alpha + \frac{\cos(\theta+\alpha)}{1+a_1}.\sin\theta$$

Hence,

$$u = v\left[A_2 - \frac{A_1.\cos(\theta+\alpha)}{1+a_1}\right] + \left[\frac{\cos(\theta+\alpha)}{1+a_1}.\sin\theta - (1+\delta)\sin\alpha\right] + \left[-l_1(1+\delta)\sin\alpha\frac{\dot{\alpha}\,\dot{q}^2}{(\cos\alpha)^2} -\right.$$
$$\left.\sin(\theta-\alpha)\dot{\theta}^2 + \partial(1+\delta)[\cos(2\alpha)\ddot{\alpha} + \sin(2\alpha)\dot{\alpha}^2] - \frac{\cos(\theta+\alpha)}{1+a_1}\left[-\partial\cos(\theta-\alpha)\ddot{\alpha} +\right.\right.$$

$$\partial \sin(\theta + \alpha)\dot{\alpha}^2 \; - l_1 \sin\theta \frac{\dot{\alpha}\,\dot{q}^2}{(\cos\alpha)^2}\Big]\Big] \tag{3.16}$$

This partial feedback linearized control input of the robot, *u*, can be computed from (3.16) given the input *v*, an additional control input yet to be defined. The feedback system equivalent to the normalized system of dynamic equations with new control input v is as following:

$$\ddot{q} = v \tag{3.17}$$

$$\ddot{\theta} = \frac{[-\emptyset_1 - v.A_1 - h_1]}{1+a_1} \tag{3.18}$$

We see the input/output system from v to q in (3.17) is linear and second order. The equation (3.18) therefore represents the internal dynamics of the TWR. This set of equations can be expressed now in the affine form (3.11). If $v = 0$ and $\theta \, \epsilon \, [0, 2\pi]$, the system has two equilibrium points. One is a stable equilibrium point as $\boldsymbol{X} = (0, \pi, 0)$ and the second is an unstable equilibrium point as $\boldsymbol{X} = (0, 0, 0)$.

Controller synthesis for motion on uneven terrain

In this section Lyapunov functions for two and three states are proposed and developed separately to make the controller flexible. Then the controller based on the developed Lyapunov function is synthesised for the partially linearized system. The objective of control synthesis is to stabilize the IB at its unstable equilibrium point and track the robot velocity.

(a) Lyapunov function and its derivative to control pitch and pitch rate (θ and $\dot{\theta}$)

The affine form of the TWR system equations has four integrators $\dot{\theta} = \int \ddot{\theta}$, $\theta = \int \dot{\theta}$, $\dot{q} = \int \ddot{q}$, $q = \int \dot{q}$. A constraint function proposed and used to devise a Lyapunov function for the IB is:

$$[k_1 cos^2(e_\theta) - l] \tag{3.19}$$

where $k_1$is a positive constant;

$e_\theta = \theta_d - \theta$ such that θ_d =desired equilibrium pitch and θ is actual pitch.

The constraint function bounds the pitch θ of the IB. This function is positive unless

$k_1 cos^2(e_\theta) - l = 0$. This produces a constraint on the system that θ should be less than $\left(\left[cos^{-1}\left(\sqrt{\frac{l}{k_1}}\right)\right]\right)$. The constrained pitch will be denoted as $\tilde{\theta}$ in rest of the document.

A Lyapunov function, originated from the energy equation of the IB of the TWR and based on the constraint function (3.) is proposed in the following equation (3.20):

$$V_0(e_\theta, \dot{e_\theta}) = \frac{1}{2}[k_1 cos^2(e_\theta) - l]\dot{e_\theta}^2 + l.[1 - cos(e_\theta)] \quad (3.20)$$

where, l is the height of the center of mass of the IB and has a positive value. This function represents two states of the TWR, pitch and pitch rate. Both the states relate to the IB. Therefore this function is used to synthesize the controller for pitch and pitch rate of the TWR. The proposed Lyapunov function (3.20) is, therefore, positive definite for:

(i) $k_1 > l$, because $V_0(e_\theta, \dot{e_\theta})$ is a locally convex function with a minimum at the origin if $k_1 > l$. k_1 is a constant that controls the boundary of initial pitch as well as performance of the controller.

(ii) $|\theta| < \tilde{\theta}$.

The time derivative of Lyapunov function is :

$$\dot{V}_0 = \dot{e_\theta}\, cos(e_\theta)\left[k_1 cos(e_\theta) - \frac{l}{cos(e_\theta)}\right]\ddot{e}_\theta - \left[k_1 \sin(e_\theta)\, \dot{e_\theta}^2 - l \tan(e_\theta)\right]$$

where

$$\ddot{e_\theta} = \ddot{\theta_d} - \ddot{\theta}$$

Substitute (3.18) for $\ddot{\theta}$ in $\dot{V}_0$and replacing corresponding expressions for $A_1, \emptyset_1, h_1$:

$$\dot{V}_0 = \dot{e_\theta} cos(e_\theta)\left[v\gamma(\theta, \alpha) + k_1\beta\left(\theta, \dot{\theta}, \alpha, \dot{\alpha}, \ddot{\alpha}\right) - \frac{l}{cos(e_\theta)}\left(\ddot{\theta_d} - \sin(e_\theta) + \frac{\emptyset_1 + h_1}{1+a_1}\right)\right] \quad (3.21)$$

where,

$$\gamma = \frac{A_1}{(1+a_1)cos(e_\theta)}[\, k_1 cos^2(e_\theta) - l] \quad (3.22)$$

$$\beta = cos(e_\theta)\left[\ddot{\theta_d} + \frac{\emptyset_1 + h_1}{1+a_1} - sin(e_\theta)\dot{e_\theta}^2\right] \quad (3.23)$$

In order to derive a control law for two states (pitch and pitch rate) control only, we can find an expression for v which makes $\dot{V}_0 \leq 0$, semi negative definite, and it converges $\theta, \dot{\theta}$ asymptotically to zero.

(b) Lyapunov function and its derivative to control pitch, pitch rate and velocity ($\theta, \dot{\theta}$ and $\dot{q}$)

To control the robot velocity as well as pitch and pitch rate, a quadratic term is added to the Lyapunov function constructed in the previous section such that the time derivative of the additional term has the same structure as the equation of derivative of Lyapunov function (3.23).

New Lyapunov function is, therefore, proposed as (3.24):

$$V_1 = k_d\, V_0(\theta, \dot{\theta}) + \frac{1}{2} W^2 \tag{3.24}$$

W is an unknown variable. The time derivative of this variable is a function of $\theta, \dot{\theta}$ and $\dot{q}$ and has the same structure as $\dot{V}_0$. This is written as following:

$$\dot{W}(\theta, \dot{\theta}, \dot{q}) \dot{e_\theta} cos(e_\theta) = \dot{V}_0(\theta, \dot{\theta}) \tag{3.25}$$

Integration of (3.25) and substitution of (3.21) gives:

$$W(\theta, \dot{\theta}, \dot{q}) = \frac{A_1 + 1 + a_1[k_1 \cos(e_\theta) \dot{e_\theta}]}{1 + a_1} - \frac{l A_1 \dot{e_q}}{(1 + a_1)\cos(e_\theta)}$$

Where $e_q = q_d - q$ and $\dot{e_q} = \dot{q_d} - \dot{q}$ such that q_d = desired velocity ; q = actual velocity.

The variable W must also satisfy

$$\dot{W}(\theta, \dot{\theta}, \dot{q}) = \dot{\theta} \frac{\partial W}{\partial \theta} + \sin\theta \frac{\partial W}{\partial \dot{\theta}} + \left(\frac{\partial W}{\partial \dot{q}} - \cos\theta \frac{\partial W}{\partial \dot{\theta}}\right) v \tag{3.26}$$

Time derivative of the Lyapunov function V_1 (3.24) is:

$$\dot{V}_1 = k_d \dot{V}_0\,(\theta, \dot{\theta}) + W\dot{W}$$

Substituting (3.21), (3.25), (3.26) for $\dot{V}_0$ W and $\dot{W}$ gives:

$$\dot{V}_1 = \left(v\gamma + k_1\beta - \frac{l}{\cos(e_\theta)}\left(\ddot{\theta_d} - \sin e_\theta + \frac{\emptyset_1 + h_1}{1 + a_1}\right)\right)\zeta \tag{3.27}$$

Where γ and β are given in (3.22) and (3.23) and ζ is as following:

$$\zeta = \dot{e_\theta} \cos e_\theta \left[k_d + \frac{k_1 A_1}{1+a_1} + \frac{k_1 e_\theta \cos e_\theta}{2}\right] - \frac{\mathrm{l} A_1 e_{\dot{q}}}{(1+a_1)\cos e_\theta} \tag{3.28}$$

(c) Control Law

A Lyapunov function based control law is developed finding an expression for the control input v which produces negative derivative of the Lyapunov function.

In order to make $\dot{V}_1 \leq 0$, semi negative definite Let,

$$k_1\beta + v\gamma - \frac{l}{\cos(e_\theta)}\left(\ddot{\theta_d} - \sin e_\theta + \frac{\emptyset_1 + h_1}{1+a_1}\right) = -\zeta$$

$$v = \frac{-\zeta - k_1\beta + \frac{l}{\cos(e_\theta)}\left(\ddot{\theta_d} - \sin e_\theta + \frac{\emptyset_1 + h_1}{1+a_1}\right)}{\gamma}$$

$$v = \frac{-1}{\gamma(\theta)}\left(\zeta + k_1\beta(\theta, \dot{\theta}, \dot{q}) + \frac{l}{\cos(e_\theta)}\left(\ddot{\theta_d} - \sin e_\theta + \frac{\emptyset_1 + h_1}{1+a_1}\right)\right) \tag{3.29}$$

This control law gives:

$$\dot{V}_1 = -\zeta^2$$

which converges $e_\theta, \dot{e_\theta}$ and $\dot{q}$ asymptotically to zero.

(d) ***Controller constraints***

i. $\tilde{\theta} = \cos^{-1}\left(\sqrt{\frac{l}{k_1}}\right) < \frac{\pi}{2}$ is the constrain function or nonlinear perturbation bounded by square of the state θ.

ii. $k_1 > l$ because value of k_1 less than l will not fulfil the constraint function as the value of cos θ more than l is invalid.

iii. $k_d > 0$

iv. $\tilde{\theta} > |\theta|$ and $\gamma < 1$ for all times.

The controller synthesized for an uneven terrain can be used for inclined and horizontal terrain. For an inclined terrain one might need to replace $\dot{\alpha} = \ddot{\alpha} = 0$ in simplified and normalized set of equations of motion, in partial feedback linearized system, in control law as well as in control constraints. The same can be implemented for a horizontal terrain replacing

$\alpha = 0$ in addition to $\dot{\alpha} = \ddot{\alpha} = 0$. The overall control algorithm based on the Lyapunov function is shown in Figure 3-6.

3.3.6. Stability Analysis

Stability of the proposed controller is analyzed in chapter 4-6 by obtaining if Lyapunov function V_0 becomes locally convex function with a minimum at origin for $k_1 > l$, a constraint of the controller. This is checked by plotting level curves. For other constraints a set is defined and determine whether it is a compact set and for what initial conditions. Semi negative definiteness of the derivative of the Lyapunov function is concluded as the controller was developed with this assumption. We then apply LaSall's theorem to prove the asymptotic stability of the equilibrium point of the TWR. LaSall's theorem defines that if every solution starting in the defined compact set approaches the largest invariant set as time approaches to infinity then the asymptotic stability is guaranteed.

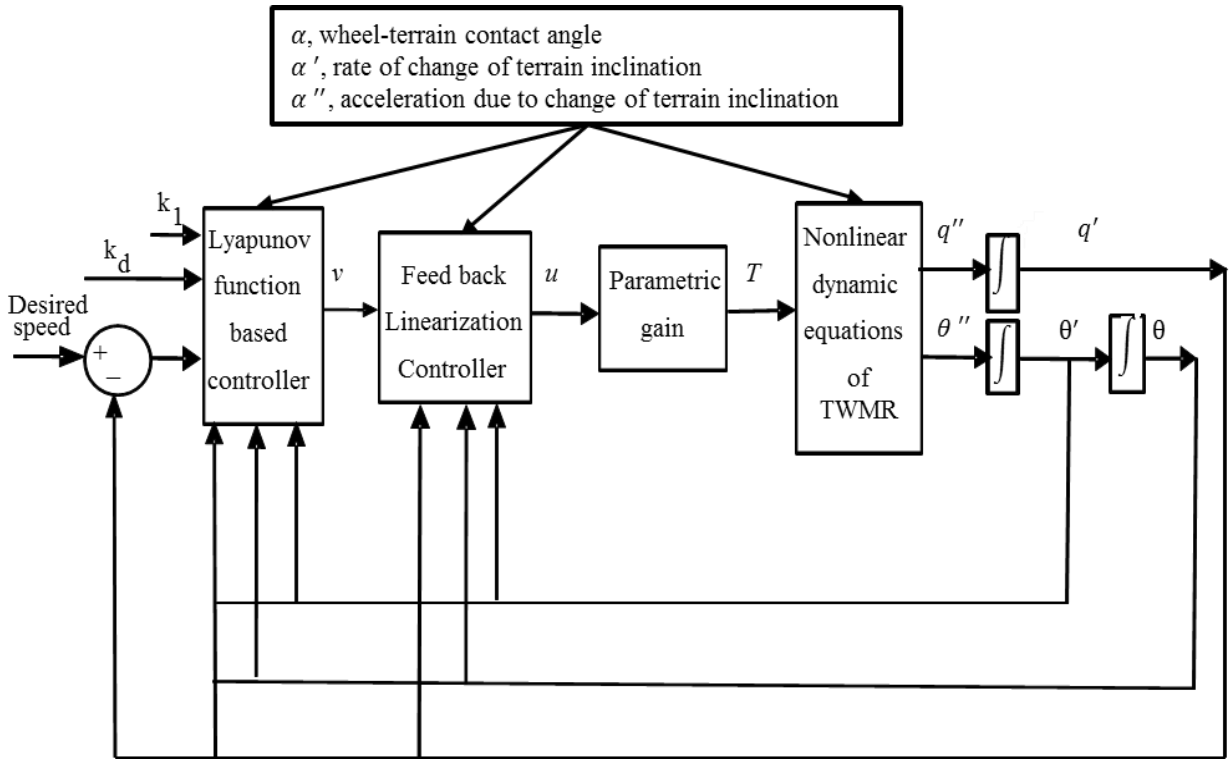

Figure 3-6: Lyapunov function based nonlinear controller - block diagram

3.3.7. Stability Region

A region of attraction of the TWR with proposed Lyapunov function based controller can be computed from the defined compact set. We shall compute the condition that avoid singularity and belong to the neighbourhood of the origin.

3.4. Performance Quantification

One of the key requirements for statically unstable two wheeled mobile robots is to dynamically stablize the intermediate body. This can be achieved by minimizing an error to the equilibrium position and velocity tracking. An autonomous navigation of the robot demands a distance covered in minimum time. Another important issue in battery operated mobile robots is power consumption required to complete the tasks. With minimum energy consumption, the battery usage can be improved. In this research three types of controllers are tested in simulation to understand their limits and feasibility. Later, they are implemented on a physical hardware to investigate their practical applications. Major objectives for their performance quantification are following:

i. To prevent the intermediate body from fall. This should be valid at different terrain angles
ii. To complete given distance in minimum time
iii. Low energy consumption
iv. Maximum region of attraction / stability region

These performance metrics are proposed to meaningfully quantify the performance of the system on different types of terrain. A cost function is assigned to each of the first three objectives in the above list as described below. The stability region will be computed or simulated as per methods described in sections 3.2.3 and 3.3.5.

A TWR is defined to be in a stable steady state posture when the center of mass of the IB lies above the contact point of its wheels with the terrain. A function related to prevent fall of intermediate body while traversing on a terrain is expressed as an Integrated Squared Error (ISE) as shown in (3.30).

$$ISE = \int_{t_0}^{t_f} (\theta_c - \theta_e)^2 dt \tag{3.30}$$

θ_c is the current pitch angle and θ_e is the desired equilibrium pitch angle. The desired pitch angle is a function of wheel-terrain contact angle, computed at steady state as (2.19):

A total time taken by the robot to traverse over a given path to complete a given distance, in simulation or experiments, is given as (3.31):

$$C_t = t_f - t_0 \tag{3.31}$$

t_f is the final or travel completion time and t_0 is the initial or travel starting time.

The energy consumption, neglecting mechanical and electrical losses in motors, is computed as (3.32):

$$C_e = \int_{t_0}^{t_f} T.\omega.dt \tag{3.32}$$

C_e is the integrated mechanical power over the simulation or physical travel time to represent the total energy consumed by the robot. T is the torque supplied by both the motors and ω is an angular velocity of each drive wheel.

.

Chapter 4. Control of a Two-Wheeled Robot on Horizontal Terrain

Stability control of two wheeled mobile robots on smooth horizontal terrain is important for their applications in plane areas. A plane area is a flat or relatively very low relief land; a flat footpath, smooth roads and industrial or commercial indoor workspaces are the environments where two wheeled robots can be used. This chapter presents two control schemes which allow a two wheeled mobile robot to stabilize its intermediate body and track the desired velocity of the robot. One of the control schemes is based on linear approximation of the TWR plant dynamics and the other is nonlinear controller. An optimal full state feedback controller, developed in the previous chapter, was implemented in simulation for a TWR. The results show that the TWR is able to regulate the pitch and pitch rate as well as track the desired velocity. This can be performed at equilibrium and neighbourhood which gave very small stability region. To increase the stability region a Lyapunov function based nonlinear controller was developed. The simulation results of the nonlinear controller demonstrate the advantage it has over the linear controller in stabilization and the stability region.

4.1. Baseline Controller

The objective of a baseline controller design is to stabilise the balance of IB of a TWR with a zero pitch rate and track the desired robot velocity on a horizontal terrain. The baseline controller is a linear full state feedback controller (FSFBC) designed using linear quadratic regulator (LQR). The LQR based FSFB control method involves realizing the control law that drives the states of the system as fast as possible at the lowest control torque possible whilst finding the closed loop gain matrix K that minimizes the performance index. An important attribute of the linear quadratic regulator is that it finds the best compromise between the speed and the control torque. This ensures that actuator saturation does not happen and the IB is not driven out of the region where the linear approximation of the system holds. For the robot system, too much control torque might tilt the IB too far to return it back to the equilibrium position. The weightings in the performance index setup by a trade-off between response speed and the control effort are, therefore, adjusted by the user as required. In order to gain more response speed, small weighting of the state variables is

recommended and for small control effort high weighting of the control variables is recommended.

4.1.1. Controller formulation

The objective of linear control design is to find controller parameters that stabilize the upright position and follow the desired velocity, minimizing the performance criteria. This FSFB controller is designed based on the assumption that all the states are available for feedback. We used MATLAB and SIMULINK to evaluate these controller parameters. A block diagram of the closed loop control system is shown in Figure 4-1. This implements the control law (3.3):

$$u = -K_x \boldsymbol{X} - K_r e_r$$

In this control law, FSFB gain matrix K_x and the velocity reference tracking gain K_r were tuned using MATLAB. As mentioned in the previous chapter, LQR work out the best closed loop pole locations satisfying the performance index presented in section 3.4. To design a linear quadratic regulator, a MATLAB control system tool box command 'lqr' is used. This command applies LQR method to find the controller gains, minimizing the performance index using the optimal cost function. With this command, selection of appropriate Q and R weighting matrices is the main task to perform. These matrices are set up so that only their diagonal elements are nonzero and nonnegative, following the condition that these matrices should be positive semi definite. As a starting point both the matrices were set up as identity matrix giving same weight to both state and input variables. R matrix reduces to a constant because there is only one input. On calling the 'lqr' command with the linear plant model and weighting matrices as input arguments, command computes the gain matrix K which is split into two separate gain matrices as K_x and K_r . After calculating the input torque the performance of the controller is evaluated and the controller gains are finalized by tuning in nonlinear plant simulations.

4.1.2. Performance Evaluation

Simulation tests were conducted to evaluate the performance of the controller in the closed loop system. The performance was measured as transient response, integrated squared error of pitch (ISE), velocity tracking and torque demanded. These metrics were to accomplish the tasks related to balancing the IB at upright position and follow the desired velocity on a flat horizontal terrain. The physical parameters of the system given in the Table 1 were used for

all experiments. These parameters represent a real-time two-wheeled robotic platform system. The tests were performed in different scenarios with different conditions to obtain confidence that the designed controller can be used on a flat horizontal terrain and also to work out the limitations of the design, if any.

The experiment is conducted in simulation to observe the controller output and transient response of the TWR such that the controller is designed for a settling time of less than 10 seconds. The initial conditions of all the states were zero except for pitch. The experiment was repeated three times for three different initial values of pitch: 5, 10 and 85 degrees. The last initial pitch angle is a pitch angle close to the boundary of upper half of the IB. Figure 4-1 shows the results of the experiments: transient behaviour of pitch and pitch rate, integrated squared error of pitch and control demand of the robot motion on a horizontal terrain in x-direction.

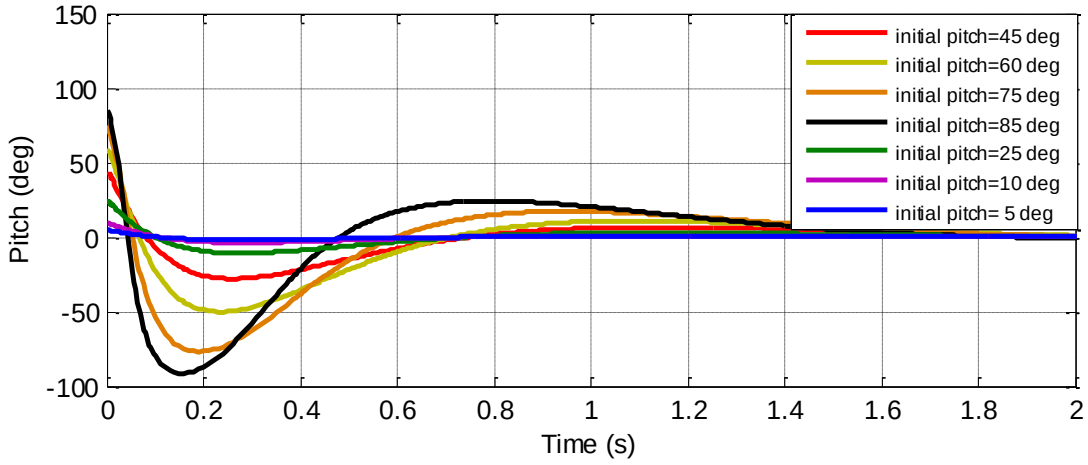

(a)

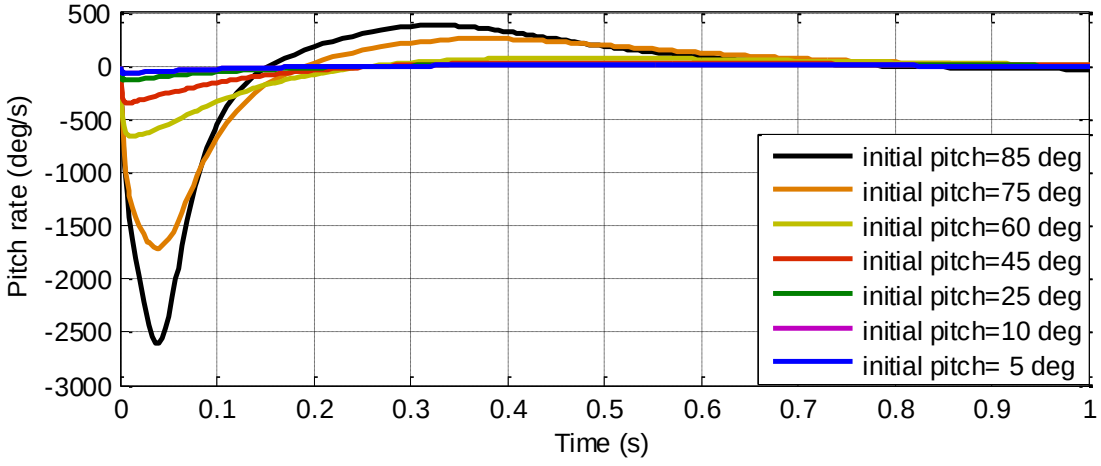

(b)

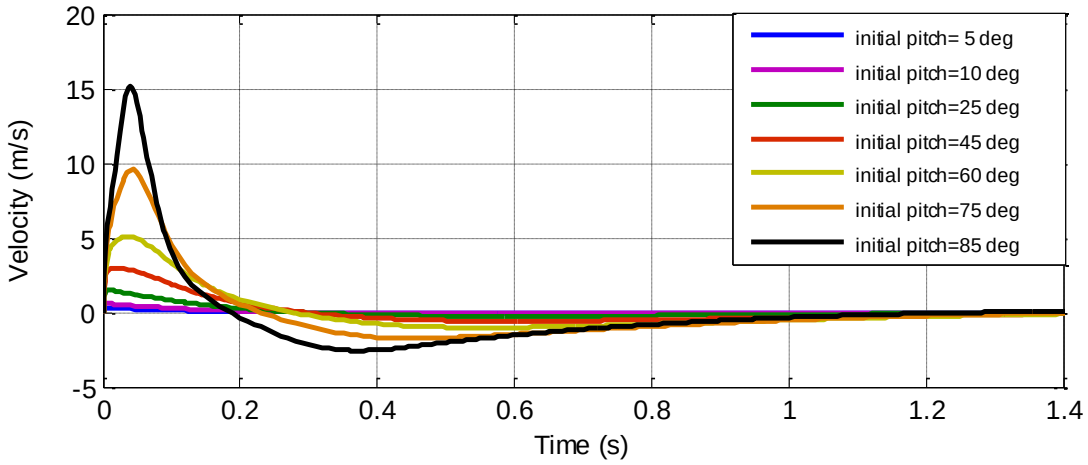
Velocity (m/s)
Time (s)
initial pitch= 5 deg
initial pitch=10 deg
initial pitch=25 deg
initial pitch=45 deg
initial pitch=60 deg
initial pitch=75 deg
initial pitch=85 deg

(c)

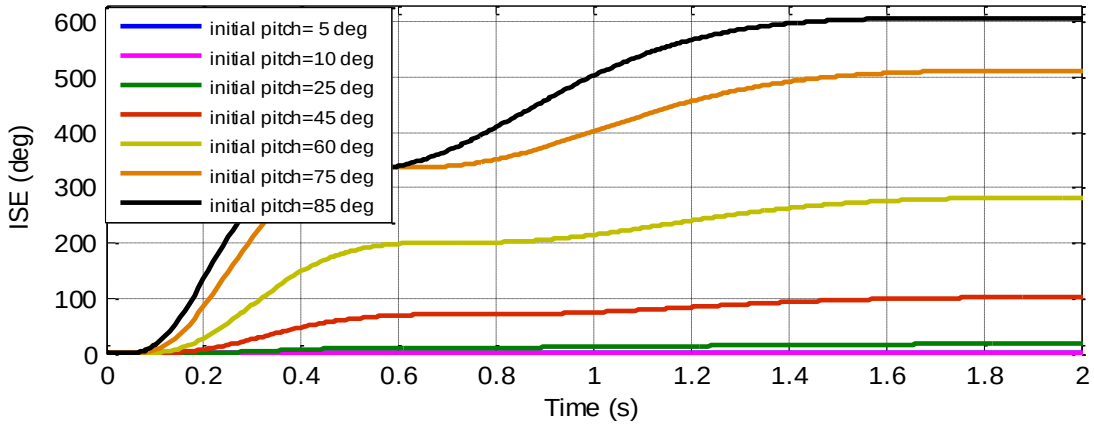
ISE (deg)
Time (s)
initial pitch= 5 deg
initial pitch=10 deg
initial pitch=25 deg
initial pitch=45 deg
initial pitch=60 deg
initial pitch=75 deg
initial pitch=85 deg

(d)

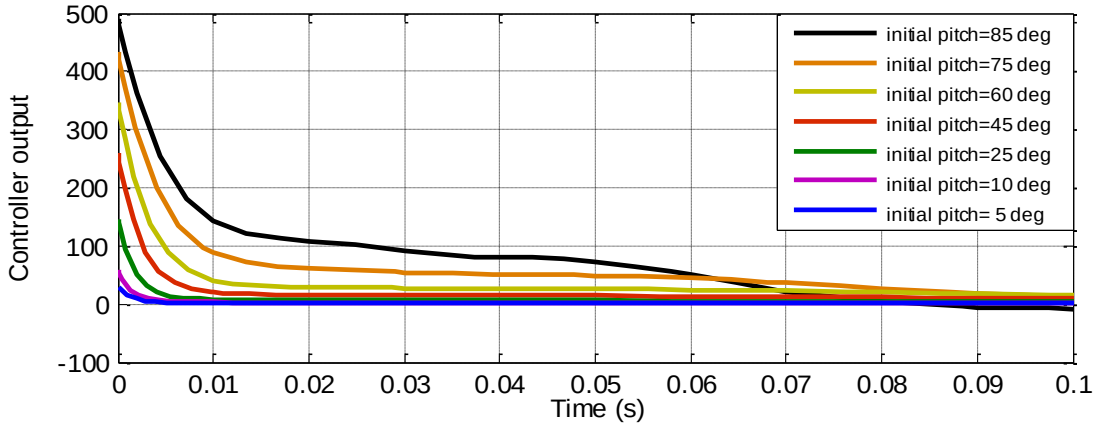
Controller output
Time (s)
initial pitch=85 deg
initial pitch=75 deg
initial pitch=60 deg
initial pitch=45 deg
initial pitch=25 deg
initial pitch=10 deg
initial pitch= 5 deg

(e)

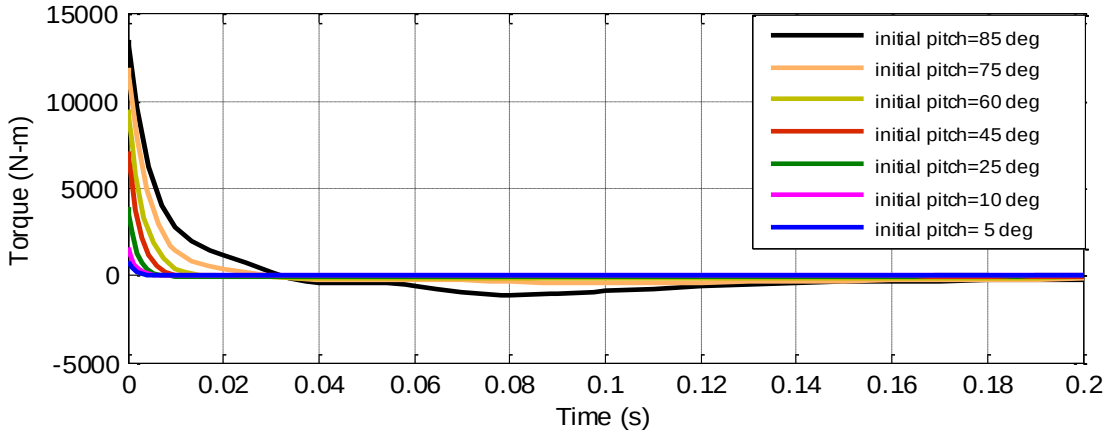

(f)

Figure 4-1: Performance of the Baseline Controller for the TWR: (a) Transient response of pitch (b) Transient response of pitch rate (c) Transient response of velocity (d) Integrated Square error in pitch (e) Controller output (f) Torque demand.

The results show high values of torques, ISE and velocity overshoot upto which seem impractical. To improve such a poor overall performance a nonlinear controller is proposed in the following sections.

4.1.3. Stability Analysis

The state matrix of the closed loop system $\boldsymbol{J}$ of the TWR with the controller designed is computed using A, B and K matrices in $\boldsymbol{J} = \boldsymbol{A} - (\boldsymbol{B} * \boldsymbol{K})$. The closed loop system matrix $\boldsymbol{J}$ is found Hurwitz and all the poles of the transfer function of the system have negative real parts. Hence, the TWR system with LQR based FSFB controller is stable as it fulfills the necessary and sufficient condition for a closed loop system to be stable.

4.2. Lyapunov Function Based Controller Formulation

The baseline controller has been designed with a linearized approximation of the nonlinear plant. The overall performance of linear design cannot be guaranteed. Therefore, a nonlinear controller is designed and implemented to seek its benefits. Nonlinear controller synthesized for TWRs (chapter 3) was a Lyapunov function based controller (LFBC). The objective of LFBC is to guarantee the stability of the control and increase the stability region in addition to the robot body balance and velocity tracking. A LFBC was developed (chapter 3) to enable two wheeled robots motion on uneven terrain. The controller was synthesised

with respect to a domain of attraction. The same controller is reduced for TWRs motion on horizontal terrain in this section.

4.2.1. Model Normalization and Partial Feedback Linearization

A horizontal terrain has no terrain height variation. The variation and rate of variation of the terrain are, therefore, zero i.e. $\dot{\alpha} = \ddot{\alpha} = 0$. The equations (2.26) and (2.27) were therefore reduced considering $\alpha = \dot{\alpha} = \ddot{\alpha} = 0$. These reduced equations of motion representing the dynamics of the two wheeled robot with kinematic constraint of no-slip and moving on a horizontal terrain are given in (2.17) and (2.18). In order to simplify the algebraic manipulation of equations of motion they have been reproduced in an affine form, through simplification and normalization, to keep the controller design easy. Hence, to clarify, (2.17) is divided by Ml^2 and (2.18) is divided by Mlr on both sides of the respective equations. The results are:

$$\left[\frac{\cos\theta}{l}\right]\ddot{x} + \left(1 + \frac{I_p}{Ml^2}\right)\ddot{\theta} - \frac{g}{l}\,sin\theta = 0 \tag{4.1}$$

$$\left[\frac{1}{l}\left(1 + \frac{m}{M}\right) + \frac{I}{r^2 l}\right]\ddot{x} + \left[\ddot{\theta}.cos(\theta) - \dot{\theta}^2.sin(\theta)\right] = \frac{T}{Mlr} \tag{4.2}$$

The normalization was performed using the same method and scaling transformations as mentioned in chapter 3 and the resulting equations for the TWR motion on a horizontal terrain are as follows:

$$(\cos\theta)\ddot{q} + (1 + a_1)\ddot{\theta} - \frac{g}{l}\sin\theta = 0 \tag{4.3}$$

$$[1 + \delta + a_2]\ddot{q} + \cos(\theta)\,\ddot{\theta} - \sin(\theta)\dot{\theta}^2\,(1 + \delta) = \frac{T}{Mlr} \tag{4.4}$$

The normalised system equations are then partially feedback linearized following the procedure described in chapter 3. The equation (4.3) has been manipulated to solve for $\ddot{\theta}$ and substitute the result in equation (4.4). The elements of the inertia, coriolis and gravitational matrices for a TWR dynamic equations developed for motion on a horizontal terrain are as follows:

$$M_{11} = 1 + a_1$$

$M_{12} = \cos\theta$

$M_{21} = \cos\theta$

$M_{22} = 1 + \delta + a_2$

$\mathbf{T} = \mathrm{u}$

$\emptyset_1 = -\sin\theta$

$\emptyset_2 = 0$

$h_1 = 0$

$h_2 = -\sin(\theta)\dot{\theta}^2$

We deduced,

$$u = v\left[(1 + \delta + a_2) - \frac{cos^2(\theta)}{1+a_1}\right] - \sin(\theta)\dot{\theta}^2 + \frac{\sin\theta.\cos\theta}{1+a_1} \quad (4.5)$$

The feedback system equivalent to the normalized system of dynamic equations with new control input v is shown in affine form is as follows:

$$\ddot{q} = v \quad (4.6)$$

$$\ddot{\theta} = \frac{sin(\theta) - v.[cos(\theta)+\sin\theta]}{1+a_1} \quad (4.7)$$

(4.6) is linear and second order while (4.7) represents the internal dynamics of the TWR system motion on horizontal terrain.

4.2.2. Controller Design

Assume that we have perfect knowledge of the states θ and $\dot{\theta}$ and $\dot{q}$. The perturbation bound proposed is as follows:

$$[k_1 cos^2(\theta) - l] \quad (4.8)$$

such that k_1 is a positive constant. A constraint function based Lyapunov function, originated from the energy equation of the IB of the TWR, is proposed. This function is developed using a constructive method. Initially a Lyapunov control function is proposed for two states of the system. Then using added integration a term is added for an additional state. The states selected at initial stage are pitch and pitch rate and then velocity of the robot is added to get a control Lyapunov function.

(a) Lyapunov function and its derivative to control pitch and pitch rate (θ and θ')

A constraint function and energy based Lyapunov function of the IB of the TWR, is proposed. This function represents two states of the TWR, namely, pitch and pitch rate. Both of the states relate to the IB. The constraint function proposed is as follows: $[k_1 cos^2(\theta) - l]$.

This function bounds the pitch θ of the IB and is positive unless

$$k_1 cos^2(\theta) - l = 0.$$

This condition produces a constraint on the system for pitch, θ. The constrained pitch is denoted as $\tilde{\theta}$ in rest of the document. The constraint is given as

$$\theta < \tilde{\theta} = \left(\left[cos^{-1}\left(\sqrt{\frac{l}{k_1}}\right)\right]\right)$$

The energy function used is : $\frac{1}{2}\theta'^2 + l.[1 - cos(\theta)]$.

The control Lyapunov function proposed is given as (4.9) which is used to synthesise controller to control pitch and pitch rate of the TWR.

$$V_{h0}(\theta, \theta') = \frac{1}{2}[k_1 cos^2\,\theta - l]\theta'^2 + l.[1 - cos\theta] \qquad (4.9)$$

The proposed Lyapunov function $V_{h0}(\theta, \theta')$ is, therefore, positive definite for:

(i) $k_1 > l$, because $V_{h0}(\theta, \theta')$ is a locally convex function with a minimum at the origin if $k_1 > l$. k_1 is a constant that controls the boundary of initial pitch as well as performance of the controller.

(ii) $|\theta| < \tilde{\theta}$, such that the initial conditions (θ_0, θ'_0) with $|\theta_0| < \frac{\pi}{2}$ satisfies that $V_{h0}(\theta, \theta') < \left(1 - cos\left(\tilde{\theta}\right)\right)$, where $\tilde{\theta} = \left[cos^{-1}\left(\sqrt{\frac{l}{k_1}}\right)\right]$.

The time derivative of Lyapunov function is given as :

$V_{h0}{}' = \theta'[k_1 cos^2(\theta) - l]\theta'' + l.sin\,(\theta)\theta'$

Substitute θ'' from (3.26) in $V_{h0}{}'$ gives:

$$V_{h0}{}' = \theta' cos(\theta)[v\gamma(\theta) + k_1\beta(\theta, \theta')] \quad (4.10)$$

where,

$$\gamma = \frac{1}{1+a_1}[l - k_1 \cos^2\theta] \quad (4.11)$$

$$\beta = \frac{\cos\theta sin\theta}{1+a_1} - sin(\theta)\theta'^2 = \sin\theta\left(\frac{\cos\theta}{1+a_1} - \theta'^2\right) \quad (4.12)$$

(b) Lyapunov function and its derivative to control pitch, pitch rate and the robot velocity $(\theta, \theta' \text{ and } q')$

A quadratic term is added to the Lyapunov function constructed as (4.9). This is added to control the robot velocity in addition to pitch and pitch rate. The quadratic term is selected such that the derivative of the additional term has the same structure as the derivative of Lyapunov function. The Lyapunov function representing three states is proposed as (4.13)

$$V_{h1} = k_d\, V_{h0}(\theta, \theta') + \frac{1}{2}W_h{}^2 \quad (4.13)$$

W_h is an unknown variable the time derivative of which should have the same structure as $V_{h0}{}'$. This variable is function of $\theta, \theta' \text{ and } q'$ and is proposed as follows:

$$W_h{}'(\theta, \theta', q')\, \theta' cos(\theta) = V_{h0}{}'(\theta, \theta')$$

or

$$W_h{}'(\theta, \theta', q') = [v\gamma + k_1\beta] \quad (4.14)$$

The variable W_h must also satisfy

$$W_h{}'(\theta, \theta', q') = \theta' \frac{\partial W_h}{\partial \theta} + \sin\theta \frac{\partial W_h}{\partial \theta'} + \left(\frac{\partial W_h}{\partial q'} - \cos\theta \frac{\partial W_h}{\partial \theta'}\right) v \quad (4.15)$$

Replacing $W_h{}'(\theta, \theta', q')$ with $[v\gamma + k_1\beta]$ in (4.15) and comparing the two sides of equation:

$$\frac{\partial W_h}{\partial q'} = \frac{l}{1+a_1} \quad ;$$

$$\frac{\partial W_h}{\partial \theta'} = \frac{k_1 \cos(\theta)}{1+a_1} \quad ;$$

$$\frac{\partial W_h}{\partial \theta} = -k_1\theta' sin(\theta)$$

This leads to

$$W_h(\theta, \theta', q') = \frac{k_1 \theta' \cos(\theta)}{1+a_1} + \frac{l\mathrm{q}'}{1+a_1} \tag{4.16}$$

Substitute W_h from (4.16) in expression of V_{h1} (4.13)

$$V_{h1} = k_d\, V_{h0}(\theta, \theta') + \frac{1}{2}\left[\frac{k_1\, \theta' \cos(\theta)}{1+a_1} + \frac{l\mathrm{q}'}{1+a_1}\right]^2 \tag{4.17}$$

Time derivative of the Lyapunov function V_{h1} (4.13), after substituting ${V_{h0}}'$, W_h and ${W_h}'$ and simplifying, is:

$${V_{h1}}' = (v\gamma + k_1\beta){W_h}' = v\gamma(\theta){W_h}' + k_1\beta(\theta, \theta'){W_h}' \tag{4.18}$$

Where

$$\beta = sin\theta\, \left[\frac{cos(\theta)}{1+a_1} - \theta'^2\right] \tag{4.19}$$

$$\gamma = -\frac{k_1 cos^2(\theta)}{1+a_1} + \frac{l}{1+a_1} \tag{4.20}$$

$${W_h}'(\theta, \theta', q') = k_d\, \theta' cos(\theta) + \frac{k_1 \theta' \cos(\theta)}{1+a_1} - \frac{l\mathrm{q}'}{1+a_1} \tag{4.21}$$

(c) Control Law

Lyapunov function based control law is established such that the control input v crafts semi negative definite derivative of the Lyapunov function (${V_{h1}}' \leq 0$), and converges θ and θ' asymptotically to zero.

In order to make ${V_{h1}}' \leq 0$, semi negative definite Let $k_1\beta + v\gamma = -{W_h}'$. This provides:

$$v = \frac{-{W_h}' - k_1\beta}{\gamma}$$

or

$$v = \frac{-1}{\gamma(\theta)}\left({W_h}'(\theta, \theta', q') + k_1\beta(\theta, \theta')\right) \tag{4.22}$$

This will produce

$${V_{h1}}' = -{W_h}'^2$$

As $V_{h1}{}'$ is semi negative definite, this converges θ, θ' and q' asymptotically to zero.

(d) *Controller constraints*

The objective of LFBC is achieved if the following constraints are observed:

v. $\tilde{\theta} = \cos^{-1}\left(\sqrt{\frac{l}{k_1}}\right) < \frac{\pi}{2}$ is the constrain function or nonlinear perturbation bounded by square of the state θ.

vi. $k_1 > l$ because value of k_1 less than l does not fulfil the constraint function as the value of cos θ more than l is invalid.

vii. $k_d > 0$

viii. $\tilde{\theta} > |\theta|$ and $\gamma < 1$ for all times.

4.2.3. Stability Region

When initial condition $(\theta_0, \theta_0{}')$ with $|\theta_0| < \frac{\pi}{2}$ satisfies that $V_{h0} < 1 - \cos\tilde{\theta}$, then $|\theta| < \tilde{\theta}$ and a set defined by (4.23) is a compact set. A compact set is a subset of topological space when for every open cover of subset a finite sub cover of subset exists.

$$\Omega_{\mathrm{h0}} = \left\{(\theta, \theta') \, \epsilon \, R^2 : \, V_{h0} < 1 - \cos\tilde{\theta}\right\} \tag{4.23}$$

This set (4.23) represents the stability region of the system with two controlled states θ & θ'. Similarly, the stability region of the system with three controlled states q', θ, θ' can be defined. Equation (4.22) suggests the system has no singularity if $|\theta| < \tilde{\theta} < \frac{\pi}{2}$. We need to find a condition when the system has a singularity at $|\theta| = \pm\tilde{\theta}$. Equation (4.23) suggests $|\theta_0|$ should be less than $\frac{\pi}{2}$ and $V_{h1} < K = k_d(1 - cos\theta)$ should belong to the neighbourhood of the origin to avoid singularity at $|\theta| = \pm\tilde{\theta}$. In other words states are bounded with $|\theta| < \tilde{\theta}$ if $|\theta(t)| < \tilde{\theta}$ and $V_{h1} < K$. $V_{h1} < K$, is an outcome from the fact that V_{h1} is a non- increasing function as $V'_{h1} = -W_h{}'^2(q', \theta, \theta')$. This also defines stability region, Ω_1, for the proposed closed loop system of the two-wheeled robot with three states (θ, θ', q').

$$\Omega_{\mathrm{h1}} = \left\{(\theta, \theta', q') \, , |\theta| < \tilde{\theta} : V_{h1} < K\right\} \tag{4.24}$$

We conclude that the unstable equilibrium point of a closed loop TWR is stable with proposed controller for all initial values of θ, θ', q' such that $|\theta| < \tilde{\theta}$ and $V_{h1} < K$. This is

stable in the sense of Lyapunov as $V_{h1}(\boldsymbol{x})$ is a positive definite function for all $\boldsymbol{x} \epsilon \Omega_1$ and $V_{h1}{}'(\boldsymbol{x})$ is negative semi definite for $\boldsymbol{x}$.

4.2.4. Stability Analysis

Stability of the proposed controller was analysed finding if V_{h0} becomes locally convex function with a minimum at origin for $k_1 > l$, a constraint of the controller. For other constraints a set is defined and determined as to whether it is a compact set and under which initial conditions. The local convexity of the function is checked by plotting level curves. A level curve is the graph of the function plotted on an interval of pitch [–pi/2 to pi/2]. These level curves are plotted for different values of k_1 as shown in Figure 4-2. The function is convex as the function graph lies below the line segment joining any two points of the graph. The Figure 4-2 shows that the function plotted for all values of $k_1 > l$ has only one minimum point which is at the origin. Hence, the Lyapunov function V_{h0} is a locally convex function with a minimum at origin for $k_1 > l = 0.19$ and the closed loop system represented by the function V_{h0} is stable on an interval [–pi/2 to pi/2].

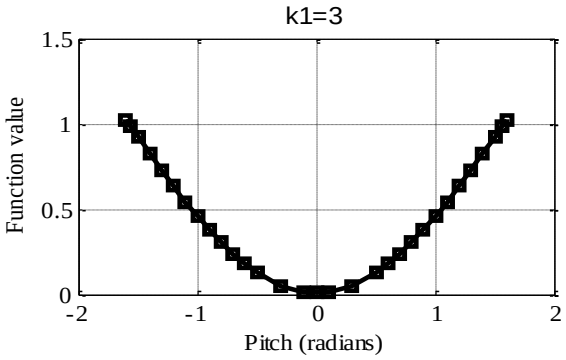

Figure 4-2: Level curve drawn for the proposed Lyapunov function as a function of pitch. The curve was plotted for a range of values (0.2-3) of the controller constant, k_1.

Since $V_{h1}(\boldsymbol{x})$ is a positive definite function for all $\boldsymbol{x} \epsilon \Omega_1$ and $V_{h1}{}'(\boldsymbol{x})$ is negative semi definite for $\boldsymbol{x}$, stability exists in the sense of Lyapunov. Next, LaSall's theorem is applied to prove the asymptotic stability of the equilibrium point of the TWR. The equilibrium point is considered at $\theta = \theta' = 0 \,\&\, q' = constant$. LaSall's theorem defines that if every solution starting in a compact set, and approaches the largest invariant set as $t \to \infty$ then the asymptotic stability is guaranteed. Therefore let D is a compact set defined for TWRs as follows:

$$D = \left\{ \boldsymbol{x} \in \Omega_1 : \left(k_d\, \theta' cos(\theta) + \frac{k_1 \theta' \cos(\theta)}{1+a_1} - \frac{l\mathrm{q}'}{1+a_1} \right)^2 = {W_h}'^2 = 0 \right\} \tag{4.25}$$

Let M is the largest invariant set in D. The Largest invariant set M is computed to ascertain if this is contained in set D. From (4.25), it is evident that on D, ${W_h}' = 0$. This reveals that the auxiliary variable

$$W_h = \left(\left(k_d + \frac{k_1}{1+a_1} \right) sin\theta + \frac{l\mathrm{q}}{1+a_1} \right) = \text{constant on set } D \text{ , and}$$

$${W_h}'' = 0.$$

Since, ${W_h}' = \left(k_d\, \theta' cos(\theta) + \frac{k_1 \theta' \cos(\theta)}{1+a_1} - \frac{l\mathrm{q}'}{1+a_1} \right)$, its time derivative is

$${W_h}'' = \left(\left(k_d + \frac{k_1}{1+a_1} \right) (\theta'' cos\theta - \theta'^2 sin\theta) + \frac{l\mathrm{q}''}{1+a_1} \right)$$

Replacing θ'' and q'' from (4.7) & (4.8), we get

$${W_h}'' = \frac{lv}{1+a_1}(1-\gamma) + \left(\frac{k_1}{1+a_1} + k_d \right) \beta \tag{4.26}$$

As ${W_h}'' = 0$, the above relation give rise to the equality

$$\beta = \frac{\frac{lv}{1+a_1}(\gamma - 1)}{\left(\frac{k_1}{1+a_1} + k_d \right)} \tag{4.27}$$

The controller was selected such that $v\gamma + k_1\beta = -{W_h}'$.

This relation then, on set D, provides $v\gamma + k_1\beta = 0$, and

$$v \left[\gamma + \frac{\frac{l}{1+a_1}(k_1 + k_1\gamma)}{\left(\frac{k_1}{1+a_1} + k_d \right)} \right] = 0$$

As $k_1(1+\gamma) > 0$, then $v = 0$ on set D. This zero control input clearly indicates the system is stable wherein $v = 0$, $q'' = 0$ and q' is a constant on set D. As ${W_h}' = 0$, $\left[\frac{k_1}{(1+a)^2} + \right.$

$k_d\Big]\theta' cos\theta = 0$. This leads to $\theta' = 0$ and $\theta^{"} = 0$ for $\theta < \frac{\pi}{2}$. Substitution of $\theta^{"} = 0$ and $v = 0$ in (4.27) leads to $\theta = 0$ on set D. Therefore, the largest invariant set M contained in the set D is the single unstable equilibrium point ($\theta = \theta' = 0$ & $q' = constant$). LaSalle's theorem, hence, proved that all the closed loop solutions starting in Ω_{h1} asymptotically converge to the largest invariant set M which is the unstable equilibrium point ($\theta = \theta' = 0$ & $q' = constant$).

4.2.5. Performance Evaluation

In order to evaluate the performance of the closed loop TWR on flat horizontal terrain and illustrate the effectiveness of the proposed control law, simulations using were performed. The tests were conducted for the evaluation of velocity tracking and stabilization of the closed-loop TWR system. The performance metrics used were transient response, velocity tracking error, torque demand, energy consumption and integrated squared error of pitch (ISE). The physical parameters of the TWR system, used for all simulation experiments, are given in the Table 2-1 which represent a physical full scale two wheeled robotic platform system. All the states (θ, θ' & q') are fed back. They are measurable and available for feedback.

The experiment was conducted to observe the stabilization of the robot at an unstable equilibrium point ($\theta = \theta' = q' = 0$) with initial pitch $\theta_0 = 57$ degrees and zero reference velocity. The experiment was repeated for reference velocities of 1-5 m/s with initial pitch $\theta_0 = 57$ degrees to investigate the controller performance for the TWR velocity tracking. The initial pitch was selected such that $|\theta_0| < \tilde{\theta} = cos^{-1}\left(\frac{l}{\sqrt{k_1}}\right)$ and keeping in mind the experimental robotic platform physical dimensional constraints. The data for different states was recorded for the purpose of performance analysis. A series of the same tests was conducted with variation of the mass, inertia and the height of centre of mass of the IB to test robustness of the controller to system parameters.

Figure 4-3 shows the results of these experiments for the closed loop system with the LFBC. Figure 4-3 (e) indicates that the states, pitch and pitch rate, converge to the origin with a smooth velocity tracking. The IB pitch, pitch rate and the robot velocity converge to steady state with a 30% overshoot in pitch. They settled within 10 seconds with no steady state error. This transient behaviour of the closed loop system was acceptable as the settling time was

within design limits and the overshoot provided sufficient clearance and no touching of the robot base to the ground. Figure 4-3 (d) shows the reference and simulated robot velocities during 20 seconds run of the TWR on a horizontal terrain. The results of velocity tracking performance for desired velocities of 1m/s and 5m/s show the maximum tracking error during transition. At steady state condition, the tracking error is zero for 1 m/s desired velocity and increases with an increase in desired velocity. The gravity effect may be a contributing factor to the tracking error at high velocity.

The results of the first experiment are also presented in phase space form in Figure 4-3 (e). This shows the relationship between angular position (pitch) and angular velocity (pitch rate) of the IB and the convergence of both states. The IB was initially located at 57 degrees far from the vertical top position; the proposed controller brought both the states close to the unstable equilibrium point of the TWR. The robustness of the controller to the system parameters is also confirmed by checking the results. The controller was designed for 45 kg robot mass having 1.3 kg-m^2 inertia and 0.19 m height of IB centre of mass. The LFBC strategy proved robust for large mass range, inertia range and for high centre of mass positions of the IB. (40-100 kg), (0.05-1.40 kg-m^2), (0.1 - 1 m).

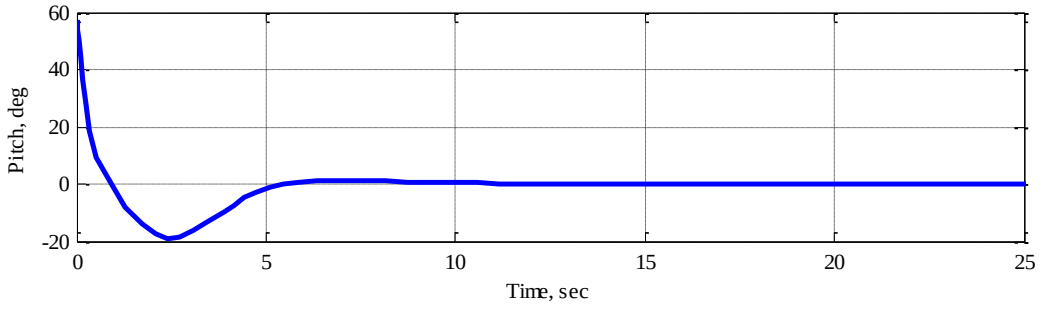

(a)

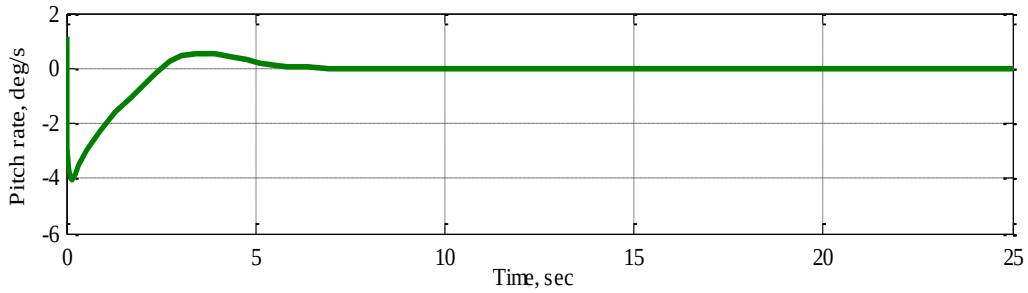

(b)

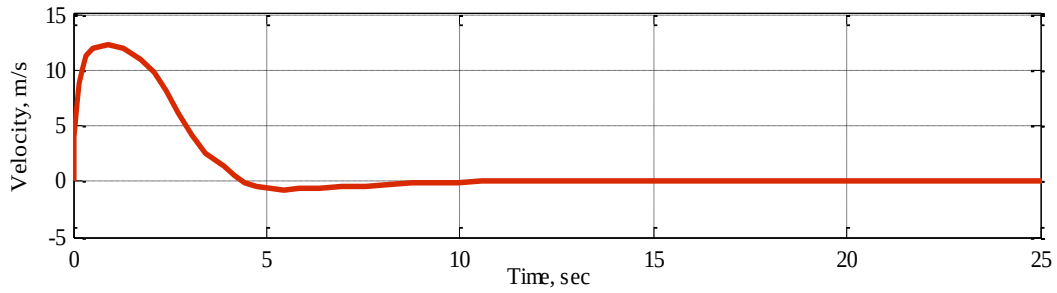

(c)

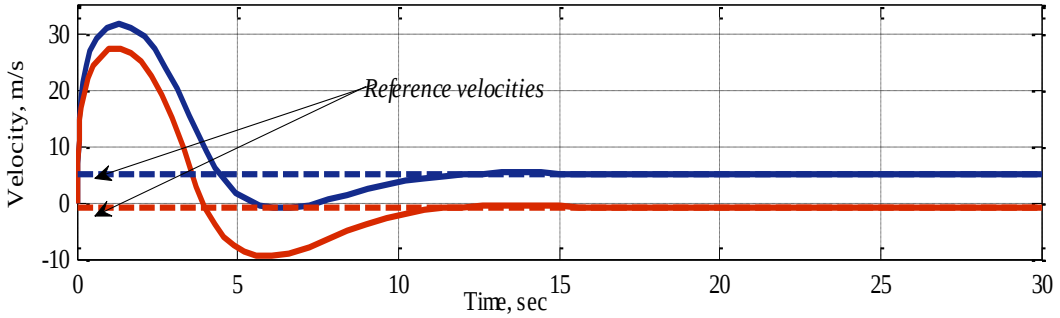

(d)

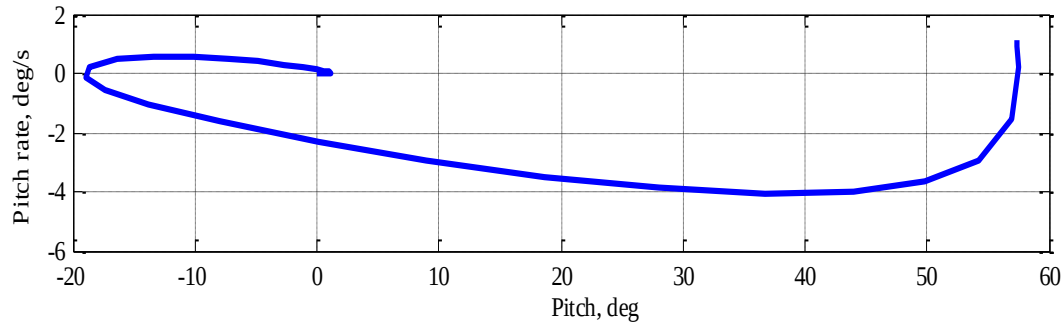

(e)

Figure 4-3: Performance of the LFBC for the TWR: (a) Transient response of pitch (b) Transient response of pitch rate (c) Transient response of velocity (d) Velocity tracking (e) Attraction of pitch and pitch rate to the equilibrium point.

4.2.6. Performance Comparison

Performance of the nonlinear LFBC is compared with the baseline linear controller. Three experiments were designed. An objective was to identify if the nonlinear control algorithm is more advantageous than the linear control. The controllers were tuned keeping one of the performance metrics constant for both the closed loop TWR systems. This was to allow for a fair comparison between two the different controllers. The performance was measured as

transient response, integrated squared error of pitch (ISE), velocity tracking and torque demanded to accomplish the task.

The first test was simulated with an objective to compare the controller output and transient response of the closed loop TWR with the same settling time. The controller gains were tuned such that both the systems response would have the same settling time. Maximum settling time was aimed within 10 seconds. The initial conditions of all the states were zero except pitch which was 85 degrees, a pitch angle close to the boundary of initial pitch calculated using $\tilde{\theta} = cos^{-1}\left(\frac{l}{\sqrt{k_1}}\right)$. These initial conditions were kept the same for both the closed loop TWR systems moving on a horizontal terrain. The data was collected for 20 seconds after the start indicating the initial conditions as described above.

Figure 4-4 illustrates a comparison of the transient behaviour of pitch, pitch rate, integrated squared error of pitch and control demand of the robot for its motion. Figure 4-4 shows the pitch settles very smoothly within 10 seconds for the LFBC. Response with BLC reveals that although the pitch oscillated expeditiously it damped very slowly before settling. These oscillations may harm sensors and measurements of or at different states. The same response was observed for pitch rate and control demand with BLC. Such a rapid variation in the control demand may damage actuators. The peak control demand, however, is higher with LFBC and the LFBC produced higher integrated squared error (ISE) of pitch. High ISE is due to a single unrepeated overshoot which is acceptable as the wheel base did not touch the terrain. This comparison of closed loop systems response of both the BLC and LFBC having same settling time, suggests the LFBC is better in terms of a smooth transition of the states.

First test demonstrated or showed higher initial torque demand by the LFBC. The second test was, therefore, designed to check whether the transient performance would decline if both the controllers produce the same initial torque at the same initial conditions. In this experiment the response of the closed-loop TWR systems was aimed to observe such that both controllers produce the same control demand initially. The controller gains were selected for both the controllers in order to produce the same initial control input demand under the same initial conditions of the states. All the states were kept at zero initial condition except that pitch had an initial value of 85 degrees.

The results shown in Figure 4-5 compare the transient behaviour of the IB position or pitch. The response of LFBC depicts smooth transition with a settling time of 10 seconds. Although the settling time with BLC at, for example, 3.5 seconds is less than LFBC, the BLC response

for pitch had a number of oscillations before settling. Such oscillations limit applications of the TWR. The rate of the IB pitch, plotted in Figure 4-5, shows a steady state error of 15 deg/s. This leads to a continuous vibration around equilibrium point which is unacceptable. The control demand for the robot (Figure 4-5c) motion in longitudinal direction for the LFBC TWR is very low as compared to the BLC controller. The results show that although the LFBC settles slowly, it drops down the control demand over transition very smoothly and gradually, as compared to the oscillated behaviour of the linear controller.

The objective of the third experiment was to observe the way in which both of the controllers were able to perform close to the equilibrium states of the TWR and to evaluate how they perform at the initial conditions far from the equilibrium point. This experiment monitored the performance and control demand of the TWR system having same closed loop characteristic polynomial. The parameters of the LFBC law were tuned and chosen such that the system would show the same performance as in previous section. The initial conditions were fixed at the origin except for the pitch of the IB. This was scheduled to be as or at 28 degrees.

The results shown in Figure 4-6 compare the transient behaviour of the IB position (pitch), integrated squared error, control demand and the velocity of the robot motion in longitudinal direction for two closed loop TWR systems. At the time the initial system is made equivalent to the closed loop system the LFBC showed good results whilst the BLC could not stabilize the system and caused large oscillations.

4.2.7. Conclusions

A linear FSFB controller was designed as a baseline controller to control stability and track the velocity of two-wheeled mobile robots on horizontal terrain. The linear control algorithm stabilizes the TWR in the neighbourhood of the equilibrium points. Then a nonlinear Lyapunov function based control scheme was developed with the same objective. This control scheme allows computation of stability region of the TWR which turned out to be a large region. In order to compare performance of the proposed nonlinear LFBC with a linear FSFB controller, stability region was computed and the controllers were evaluated in three scenarios. In each scenario the controllers were tuned whilst maintaining one of the performance metrics common.

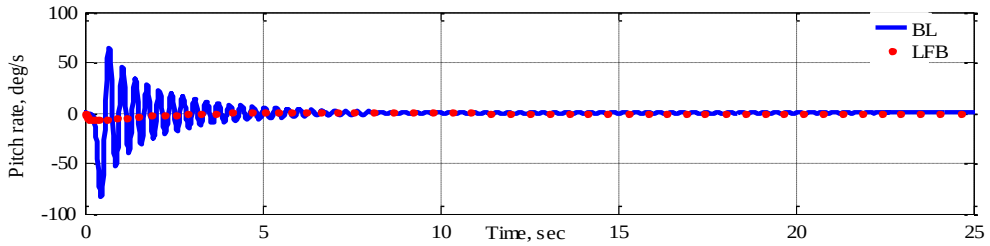

(a)

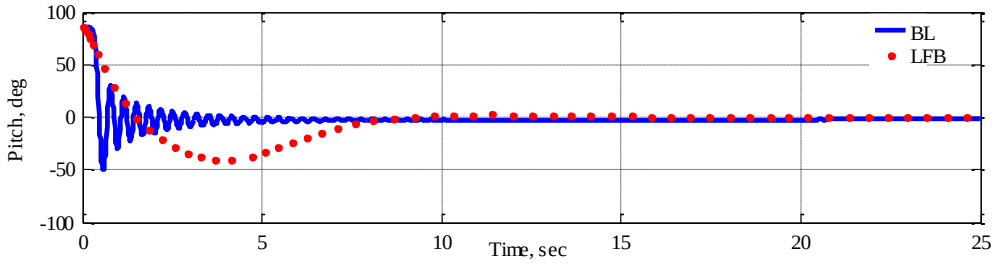

(b)

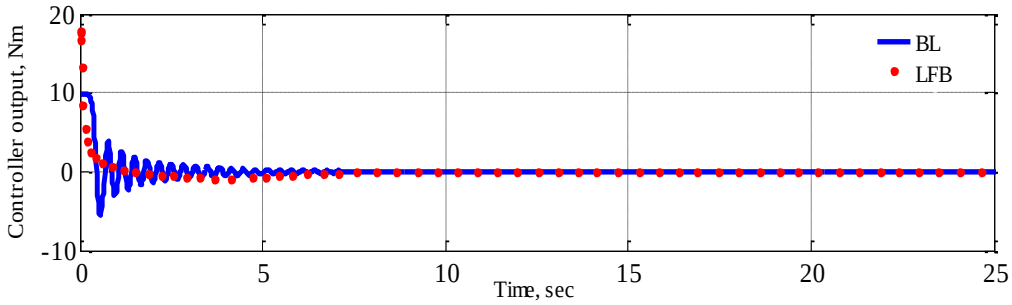

(c)

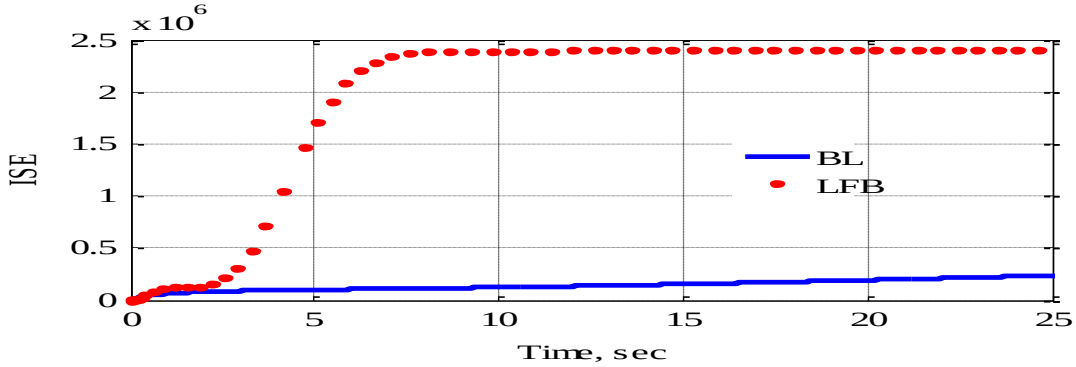

(d)

Figure 4-4: Comparison of performance and control input of baseline and Lyapunov function based controllers for the same settling time: (a) transient performance of pitch rate (b) transient performance of pitch (c) Control input generated by each controller (d) Integrated squared error of pitch.

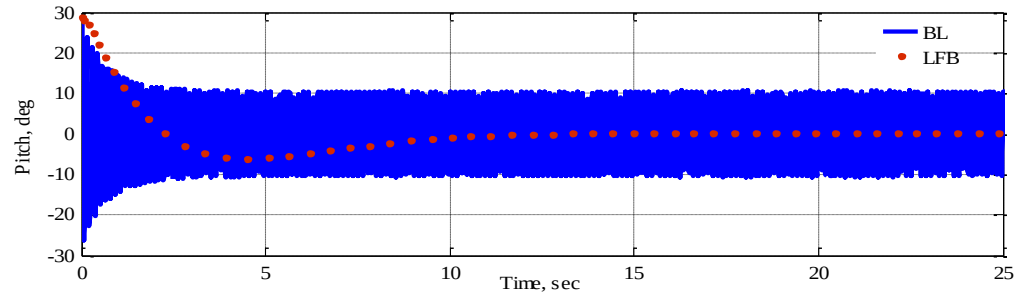

(a)

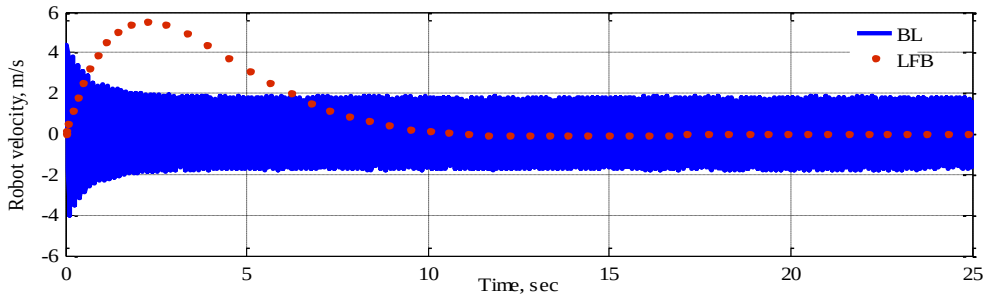

(b)

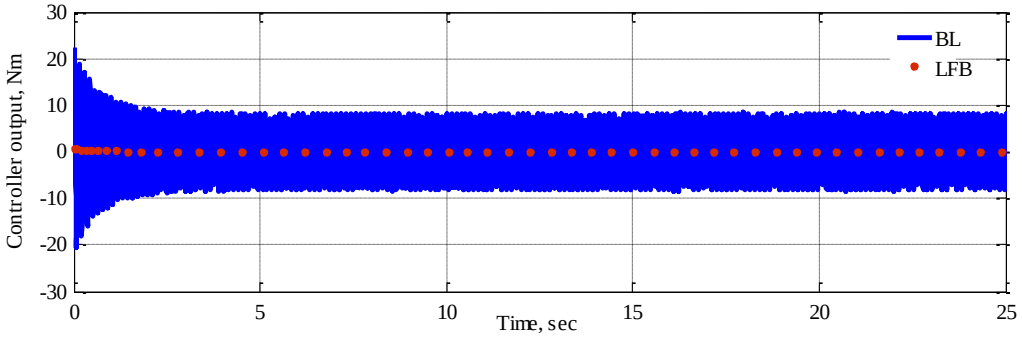

(c)

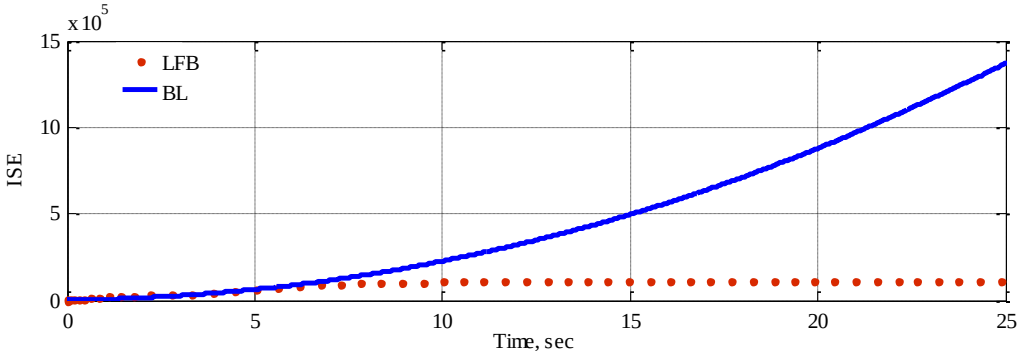

(d)

Figure 4-5: Comparison of performance and control input of baseline and Lyapunov function based controllers for same closed loop polynomials: (a) transient performance of pitch rate (b) transient performance of pitch (c) Control input generated by each controller (d) Integrated squared error of pitch.

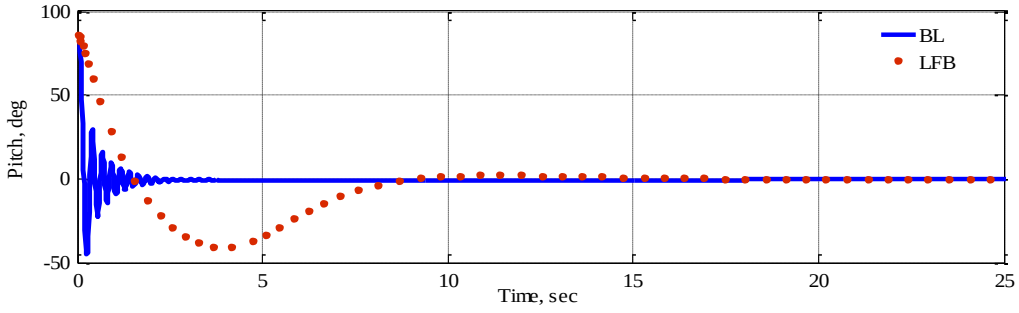

(a)

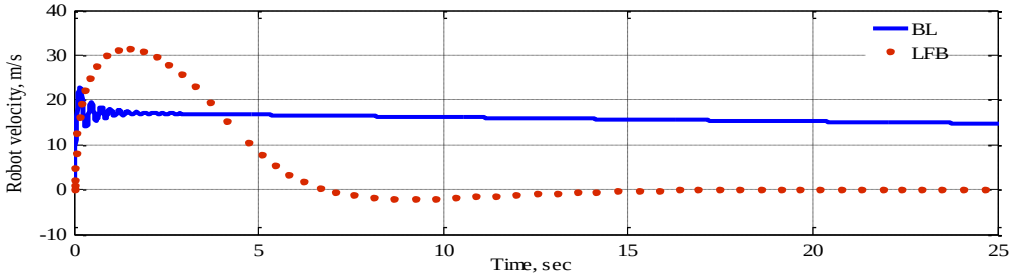

(b)

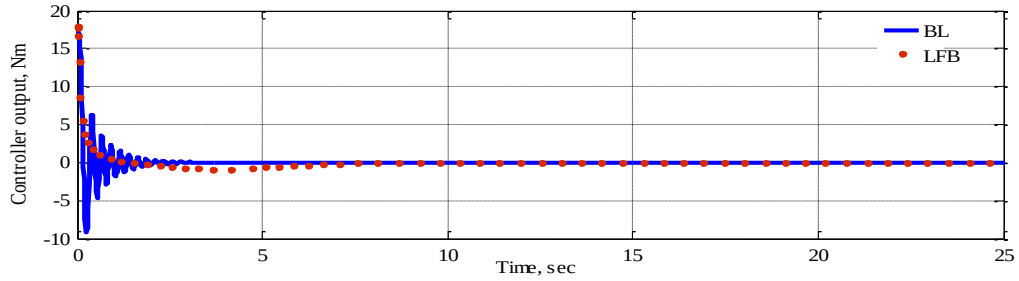

(c)

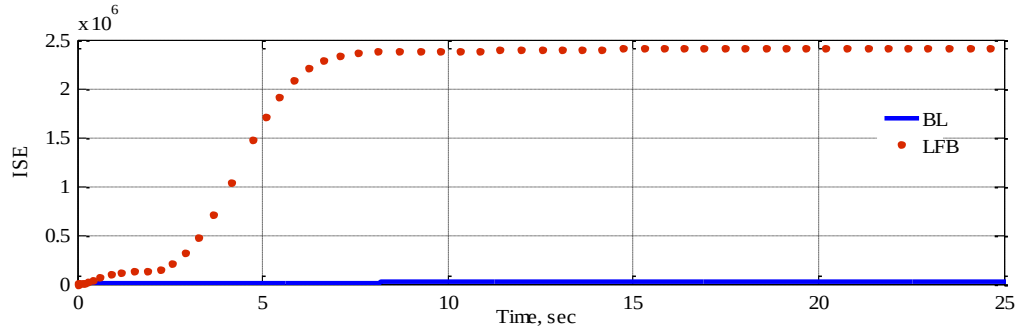

(d)

Figure 4-6: Comparison of performance and control input of baseline and Lyapunov function based controllers for the same initial control demand: (a) transient performance of pitch rate (b) transient performance of pitch (c) Control input generated by each controller (d) Integrated squared error of pitch.

Simulation results illustrate the performance of the linear and nonlinear control schemes for the TWR on horizontal terrain. It was shown that the FSFB control law was able to stabilize the IB and run the robot with reference velocity in a few scenarios however it did not succeed at the point or stage the same initial torque was supplied at the same initial conditions. The linear controller, as compared to the proposed controller, produced a high control demand that limits its practical use. Velocity tracking performance of the linear controller was not to the desired standard. The LFBC law was able to successfully stabilize the IB and run the robot with reference velocity in all tested situations. This proposed controller tracked the velocity and stabilized the IB position from far initial pitch within 10 seconds and with a low power demand. LFBC imparts or transmits all the advantages of conventional FSFB control and guarantees the stability with a broader stability region by utilizing a novel control Lyapunov function. The LFBC law is smoother than FSFB control, eliminating the effect of variation in TWR physical parameters utilizing control Lyapunov function. For these reasons LFBC is recommended for use as a basic nonlinear controller for the application of the TWR on inclined (Chapter. 5) and uneven (Chapter. 6) terrain.

Chapter 5. Control of a Two-Wheeled Robot on Inclined Terrain

The wheel-terrain contact angle remains unchanged for an inclined terrain; although different inclined terrains have different inclination angles. Change in height of a terrain induces dynamic disturbance forces. They are generated at the wheel-terrain contact point due to a change in contact force. The disturbance forces affect the operations performed by the mobile robot. The aim of this study is to stabilize two wheeled mobile robots on inclined terrain. The robot velocity tracking has been an additional objective of this study. Three control schemes have been designed and their performance has been investigated in simulations. A dynamic model developed (chapter 2) for two wheeled robots motion on inclined terrain has been utilized. A linear FSFB controller, designed for zero slope (chapter 4), has been tested on inclined terrain. An LQR based gain scheduled (GS) controller has been designed utilizing wheel-terrain contact angle as a scheduling variable. To guarantee the stability of the closed loop system and increase the stability region, a Lyapunov function based nonlinear controller has been designed for TWR motion on inclined terrain and the stability region has been calculated or computed. The simulation results of the nonlinear controller demonstrate that it is more advantageous for TWR on inclined terrain, compared to the FSFB and GS controller.

5.1. Effect of Terrain Inclination

This section presents control of the stability of closed-loop TWR at the desired velocity on a horizontal terrain and evaluates performance as well as stability region on flat horizontal and inclined terrain. The objective was to identify the effects of terrain inclination on performance and stability regions. A numerical approach using computer simulation [25-27] of the nonlinear dynamics of a system was utilised to evaluate the stability region. The Dormand and Prince method for numerical solution of the differential equations was used. An FSFB controller was implemented in simulations. The performance of the controller was evaluated in a number of scenarios utilizing transient response of pitch and velocity. The performance was tested at a range of initial conditions of sets of states which determined the boundary of initial conditions where the system became unstable. That boundary was drawn to locate the stability region.

5.1.1. Controller Design

A full state feedback (FSFB) controller based on LQR (chapter 4) was selected for the performance and stability region quantification as it guarantees stability for linear systems. The states vector used for the controller design was $\underline{x} = \left[\int(\dot{x} - v_{ref})dt \quad \dot{x} \quad \theta \quad \dot{\theta}\right]^T$. In the state vector v_{ref} is the desired velocity of a TWR. A block diagram of the closed-loop system is shown in Figure 5-1. The overall control law implemented was $= -K\underline{x}$.

The state weighting matrix, Q and input weighting matrix, R were tuned in simulation on nonlinear dynamics of TWR such that they fulfilled the control objective. The gains were optimized for minimum steady state error in pitch (θ), a quick response and least possible overshoot of pitch from the equilibrium position. The resulting controller gains matrix was found as $K = [-316 \; -374 \; -1033 \; -512]$.

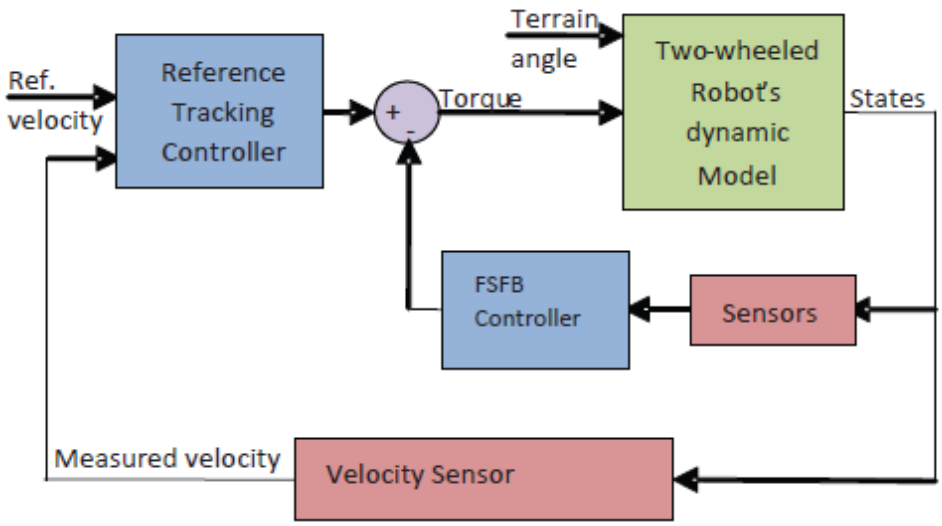

Figure 5-1: Closed loop system of two wheeled robots to assess the effect of terrain inclination.

5.1.2. Performance Quantification

The performance of the closed loop TWR system was observed in the following scenarios:

1. Stationary balancing on a horizontal flat terrain
2. Balancing during motion at a desired velocity on a horizontal terrain
3. Stationary balancing on inclined terrain

In the first case, initial conditions for velocity of the robot and pitch rate of IB were assumed to be zero and the IB pitch was set to 5 degrees. In second scenario, the initial values of pitch and pitch rate were assumed to be zero and the system was run at three desired velocities. These desired velocities were 0.5, 1 and 2 m/s. They were selected to represent the slow walk, the brisk walk and the running speed of a human. In the third case, the response was simulated for balancing of IB on inclined terrain. The wheel-terrain contact angles selected were 10^o and 20^o, whereas the initial values of velocity and pitch were assumed to be zero.

In order to go-over closed loop system performance for velocity control, the transient response of the system was observed in all three cases. The results, shown in Figure 5-2, demonstrate that even though the system stabilized within 4 seconds, in all the conditions, an overshoot in the velocity increased with an increase in the desired velocity. The same trend was observed with an increase in the wheel-terrain contact angle. This is concluded from results that increase in velocity and terrain inclination affects the performance of the velocity tracking unfavourably.

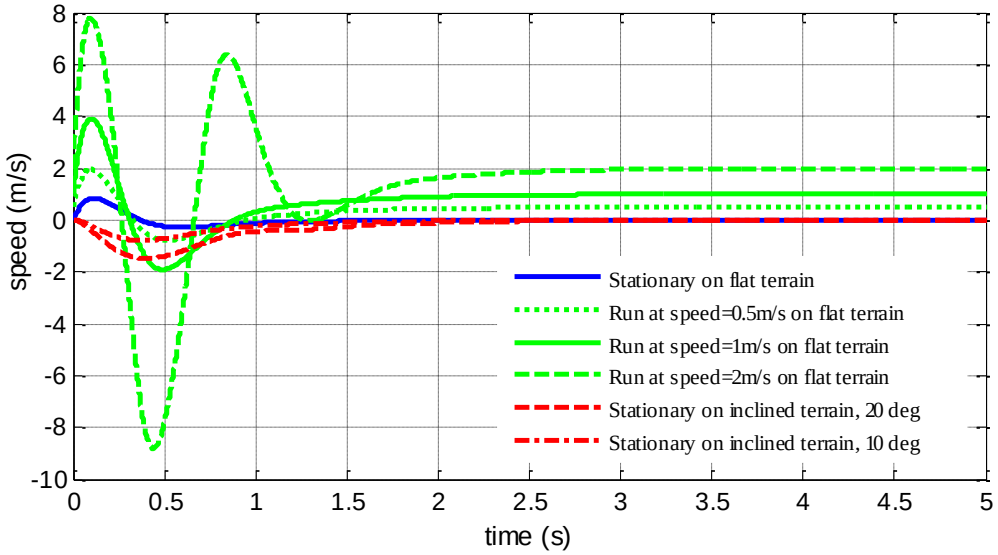

Figure 5-2: Performance of speed control and tracking on horizontal and inclined terrain.

The transient response of closed loop system to the pitch in three cases is shown in Figure 5-3. Figure 5-3 shows the system was stabilized within 4 seconds only up to 10 degrees of terrain inclination and to a desired velocity of 0.5 m/s. The percentage overshoot also increased as the desired velocity and terrain inclination angle increased. Hence, the performance of IB balance was deteriorated from the designed criterion for inclination angle above 10^o and velocity above 0.5 m/s. Figure 5-3 also displays the IB of the robot is balanced at an angle other than zero with a change in the wheel-terrain contact angle. These nonzero

equilibrium angles increased as the terrain inclination angle increased. A relationship between equilibrium pitch and wheel-terrain contact angle was established (chapter 2) for the steady state operating condition using the dynamics equations.

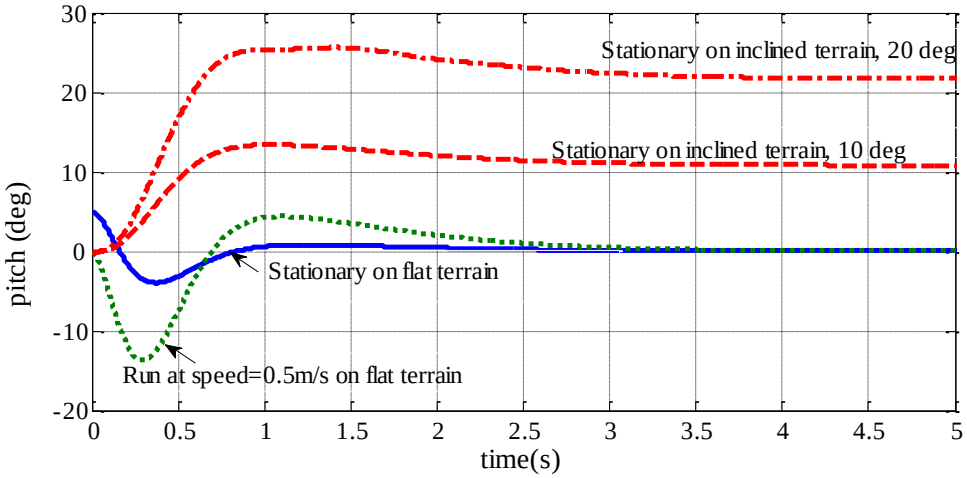

Figure 5-3: Performance of pitch control on horizontal and inclined terrain.

5.1.3. Stability Region

A stability region is a subset of the system states for which system stability can always be maintained. Once stability of the linearized TWR system is verified at the equilibrium point, the system is assumed to be stable at all initial conditions. As the real system of two-wheeled mobile robots is nonlinear it is expected that there exist certain states of the physical system from which the intermediate body cannot revert back to the upright position or the system becomes unstable. In other words, a confined stability region is expected due to nonlinearities. The stability region for the closed-loop system on horizontal and inclined terrain was, therefore, estimated in simulations.

Integrated error in velocity, velocity, pitch and pitch rate were four states of the TWR system and terrain angle was a disturbance considered for the design of the controller in this section. It was difficult to visualize the variation of all the states and disturbance in one plot. The stability region, therefore, was estimated for pairs of state variables. In order to estimate the boundary of stability region numerically, value of initial condition of one state variable from a selected pair of states was fixed. The initial conditions of remaining state variables of the system were assumed to be zero. The maximum and minimum initial values of other state variable of the pair were evaluated. These are the values beyond which the system became unstable.

Simulations were accomplished for a TWR traversing on two types of terrain, horizontal and inclined. The motion of the robot on horizontal flat terrain was evaluated where no disturbance due to terrain inclination was considered. The experiments were conducted at different sets of initial conditions of the system states. The simulations were terminated at which time a set of initial state values approaches occurred for which the robot did not show the desired performance. Later the motion on inclined terrain was considered to assess the effects of terrain disturbance. The combinations of initial values of the states in unstable cases were recorded and plotted as a boundary of the stability region.

5.2.3.1. Stability Region on Horizontal Terrain

In order to plot stability regions the state variables, for robot motion on a horizontal terrain, are divided into three pairs: $\dot{x} \sim \theta$; $\theta \sim \dot{\theta}$; $\dot{x} \sim \dot{\theta}$. For the first pair of states $\dot{x} \sim \theta$ initial velocity was selected from zero to 4m/s with an increment of 0.01 m/s for each simulation. The initial pitch was selected from -90^o to 90^o with increments of 5^o. The initial conditions for all other state variables and disturbance were fixed to zero. For each reference velocity, the maximum and minimum initial pitch from which the IB returns to the upright equilibrium position within 4 seconds was assessed. The pitch range appraised at different reference velocities assuming no disturbance is shown in Figure 5-4. The horizontal and vertical axes of Figure 5-4 stand for the initial values of reference velocity in m/s and pitch in degrees respectively. The results show that there exists a region of stability for the upright position in the $\dot{x} \sim \theta$ plane at zero initial displacement and pitch rate.

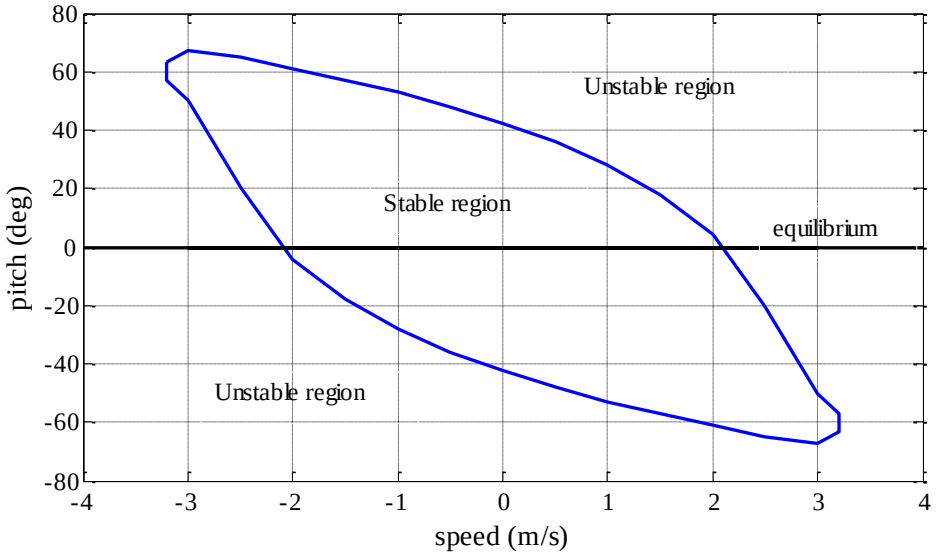

Figure 5-4: Stability region of initial values of pitch and linear speed.

For the second pair, the pitch was evaluated at different pitch rate of the IB assuming no disturbance. The initial pitch rate of the IB was selected with increments of 10 degrees/s. The initial pitch was selected for a range from -100^{o} to 100^{o} with intervals of 5^{o}. The initial conditions for all other state variables were fixed to zero. For the same performance criterion described above the stability region of the pitch corresponding to the pitch rate of the IB is shown in Figure 5-5 whereby horizontal and vertical axes represent the initial values of pitch rate in degrees/s and pitch in degree respectively.

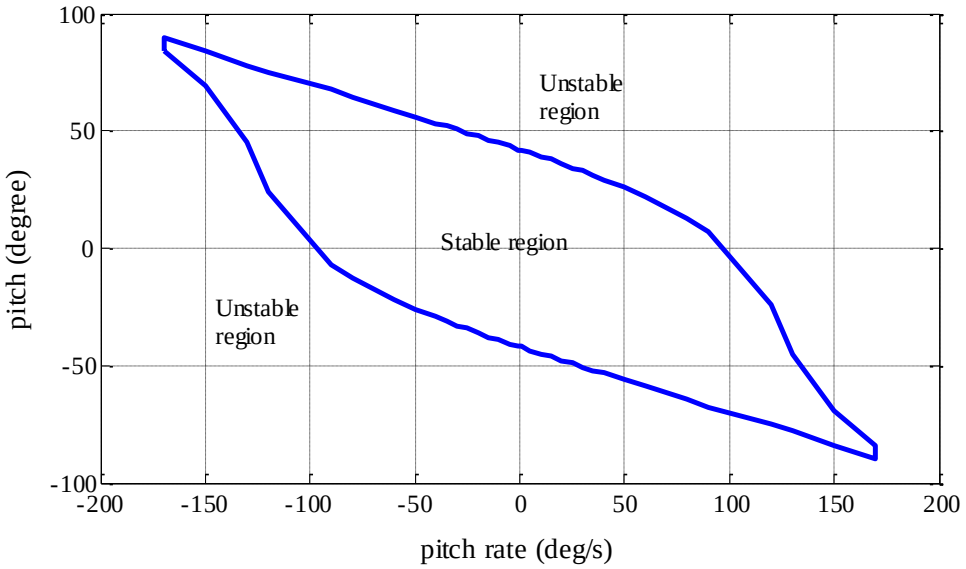

Figure 5-5: Stability region of initial values of pitch and pitch rate

The initial velocity for the third pair of states was selected with intervals of 1 m/s. The initial pitch rate was selected every 15 degrees/s for a range from -500^{o} to 500^{o} per seconds. For such a selected reference velocities the maximum pitch rate that stabilized the system within 4seconds was estimated. Figure 5-6 shows the stability region of the pitch rate and reference velocity of the system. Here, the horizontal and vertical axes are the initial values of reference velocity in m/s and pitch rate in degrees/s respectively.

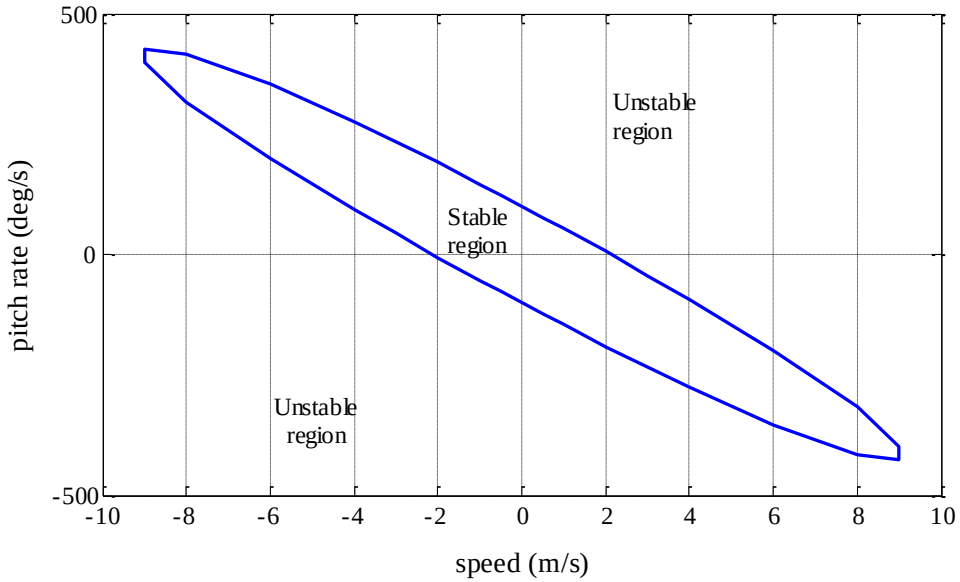

Figure 5-6: Stability region of initial values of pitch rate and linear speed

5.2.3.2. Stability Region on Inclined Terrain

A terrain inclination is represented by the wheel-terrain contact angle which is defined as an angle drawn by an inclined terrain with a horizontal plane. To see the way in which an inclined terrain affects the motion of TWR, the simulations were performed on a terrain of different inclinations. It was known that the equilibrium points on inclined terrain vary depending upon the wheel terrain contact angle. The stability regions were assessed with the TWR performance for static stability. Static stability signifies that the initial and steady state velocity of the robot was assumed to be zero. Initial conditions for pitch were selected as pitch equilibrium points and velocity error was computed from the control input demand of the reference tracking controller at equilibrium point. This was obtained by dividing the controller output by the controller gain giving the initial condition of error integrator. All these initial conditions were set as the initial value of the respective integrators.

In each experiment, a wheel-terrain contact angle was fixed to assess the stability region and the initial conditions of pitch from equilibrium pitch were increased and decreased, until the system became unstable. Then the wheel-terrain contact angle was changed and the above procedure was repeated. The results were plotted as shown in Figure 5-7, wherein the horizontal axis stands for the value of wheel-terrain contact angle, in degrees, and the vertical axis represents the initial values of pitch of IB, in degrees. The equilibrium pitch of IB corresponding to each wheel-terrain contact angle is plotted as a red line in Figure 5-7 to observe the variation of actual pitch from equilibrium.

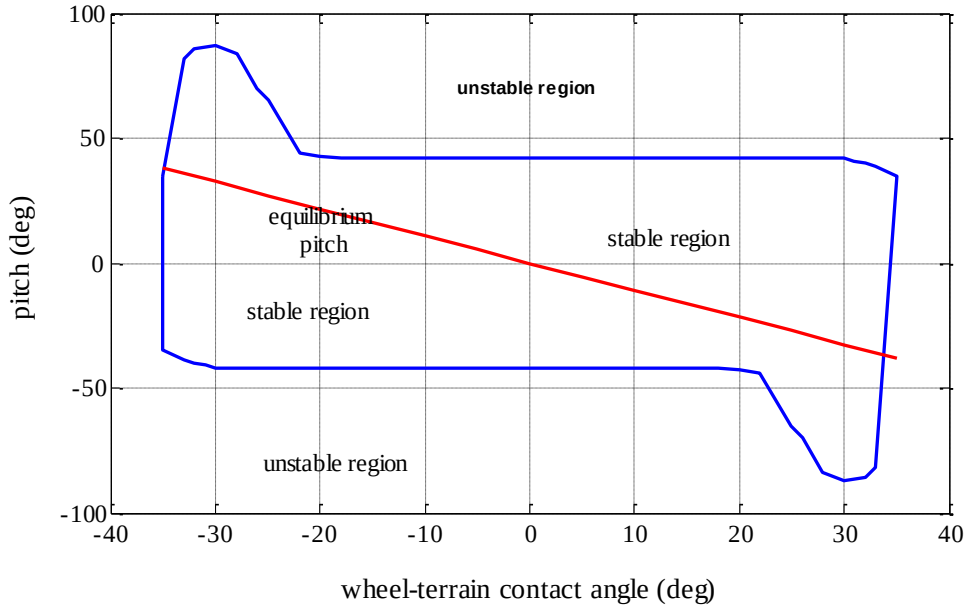

Figure 5-7: Stability region boundary of body pitch angle with respect to change in the slope of the terrain surface.

5.1.4. Results and Discussions

The performance criterion, selected for the stability control in this section, included a settling time of 4 seconds with no steady state error and minimum overshoot in pitch. Figure 5-2 and Figure 5-3 demonstrates that the settling time of the pitch of the robot was increased from 4 seconds as the velocity and wheel-terrain contact angle increased. This increase was more significant above 20 degrees of terrain inclination. Similarly an overshoot in velocity increased with an increase in desired velocity. The same trend was observed with an increase in the wheel-terrain contact angle. The robot performed well to the designed criterion only up to 10 degrees of terrain inclination and to a desired velocity of 0.5 m/s. These results reveal that an increase in velocity and terrain inclination deteriorates the performance of two wheeled robots on inclined terrain.

Stability regions of pitch for a speed range from -4 to +4 m/s can be seen in Figure 5-4. The velocity range -1 to +1 m/s is close to the brisk walking speed of a human. For an initial velocity range -0.01 to 0.01 m/s the system stabilized up to initial pitch 40^{o}. For an initial velocity beyond ±0.01 m/s, stability region varied with a change of initial condition of velocity. It is worth noting that the total pitch range around the upright equilibrium position of the IB did not change more than 3^{o} within a speed variation of ±1 m/s. The results suggest the equilibrium point at a stationary condition may be different from the equilibrium point at

a dynamic condition. A tool edged shape of pitch that appears in Figure 5-7 is an effect of nonlinearities in the system. The results also show that the terrain inclination 0 - ±20 degrees has no effect on the stability region of IB pitch with the controller, although the system becomes stable up to 30 degrees however this response has oscillations and delay. Closed loop poles were determined at different terrain angles without changing controller gains. A variation in the closed-loop poles of the system was observed. The dominant closed-loop pole was getting closer to the imaginary axis and became complex. The other poles were moving farther away indicating that the system was moving towards instability.

5.1.5. Conclusions

A FSFB controller based on LQR showed promising results for the stable motion of the robot on flat horizontal terrain. The controller performed well up to human walking speed, for example, 1m/s (4km/h). The boundaries of the stability regions of different states of the system were found in closed shape. However the performance and the stability region of the pitch on flat inclined terrain declined. This indicates that the terrain inclination has dynamic effects on the stability of two-wheeled mobile robots as dynamics change with change of wheel-terrain contact angle. The equilibrium point for pitch at stationary condition was also affected by the speed of the robot. It is concluded, therefore, that the control of two wheeled robots on inclined terrain must take into account the terrain inclination, in particular when they navigate at high inclination paths. The dynamic effects of terrain inclination angle might be modelled and designed to compensate accordingly.

5.2. Gain-Scheduled Control of TWRs

There is a strong need to provide compensation of dynamic effects produced by an inclined terrain [ref of own paper and maria's paper 'effects of terrain irregularities']. The two wheeled robot should be capable of balancing its IB on inclined terrain and standing or keep moving at a desired velocity to take advantage of no tip-over property. This is usually referred as stabilization control and reference tracking control. The linear optimization controller designed for the TWR (chapter 4) was unable to compensate for the terrain inclination after certain limit. Therefore, gain-scheduled control for a TWR with wheel-terrain contact angle variation is an important task.

Gain scheduling has been used to control nonlinear plants in a variety of engineering applications such as process control [136] and flight control [137]. This method has also been

seen in other applications such as ship steering, PH control, combustion control and engine control. Jiang scheduled the gains of a PID controller of a two-cylinder diesel engine [138]. A Gain scheduling is a controller wherein controller gains are changed according to the current value of scheduling variable. Scheduling variable may be external and/or internal to the plant [139]. The values of scheduling variable are unknown *a priori* but can be measured online [129]. A main approach, namely traditional gain-scheduled control [140], is considered in this research. A major challenge in designing a gain-scheduled controller is the stability and performance problem caused by the dynamics of changing scheduling variable. In the current study this dynamic was ignored in the design process and ruled out stability problems through extensive simulations.

5.2.1. Controller Formulation

The objective of a gain-scheduled (GS) controller design is to balance the IB of a TWR at the equilibrium pitch with zero pitch rates and track the desired robot velocity on inclined terrain. Gains of FSFBC, designed using LQR, were scheduled. This scheduling varies with the wheel-terrain contact angle. The Wheel-terrain contact angle was assumed to be measured in advance as a scheduling variable. The range of allowable wheel-terrain contact angle on inclined terrain depends on the geometry of a robot [33], for example, the clearance of the IB base from the horizontal terrain and width of the IB base. The maximum permitted inclination angle of terrain was computed using (chapter 3).

The allowable range of wheel-terrain contact angle was divided into equal step size of 5^{o} of discrete operating conditions. For each operating condition, a linearized model was extracted. GS controller implements the control law (5.1):

$$u = -K_x(\boldsymbol{\alpha})\boldsymbol{X} - K_r(\boldsymbol{\alpha})e_r \tag{5.1}$$

The controller gains $K_x(\boldsymbol{\alpha})$ & $K_r(\boldsymbol{\alpha})$, in this control law, were determined by tuning the weighting matrices of LQR for the system running in simulation on respective operating condition. The $\boldsymbol{Q}$ and $\boldsymbol{R}$ matrices were selected such that they minimize the performance index for the closed loop system and present the best compromise between the robot velocity and the control torque. The state space matrices were evaluated using the physical parameters of the robot listed in Table 2.1, chapter 2. The equilibrium pitch is different for each inclined terrain as it varies with wheel-terrain contact angles. This is updated for the plant and

controller as a function of wheel-terrain contact angle using (2.19). The relationship (2.19) is valid for the steady state of each operating condition.

5.3.2 Interpolation between Gains

The operating conditions, other than those in which the system was linearized and for which the gains were determined, were interpolated from the known data of the simulated controller gains. Many interpolation methods have been successfully applied in control literature. These methods are either ad-hoc which require a lot of trial and error or are too complex to implement in computer simulation and in real time. Moreover, methods that use the transfer function form for interpolation can be numerically ill conditioned for high-order systems. Small errors in the coefficients of the denominator polynomial may result in a large difference of the pole locations. The sensitivity grows if multiple poles occur in high-order systems. A linear interpolation method was, therefore, used for this study [124]. This makes an interpolation between the gains of the local controllers. Such an interpolation is simple, quick and converts local controllers into a global varying controller and it is easy to implement. Figure 5-8 gives a wide view of variation of individual gains scheduled for the GS controller which is implemented in the next section.

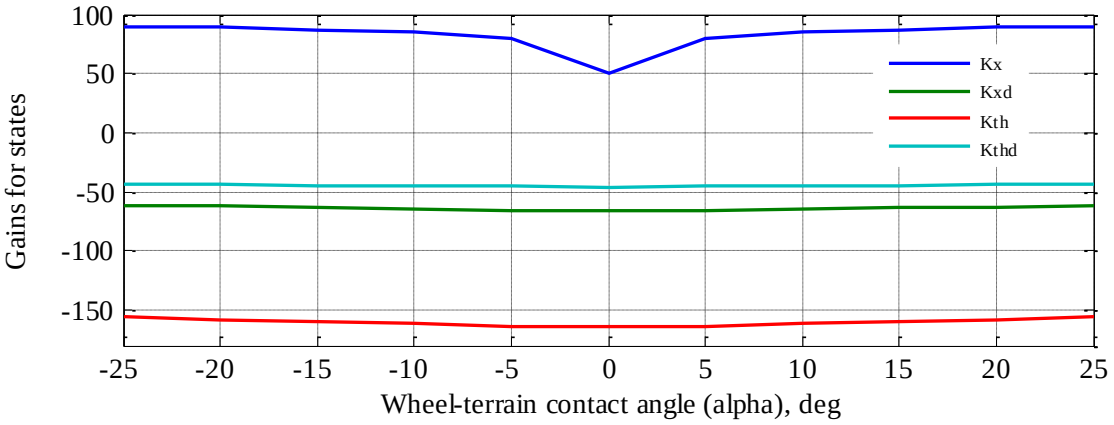

Figure 5-8: FSFB controller gains variation with the wheel-terrain contact angle.

5.2.2. Performance Evaluation

The performance was evaluated in simulations. The nonlinear plant model was utilised which represents the TWR dynamics on inclined terrain. Linear interpolation blocks were implemented one for each gain. Three gains were for three states and one gain for velocity tracking. These gains vary with wheel-terrain contact angle. For velocity tracking experiments,

the initial conditions for linear displacement and pitch rate were set at zero. The pitch was selected as 15 degrees for an inclined terrain with -15 deg wheel-terrain contact angle. The initial and reference velocity were kept the same. These were 0.05, 0.1 and 0.5 m/s. The results are shown in Figure 5-9.

The performance was evaluated on five inclined terrain, the inclinations of which were 5^o, 10^o, 15^o, 20^o, 25^o. The initial conditions for pitch rate, position, velocity and reference velocity were zero while initial condition for pitch was the same as wheel-terrain angle except with opposite sign. The performance metrics of transient response, integrated squared error of pitch (ISE), velocity tracking and torque demanded (chapter 3) were used for performance quantification. The objectives of this performance evaluation were to find how well the GS controller stabilizes the IB on inclined terrain of high inclinations; how much torque demand the controller produces; what level of balancing error it produces and to determine the tracking error in velocity. The results can be seen in Figure 5-9 (a-d).

The states are regulated by the GS controller at equilibrium pitch relative to the wheel-terrain contact angle, zero pitch rate and stationary position of the robot. The torques demanded by the controller to regulate these states increases with the increase of the wheel-terrain contact angle as shown in Figure 5-9 (c). Even though the GS controller regulates the equilibrium pitch, the error from the equilibrium, integrated over time, increases as the slope continues to increase.

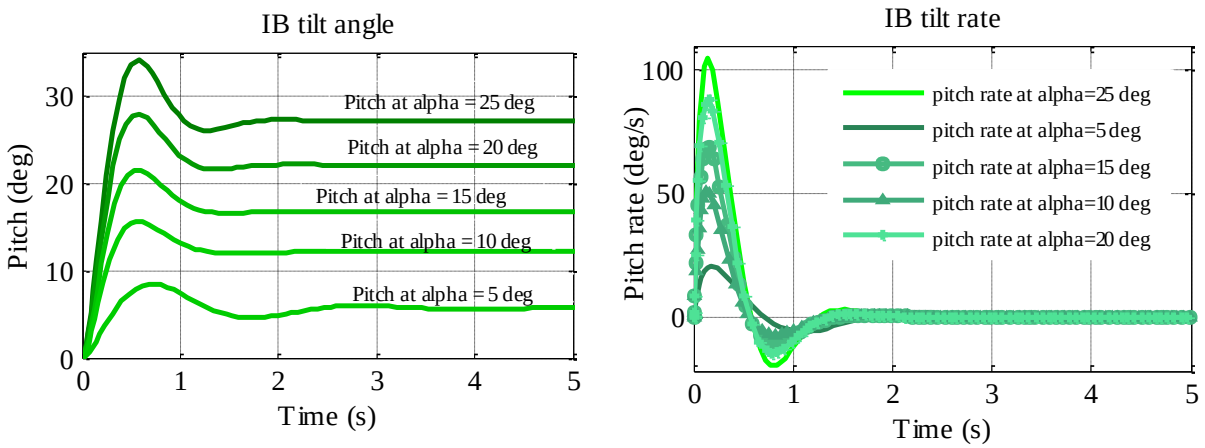
IB tilt angle
Pitch (deg)
Time (s)
Pitch at alpha = 25 deg
Pitch at alpha = 20 deg
Pitch at alpha = 15 deg
Pitch at alpha = 10 deg
Pitch at alpha = 5 deg
IB tilt rate
Pitch rate (deg/s)
Time (s)
pitch rate at alpha=25 deg
pitch rate at alpha=5 deg
pitch rate at alpha=15 deg
pitch rate at alpha=10 deg
pitch rate at alpha=20 deg

(a)

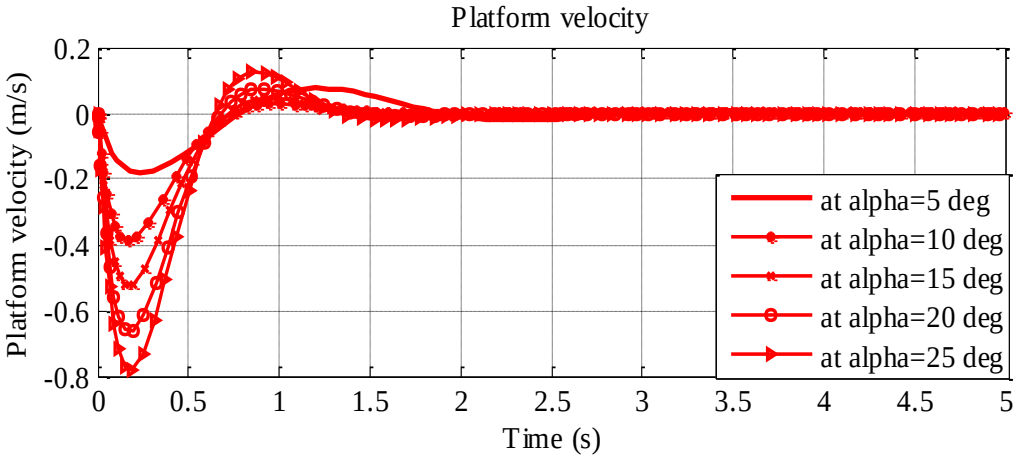
Platform velocity
Platform velocity (m/s)
Time (s)
at alpha=5 deg
at alpha=10 deg
at alpha=15 deg
at alpha=20 deg
at alpha=25 deg

(b)

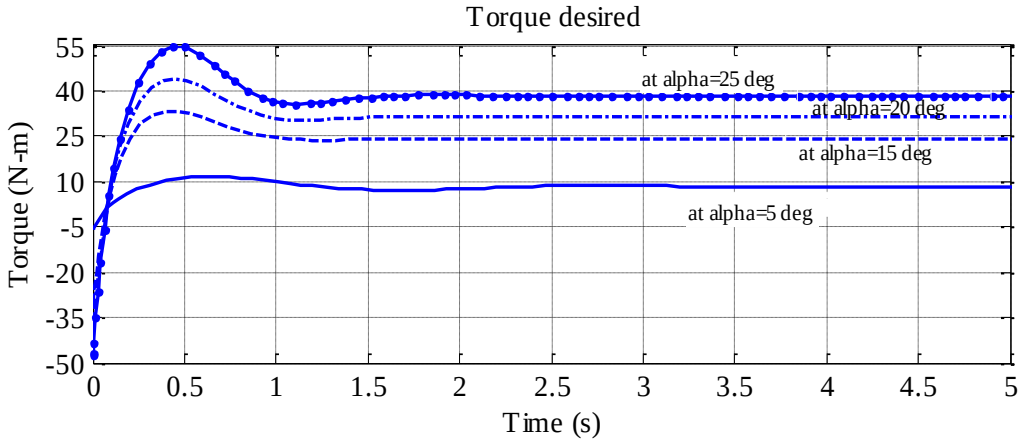
Torque desired
Torque (N-m)
Time (s)
at alpha=25 deg
at alpha=20 deg
at alpha=15 deg
at alpha=5 deg

(c)

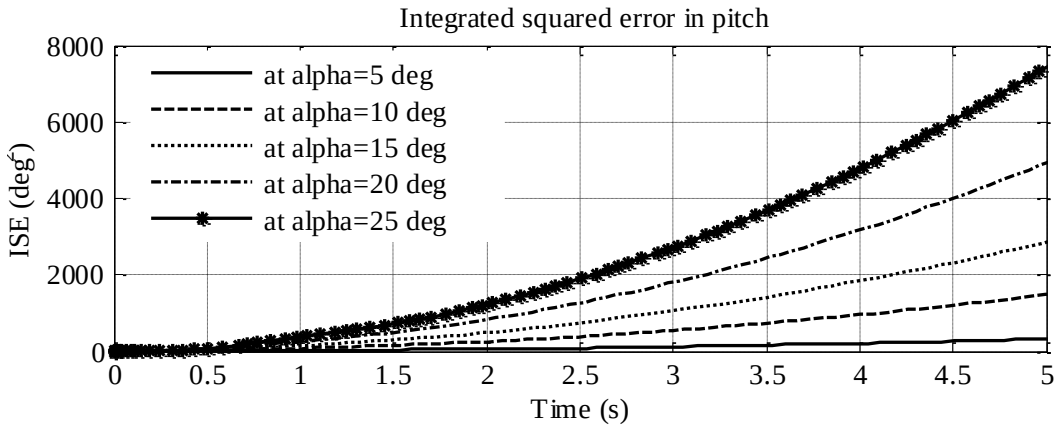

(d)

Figure 5-9: Performance of the GS controller on inclined terrain (a) Transient response of pitch and pitch rate (b) Transient response of velocity (c) Torque demand (d) Integrated squared error of pitch.

5.2.3. Stability Analysis

The local closed loop system matrices of the TWR with the GS controller were found Hurwitz as their poles of the system transfer function were negative real parts. The local controllers, therefore, fulfil the necessary and sufficient condition for a closed loop system to be stable. The stability of the global gain-scheduling controller was ensured in simulations by interpolating between the local controllers for this setup by starting and finishing the run on same inclined terrain. This fulfils the first condition of stability [129], namely, to keep very slow change in scheduling variable. In order to fulfil the second condition, that the scheduling variable captures nonlinearities of the plant; the states of the systems were considered as a function of the scheduling variable in their dynamic equations (chapter 2). The variation of the pitch and pitch rate is shown in Figure 5-10. The plot describes the instability of the robot beyond 60 degrees of initial pitch.

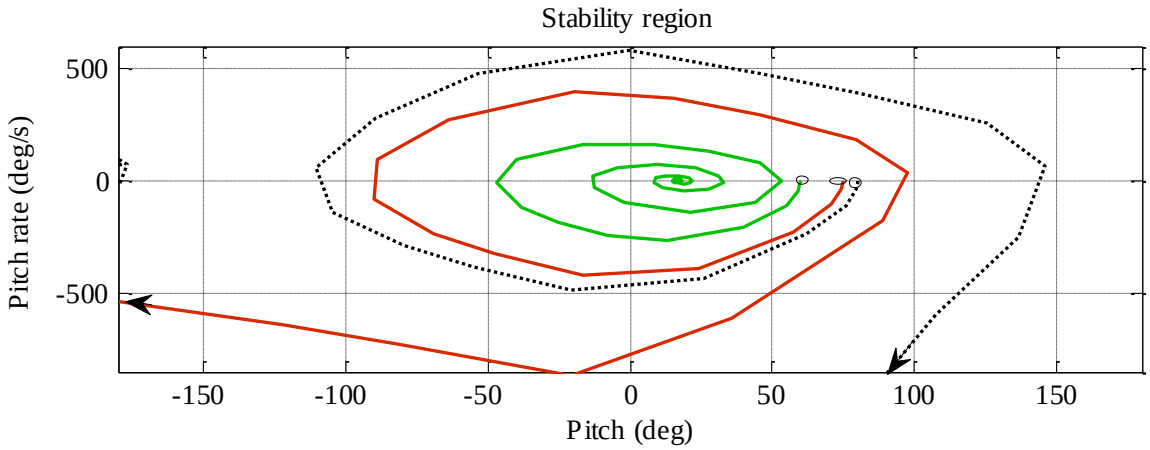

Figure 5-10: Stability of the TWR on an inclined terrain with the GS controller.

As Figure 5-10 illustrates, the stability of the robot above 60 deg inclined terrain is not guaranteed. In the next section, therefore, a nonlinear controller is designed and presented to control the TWR on inclined terrain with augmented stability region.

5.3. Lyapunov Function Based Control of TWRs

A baseline controller was designed for TWRs with a linearized approximation of the nonlinear plant. There is no guarantee of overall performance of linear design and therefore a nonlinear GS controller was designed for TWR motion on inclined terrain. The GS controller which guarantees the stability of local controllers does not guarantee the same stability at intermediate operating points where the gains were interpolated as well as stability region is limited. To overcome this problem, a nonlinear Lyapunov function based controller is designed and presented in this section. The objective of LFBC was to guarantee the stability of the control on inclined terrain and increase the stability region as well as control the robot body balance and velocity tracking. A LFBC was developed (chapter 3) for two wheeled robots motion on uneven terrain. The controller was synthesised for a domain of attraction. The same controller is reduced for TWRs motion on inclined terrain as given in the following subsections.

5.3.1. Model Normalization and Partial Feedback Linearization

In order to design the LFBC for the TWR motion on inclined terrain, the dynamic equations of motion of the system (2.13) & (2.14) were reduced to (2.15) and (2.16). These are simplified, normalized and partially linearized to convert into an affine form which is used for LFBC design.

(a) Model simplification

The equation (2.15) is divided by Ml^2 and (2.16) is divided by Mlr to simplify the set of reduced dynamic equations. The results are as follows:

$$\left[-\frac{1}{l}(\tan\alpha.sin\theta+\cos\theta)\right]\ddot{x}-\left(1+\frac{I_p}{Ml^2}\right)\ddot{\theta}+\frac{g}{l}\,sin\theta\;=0 \tag{5.2}$$

$$\left[\frac{1}{\mathrm{l}.\cos\alpha}\left(1+\frac{m}{M}\right)+\frac{I}{Mlr^2}\right]\ddot{x}\;-\frac{r}{l}\left(1+\frac{m}{M}\right)sin(\alpha)+\left[\ddot{\theta}.cos(\theta+\alpha)-\dot{\theta}^2.sin(\theta-\alpha)\right]=\frac{T}{Mlr} \tag{5.3}$$

(b) Model normalization

The following scaling transformations were substituted in (5.2) and (5.3) to achieve normalization:

$$q=\frac{x}{l}\;;\qquad \dot{x}=l\dot{q};\qquad \ddot{x}=l\ddot{q};\qquad \delta=\frac{m}{M}\;;\qquad a_1=\frac{I_p}{Ml^2}\;;\qquad a_2=\frac{I}{Mr^2}\quad ;u=\frac{T}{Mlr}$$

The dynamic equations, with scaling factors, appear as

$$A_1\ddot{q}+(1+a_1)\ddot{\theta}-\frac{g}{l}\sin\theta=0 \tag{5.4}$$

$$A_2\ddot{q}+\cos(\theta+\alpha)\,\ddot{\theta}-\frac{g}{l}(1+\delta)\sin\alpha-\sin(\theta-\alpha)\dot{\theta}^2\;=u \tag{5.5}$$

where,

$A_1=\sin\theta\tan\alpha+\cos\theta$

$A_2=\frac{1+\delta}{\cos\alpha}+a_2$

(c) Partial feedback linearization

The normalised system equations (5.4) and (5.5) were partially linearized to reduce inertial coupling and the outputs collocation with the input. The inertia matrix of the system is symmetric and positive definite. The elements of the inertia, coriolis and gravitational

matrices for a TWR dynamic equations developed for motion on inclined terrain are as follows:

$$M_{11} = 1 + a_1 \; ; M_{12} = \sin\theta \tan\alpha + \cos\theta = A_1 \quad ; M_{21} = \cos(\theta + \alpha) \quad ; M_{22} = A_2$$

$$\emptyset_1 = -\frac{g}{l}\sin\theta \quad ; \emptyset_2 = -\frac{g}{l}(1+\delta)\sin\alpha \; ; h_1 = 0 \quad ; h_2 = -\sin(\theta-\alpha)\dot{\theta}^2 \quad ; \mathrm{T} = \mathrm{u}$$

$$\overline{M_{22}} = M_{22} - \frac{M_{12}.M_{21}}{M_{11}} = A_2 - \frac{(\sin\theta\tan\alpha+\cos\theta)\cos(\theta+\alpha)}{1+a_1}$$

$$\overline{h_2} = h_2 - \frac{M_{21}}{M_{11}}h_1 = -\sin(\theta-\alpha)\dot{\theta}^2 = h_2$$

$$\overline{\emptyset_2} = \emptyset_2 - \frac{M_{21}}{M_{11}}\emptyset_1 = -\frac{g}{l}(1+\delta)\sin\alpha + \frac{g}{l}\frac{\sin\theta.\cos(\theta+\alpha)}{1+a_1}$$

The new control variable u is written as (5.6), following the method used in chapter 3:

$$u = v\left[A_2 - \frac{A_1\cos(\theta+\alpha)}{1+a_1}\right] + h_2 - \frac{g}{l}\left[(1+\delta)\sin\alpha - \frac{\sin\theta.\cos(\theta+\alpha)}{1+a_1}\right] \tag{5.6}$$

The feedback system dynamic equations equivalent to the normalized system with new control input v are given as (5.7) below:

$$\ddot{q} = v$$
$$\ddot{\theta} = \frac{-\emptyset_1 - A_1 v}{1+a_1} \tag{5.7}$$

The set of equations (5.7) represents dynamics of statically unstable TWRs motion on inclined terrain in an affine form. The equation $q" = v$ is linear and second order. The second equation $\ddot{\theta} = \frac{-\emptyset_1 - A_1 v}{1+a_1}$, therefore, represents the internal dynamics of the system.

5.3.2. Controller Formulation

Assuming the system states θ , $\dot{\theta}$, $\dot{q}$ and the wheel-terrain contact angle α are known, the system perturbation bound is proposed as (3.19). k_1 , a positive constant, is used for tuning the controller to get best controller performance. A constraint based Lyapunov function is developed using a constructive method. The constructive method presents a flexibility to add more states to the Lyapunov function without changing the basic function proposed for the system. For the two wheeled robot system, initially a Lyapunov control function is proposed

for two states (θ and $\dot{\theta}$) of the system. Then a term is added for an additional state, for example, $\dot{q}$ using added integration method.

(a) Control Lyapunov function with θ and $\dot{\theta}$

The constraint function proposed for TWR on inclined terrain, $[k_1 cos^2 e_\theta - l]$, is positive unless $k_1 cos^2 e_\theta - l = 0$ and bounds the pitch θ of the IB with respect to the terrain inclination. The constrained pitch denoted as $\tilde{\theta}$ is given by:

$$\theta < \tilde{\theta} = \left(\theta_d - \left[cos^{-1}\left(\sqrt{\frac{l}{k_1}}\right)\right]\right).$$

where $e_\theta = \theta_d - \theta$ and θ_d is the desired equilibrium pitch. The control Lyapunov function proposed to synthesise controller to control pitch and pitch rate of the TWR is (5.8):

$$V_{i0}(\theta, \dot{\theta}) = \frac{1}{2}[k_1 cos^2 e_\theta - l]\dot{e_\theta}^2 + l.[1 - cose_\theta] \quad (5.8)$$

(b) *Time derivative of control Lyapunov function*

The time derivative of the control Lyapunov function for two states is given as follows:

$$\dot{V_{i0}} = \dot{e_\theta} cose_\theta \left[v\gamma(\theta, \alpha) + k_1\beta(\theta, \theta', \alpha) - \frac{l}{\cos e_\theta}\left(\ddot{\theta_d} - \sin e_\theta + \frac{\emptyset_1 + h_1}{1 + a_1}\right)\right],$$

Such that

$$\gamma = \frac{A_1}{(1+a_1)\cos e_\theta}\,[k_1 cos^2 e_\theta - l] \quad (5.9)$$

$$\beta = \cos e_\theta \left(\ddot{\theta_d} - \dot{e_\theta}^2 \sin e_\theta + \frac{\emptyset_1 + h_1}{1 + a_1}\right) \quad (5.10)$$

(c) Control Lyapunov function with $\theta, \dot{\theta}$ and $\dot{q}$

In order to track the desired robot velocity in addition to pitch and pitch rate for TWRs motion on inclined terrain, a quadratic term is added. This term is selected such that the derivative of the additional term has the same structure as the derivative of Lyapunov function proposed in section *5.3.1*. The structure of Lyapunov function representing three states is proposed as:

$$V_{i1}(\theta, \theta', q') = k_d\, V_{i0} + \frac{1}{2} {W_i}^2$$

W_i is an unknown variable which is function of $\theta, \dot{\theta}\ and\ \dot{q}$ and is derived as (5.11):

$$W_i(\theta, \theta', q') = \frac{A_1 + 1 + a_1\ (k_1 \cos\ e_\theta\ {\dot{e_\theta}}^2\ )}{1 + a_1} - \frac{\mathrm{l} A_1 e_{\dot{q}}}{(1 + a_1) \cos\ e_\theta}$$

This gives:

$$V_{i1} = k_d\, V_{i0}(\theta, \theta') + \frac{1}{2}\left[\frac{A_1+1+a_1\ (k_1 \cos\ e_\theta\ {\dot{e_\theta}}^2\ )}{1+a_1} - \frac{\mathrm{l} A_1 e_{\dot{q}}}{(1+a_1) \cos\ e_\theta}\right]^2 \qquad (5.12)$$

This control Lyapunov function not only characterises the three states of a TWR motion on an inclined terrain, it also considers the effect of wheel-terrain contact angle and control gains, representing complete closed loop energy function.

(d) Time derivative of control Lyapunov function with $\theta, \dot{\theta} and\ \dot{q}$

Time derivative of the control Lyapunov function (5.12) is as follows:

$$\dot{V_{i1}}(\theta, \theta', q') = k_d\, \dot{V_{i0}} + W_i \dot{W_i} \qquad (5.13)$$

Substituting $\dot{V_{i0}}$, W_i and $\dot{W_i}$ in (5.13) provides the time derivative (5.14).

$$\dot{V_{i1}}(\theta, \theta', q') = \left(v\gamma + k_1\beta + \frac{l}{\cos e_\theta}\left(\sin e_\theta - \frac{\emptyset_1 + h_1}{1+a_1}\right)\right)\zeta \qquad (5.14)$$

where,

$$\zeta = \dot{e_\theta} \cos e_\theta\ \left[k_d + \frac{k_1 A_1}{1+a_1}\ + \frac{k_1 e_\theta\ \cos e_\theta}{2}\right] - \frac{\mathrm{l} A_1 e_{\dot{q}}}{(1+a_1) \cos\ e_\theta} \qquad (5.15)$$

The derivative of control Lyapunov function shows the behaviour of change of energy of the TWR while moving on inclined terrain. The system stability can be derived from the direction of variation of this derivative.

(e) Control Law

A control law is synthesised for TWRs motion on inclined terrain, using the derivative of the control Lyapunov function (5.14). The control Lyapunov function based control law was

derived finding an expression for the control input v such that this makes $\dot{V_{i1}} \leq 0$, semi negative definite, and converges $\theta, \dot{\theta} and\ \dot{q}$ asymptotically to zero. Let,

$$v\gamma + k_1\beta + \frac{l}{\cos e_\theta}\left(\sin e_\theta - \frac{\emptyset_1 + h_1}{1+a_1}\right) = -\zeta$$

$$\Rightarrow \quad v = \frac{-\zeta - k_1\beta - \frac{l}{\cos e_\theta}\left(\sin e_\theta - \frac{\emptyset_1 + h_1}{1+a_1}\right)}{\gamma}$$

$$\Rightarrow \quad v = \frac{-1}{\gamma(\theta)}\left(\zeta + k_1\beta + \frac{l}{\cos e_\theta}\left(\sin e_\theta - \frac{\emptyset_1 + h_1}{1+a_1}\right)\right) \qquad (5.16)$$

This produces

$$\dot{V_{i1}} = -\zeta^2$$

As $\dot{V_{i1}}$ becomes semi negative definite, it converges $\theta, \dot{\theta} and\ \dot{q}$ asymptotically to zero.

5.3.3. Stability Region

The stability region of TWRs on inclined terrain system with two controlled states $\theta, \dot{\theta}$ is defined as a compact set (5.17).

$$\Omega_{i0} = \left\{\left(\theta, \dot{\theta}\ \right) \epsilon\, R^2 :\ V_{i0} < 1 - \cos\left(\tilde{\theta} - \alpha\right)\right\} \qquad (5.17)$$

This is a compact set when initial condition $(\theta_0, \theta_0{}')$ with $|\theta_0| < \frac{\pi}{2}$ satisfies that $V_{i0} < 1 - \cos\left(\tilde{\theta} - \alpha\right)$ and $|\theta| < \tilde{\theta}$. Similarly, the stability region of the system with three controlled states $\theta, \dot{\theta} and\ \dot{q}$ is defined as (5.18):

$$\Omega_{i1} = \left\{\left(\theta, \dot{\theta}, \dot{q}\ \right), |\theta| < \tilde{\theta} : V_{i1} < K\right\} \qquad (5.18)$$

This stability region was derived finding a condition when the TWR system has a singularity at $|\theta| = \pm\tilde{\theta}$. Equation (5.8) suggested $|\theta_0|$ should be less than $\frac{\pi}{2}$ and $V_{i1} < K = k_d\left(1 - cos(\theta - \alpha)\right)$. This should also belong to the neighbourhood of the origin to avoid singularity at $|\theta| = \pm\tilde{\theta}$. In other words states are bounded with $|\theta| < \tilde{\theta}$ if $|\theta(t)| < \tilde{\theta}$ and $V_{i1} < K$. $V_{i1} < K$, is an outcome from the fact that V_{i1} is a non- increasing function ($\dot{V_{i1}} = -\zeta^2\left(\theta, \dot{\theta}, \dot{q}\ \right)$).

The stability region of the TWR on inclined terrain, therefore, is defined as the set of all

initial values of θ, θ', q' ,such that $|\theta| < \tilde{\theta}$ and $V_{i1} < K$, which stabilize the unstable equilibrium point of the closed loop TWR with the proposed controller. This stability is in the sense of Lyapunov as it fulfils the Lyapunov stability conditions i.e. $V_{i1}(\boldsymbol{x})$ is a positive definite function for all $\boldsymbol{x} \epsilon \Omega_1$ and $\dot{V_{i1}}(\boldsymbol{x})$ is negative semi definite for $\boldsymbol{x}$.

5.3.4. Performance Evaluation

The performance of the closed loop TWR on a flat inclined terrain is evaluated to illustrate the effectiveness of the proposed LFBC law in simulations using MATLAB and SIMULINK. The tests were performed for the evaluation of velocity tracking and stabilization of the IB of closed-loop system. The performance metrics used were transient response, velocity tracking error, and torque demand. The physical parameters of the TWR system are given in the Table 2.1 which represents a real time full scale two wheeled robotic platform. All the states $(\theta, \dot{\theta}, \dot{q})$ were assumed to be measurable and are fed back for the controller.

The simulation was performed to observe the stabilization of the robot at equilibrium points each relative to the wheel-terrain contact angle. A series of the same tests were conducted for reference velocity range 0-0.5 m/s with initial pitch $\theta = 15$ degrees to investigate the controller performance for the TWR velocity tracking. After 10 seconds run, the data for different states was recorded for the purpose of performance analysis. Plots of Figure 5-11 are drawn by changing the terrain angle yet keeping the reference speed to zero and pitch to respective equilibrium point. The initial pitch was taken closer to the equilibrium pitch. The controller gains were kept the same in all simulations.

Figure 5-11 confirms the tracking of pitch positions only the pitch takes longer to settle with an increase in terrain inclination angle. The controller brings the robot close to stationary condition within 3 seconds demanding a torque which increases with an increase in wheel-terrain contact angle. Figure 5-12 shows the non-zero velocities are tracked smoothly within 2m movement of the robot. The two states are plotted in Figure 5-13 to observe the stability region of the TWR. The results show a smooth manoeuvre of states from 80 deg pitch to the equilibrium pitch 15 deg. The stability region produced with LFBC is shown in Figure 5-14 which in comparison to GS stability region (Figure 5-10) has a wide range which proves the utilization of the LFBC.

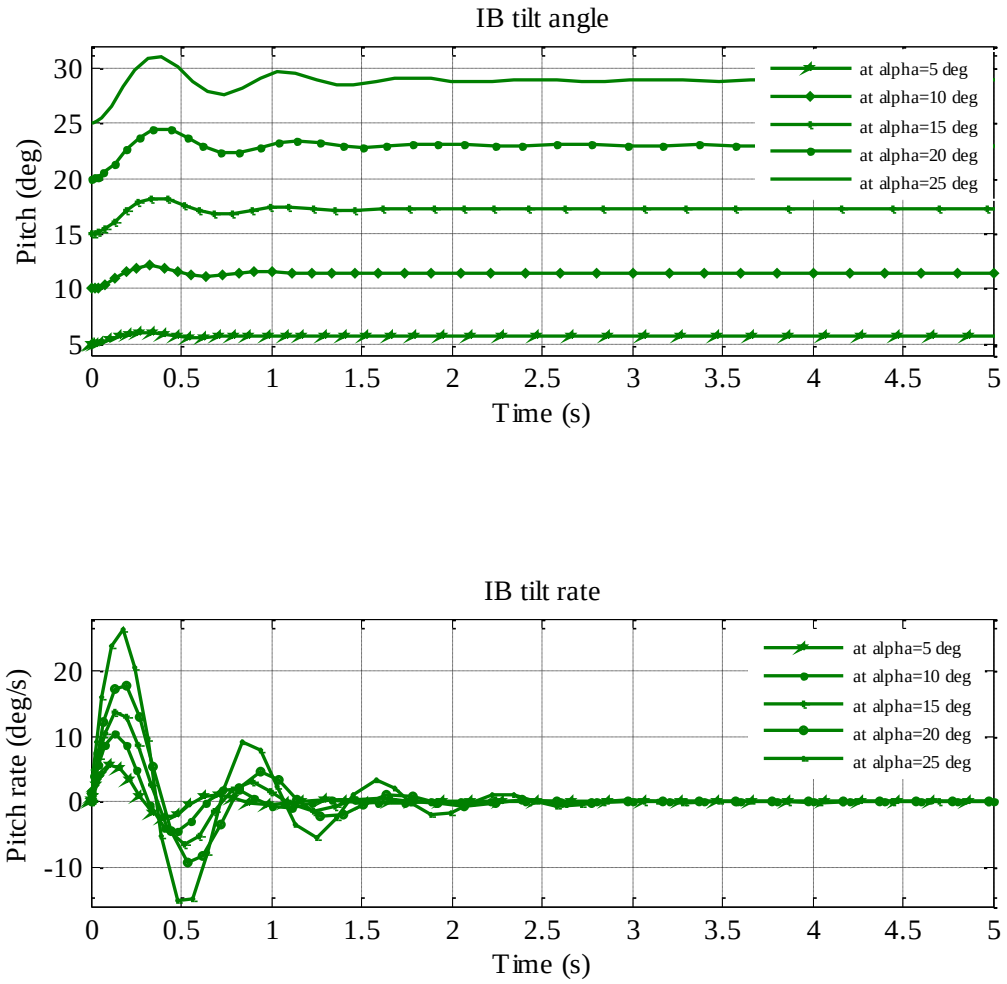

Figure 5-11: Transient response of pitch and pitch rate with LFBC for the TWR closed loop system moving on inclined terrain.

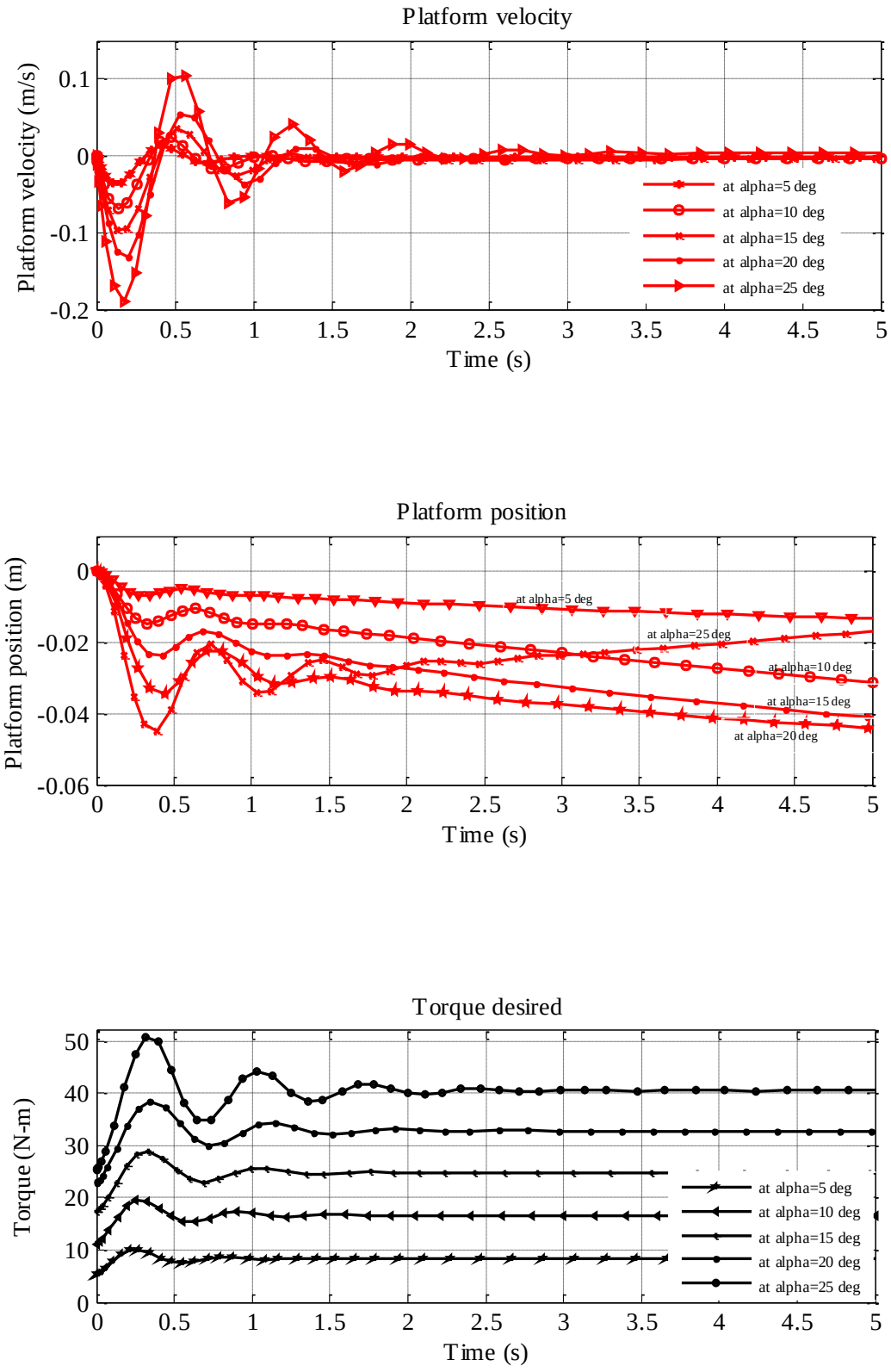

Figure 5-12: Transient response of position and velocity and torque demanded with LFBC for the TWR closed loop system moving on inclined terrain.

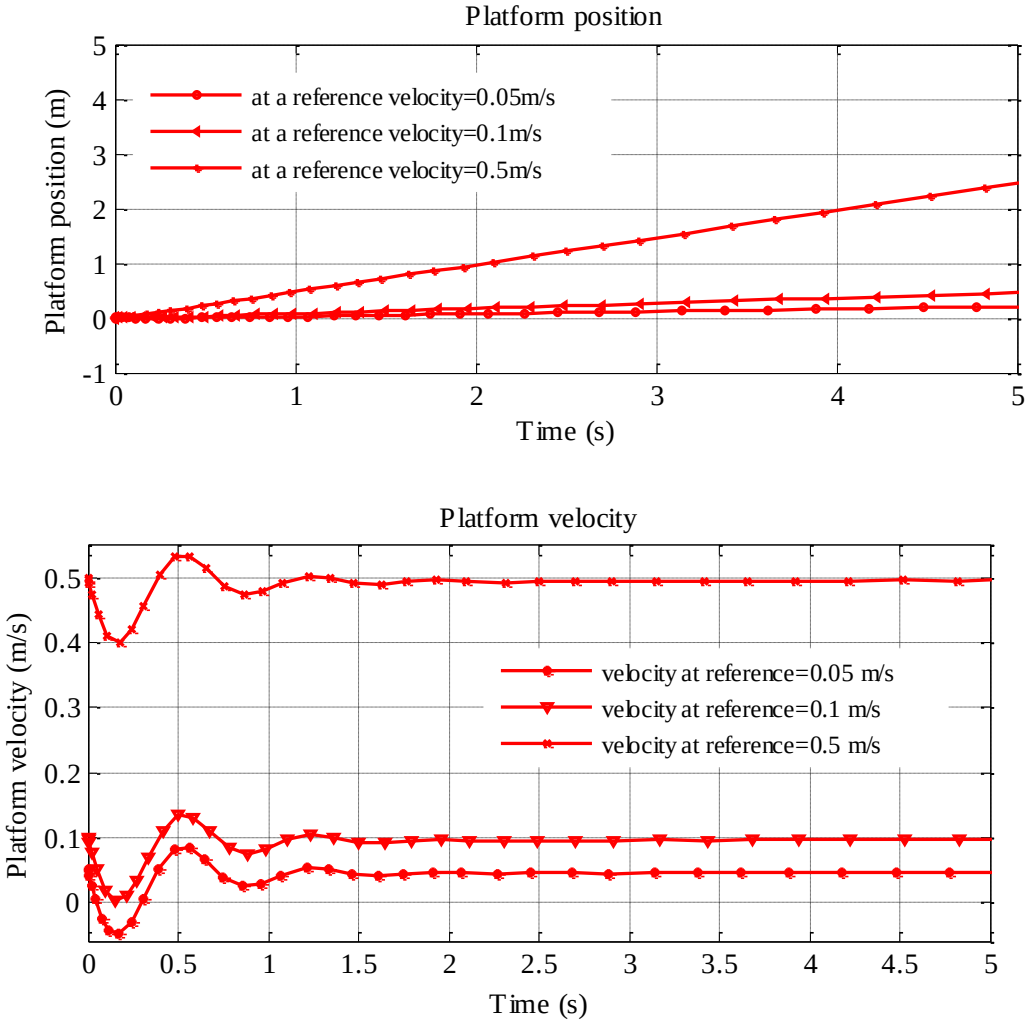

Figure 5-13: Velocity Tracking with LFBC for the TWR closed loop system moving on inclined terrain.

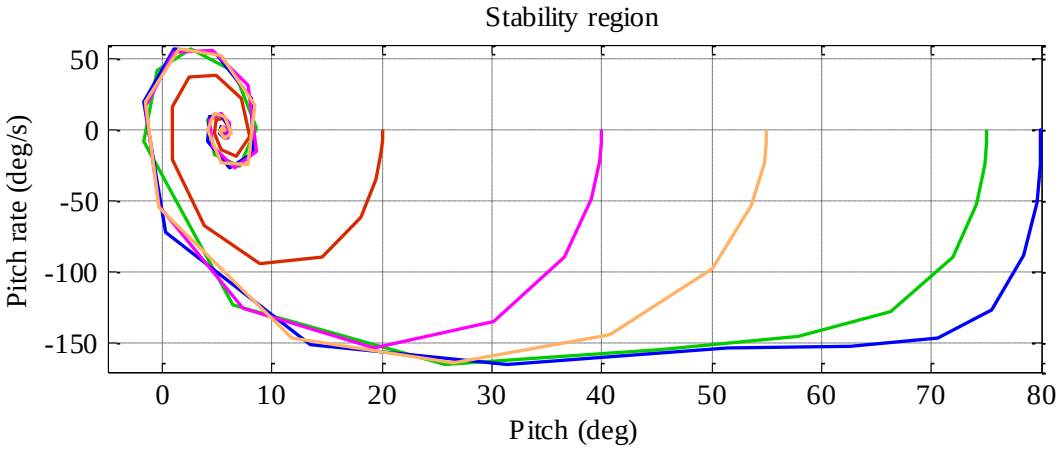

Figure 5-14: Stability region of pitch and pitch rate simulated on an inclined terrain with wheel terrain contact angle = 15 degrees.

5.3.5. Conclusions

A linear FSFB controller, designed as a baseline controller to control stability and track the velocity of two-wheeled mobile robots on inclined terrain, stabilizes the TWR in the neighbourhood of the equilibrium point. To provide a versatile control, on terrain of different inclination angles, a nonlinear GS controller was designed. Then a nonlinear Lyapunov function based control scheme was developed to enhance and guarantee the stability with the same basic control objective. This control scheme also allowed computation of stability region of the TWR. The performance of each of the control schemes was evaluated on inclined terrain. The controllers were evaluated and stability region was computed in three situations, in order to compare performance of the proposed nonlinear LFBC with a GS controller and linear FSFB controller. Simulation results illustrate the performance of the linear and nonlinear control schemes for the TWR. They reveal that LFBC delivers or demonstrates all the advantages of conventional FSFB control and guarantees the stability with broader stability region by utilizing a novel control Lyapunov function. For these reasons LFBC is tested for the application of the TWR on uneven terrain (Chapter. 6).

Chapter 6. Control of a Two-Wheeled Robot on Uneven Terrain

The disturbance forces generated at wheel-terrain contact point by a variation of slope in an uneven terrain change the dynamics of two wheeled robots. These disturbance forces depend on the rate of variation of the slope. The accelerations generated by the change in rate of slope variation cause a need for an extra control torque. In this chapter, three control schemes were designed and their performance was investigated in simulations. A linear FSFB controller, designed for horizontal terrain (chapter 4), was tested on uneven terrain. The performance of an LQR based gain scheduled (GS) controller, designed using wheel-terrain contact angle as a scheduling variable, was tested. A rapid variation in wheel-terrain contact angle did not guarantee the stability of the closed loop system and, therefore, a control Lyapunov function based nonlinear controller was developed to stabilize the TWR on uneven terrain. The stability of the proposed closed loop system was analysed using LaSalle's theorem and a stability region was computed. The simulation results show that the control Lyapunov function based controller stabilizes the TWR on uneven terrain with guaranteed stability and less power consumption as compared to the FSFB and the GS controllers.

6.1. Uneven Terrain Generation

The slope of uneven terrain changes with time or position. In this study the uneven terrain is assumed to be changing with the position of the robot. The terrain is, therefore, generated as a function of the position. For the three controllers implemented below the position of the robot is assumed to be known. The uneven terrain selected for experiments was a bump which was defined as a piecewise continuous function (6.1).

$$z(x) = \begin{cases} k\, e^{1/1-(x-2)^2} & for\ 1<x<3 \\ 0 & otherwise \end{cases} \tag{6.1}$$

This is the simplest analytical function that generates a surface with one bump which represents both uphill and downhill situations of inclination. *k* is a constant that varies the elevation of the bump. The terrain is assumed to be smooth and flat. This is designed in three segments joined together such that the first part is horizontal to a length of 1m from the starting point. Then there is a bump, modelled over a length of 2m, shown in Figure 6-1. The maximum bump height selected for simulations is 18.4cm. This height ensures that the radius of curvature of the terrain plane is always greater than the radius of the wheel of the two wheeled robot. This ensures the assumption of a single contact point of the wheel is

maintained. After the bump, terrain again becomes horizontal. Each segment of the terrain is modelled as a rigid surface.

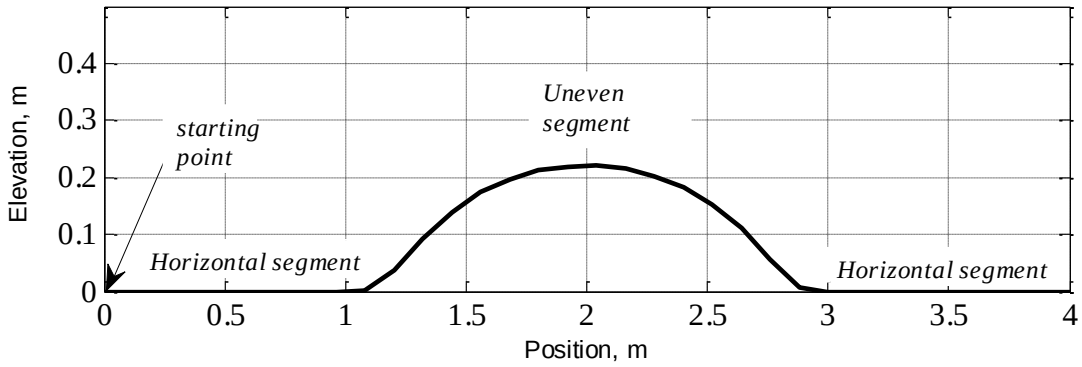

Figure 6-1: Simulated Uneven Terrain (a bump)

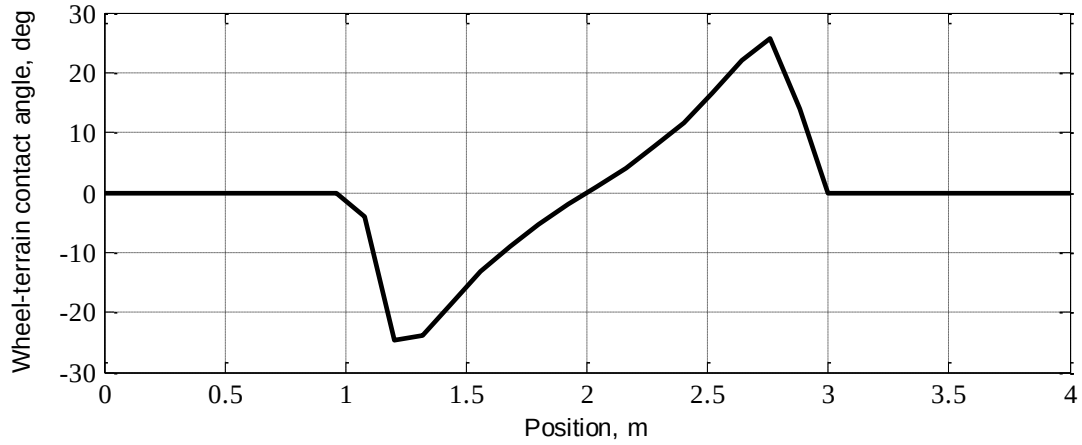

Figure 6-2: Wheel-terrain contact angle on the bump with respect to the position

The uneven terrain was generated for simulations using MATLAB-SIMULINK. The code was generated in MATLAB and was implemented in Simulink using a function block.

6.2. Baseline Controller

The full state feedback (FSFB) controller based on LQR (chapter 4) is evaluated on the bump, an uneven terrain. The controller is designed to output optimal gains to regulate the IB position and track the desired velocity of TWRs. As FSFB is a linear controller, it is stable only in the neighbourhood of the equilibrium state, so the controller tuned for horizontal terrain is implemented on the bump. The integral of velocity error is used to correct the velocity to eliminate steady state error. The objective of control is to minimize steady state error in pitch, a quick response and least possible overshoot of pitch.

In order to test the control algorithm for the TWR moving on a bump, the simulations are carried out with a reference velocity of 0.5m/s. The initial conditions for position, linear velocity, pitch rate and the pitch are set to zero. The robot is allowed to traverse over a length of 10m of the simulated terrain. The initial 3m of which is same as shown in Figure 6-2 and the rest 7m length of the terrain is flat horizontal terrain. To allow the robot to stabilise and settle the last part of the terrain was designed to be longer. The performance metrics listed in chapter 3 (section 3.4) are calculated to quantify the performance of the controller for the TWR moving on uneven terrain, to replicate a bumpy terrain.

6.2.1. Results and Discussion

A transient response of states of the TWR is unstable as shown in Figure 6-3. The response is plotted for two reference velocities: 10 cm/s and 50 cm/s. At both velocities the IB topples down and system becomes unstable at the length of 1.05 m where the bumpy terrain starts. It is, therefore, concluded that the torque demand produced by the baseline controller is not enough to compensate for the effect of dynamic forces exerted at the wheel-terrain contact point at an inclination of terrain.

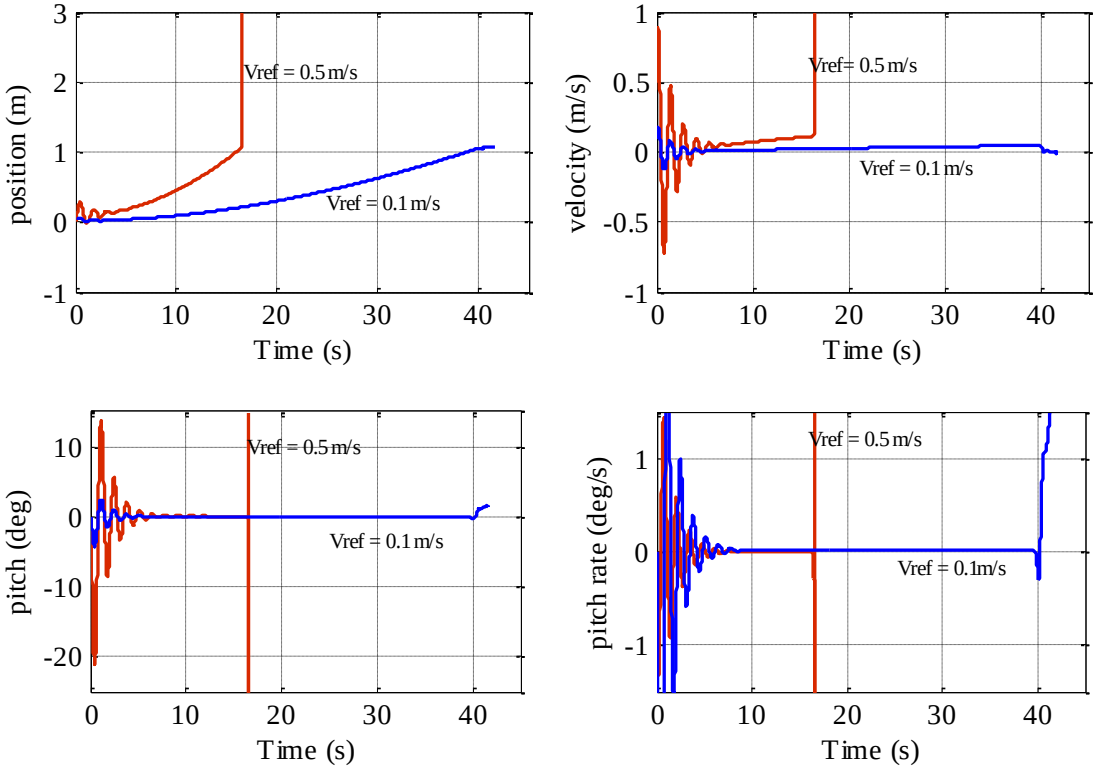

Figure 6-3: Performance of the baseline controller on the bump for a TWR shown as a transient response of position, pitch, pitch rate and velocity tracking.

Closed loop poles were calculated at different terrain angles without changing controller gains. A variation in the closed-loop poles of the system was observed. At the point the dominant closed-loop pole was getting closer to the imaginary axis it became complex. The other poles were moving far away indicating the system was moving towards instability. In order to overcome the additional forces, at the point the where the wheel touches the inclined terrain, and the force variation is at certain rate the linear controller can be tuned at a number of equally distant points. This will provide the extra push required to overcome the external acceleration components relative to the inclination of the terrain and rate of change of terrain.

6.3. Gain-Scheduled Controller

Due to a variation in the wheel-terrain contact angle the operating conditions at different points on an uneven terrain change. The rate of change of the slope on an uneven terrain also induces disturbance torque. These variations demand variable control input to the actuators. A fixed gain linear controller does not work in this situation as concluded in the previous section. A Gain-Scheduled controller is, therefore, proposed to generate variable control according to variation in the wheel-terrain contact angle. The Wheel-terrain contact angle is assumed to be available for the controller in advance as a scheduling variable. As presented in chapter 3, based on the clearance of the base of the IB from the flat horizontal terrain, the geometry of a robot IB, the relationship to find a range of allowable wheel-terrain contact angle on an uneven terrain is assumed to be at 30^o for the purposes of designing the controller.

The gain-scheduled controller designed for the TWR moving on inclined terrain (chapter 5) is used for uneven terrain in this chapter. The range of 30^o was divided into six steps with a step size of 5^o. The controller gains, calculated at designed operating conditions, were linearly interpolated for unknown operating points. The equilibrium point deemed for the control design was at zero linear velocity and zero pitch rates, even though the pitch varies with the wheel-terrain contact angle. The objective of the gain-scheduled controller design was to balance the IB of a TWR at the equilibrium point and follow the desired velocity of the robot on uneven terrain. The GS control law implemented was as (6.2):

$$u = -K_x(\boldsymbol{\alpha})\boldsymbol{X} - K_r(\boldsymbol{\alpha})e_r \tag{6.2}$$

The controller parameters were calculated for the same TWR physical parameters given in Table 2.1. The plant and controller parameters were updated during experiments as a function of the wheel-terrain contact angle.

6.3.1. Performance Quantification

A major advantage of the GS control method is its ability to generate variable control demand as a function of the wheel-terrain contact angle. The TWR is subjected to move on a bump described in section 6.2. The performance is evaluated in simulations. The nonlinear plant model was used to represent the TWR dynamics on uneven terrain and linear interpolation blocks were used for gain of each state. The initial conditions for linear position, linear velocity, pitch rate and the pitch were fixed as zero. The first set of tests is performed for stationary balancing of the TWR at different points on the bump. The second set of tests was conducted to demonstrate how the GS controller performs if the TWR is on the bump and the IB is disturbed from the equilibrium pitch.

Only two representative results for stationary balancing are shown here. The TWR is balanced at its equilibrium IB position as shown in Figure 6-4(c) using GS controller. The data for states: velocity, pitch and pitch rate are plotted for stationary balancing. It is concluded from the results that at high wheel-terrain contact angles the transient response gets worse due to rapid and large variation of terrain slope. The transient response also shows the stability region is limited to a very close neighbourhood of the equilibrium position of the IB.

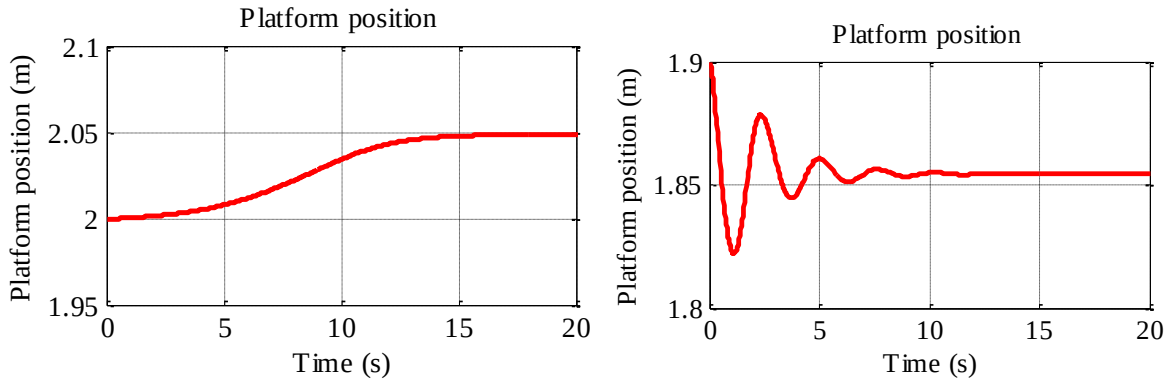

(a)

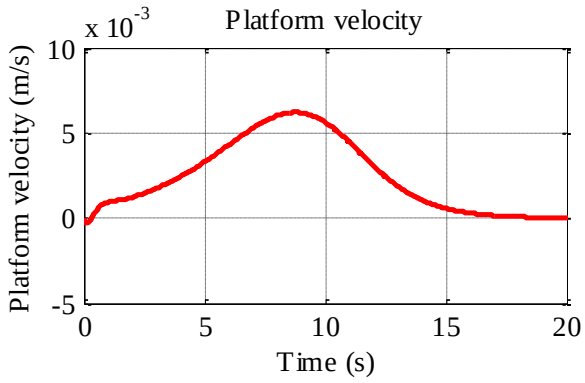
x 10^-3
Platform velocity
Platform velocity (m/s)
10
5
0
-5
0
5
10
15
20
Time (s)

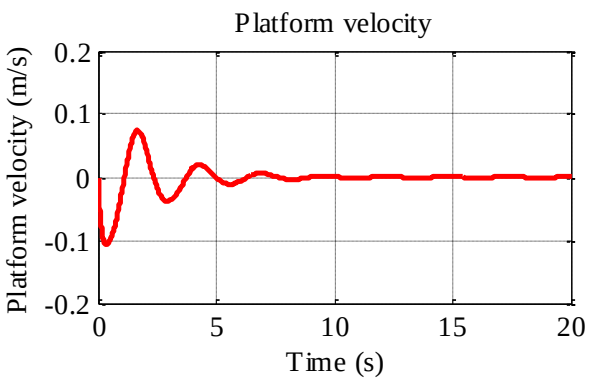
Platform velocity
Platform velocity (m/s)
0.2
0.1
0
-0.1
-0.2
0
5
10
15
20
Time (s)

(b)

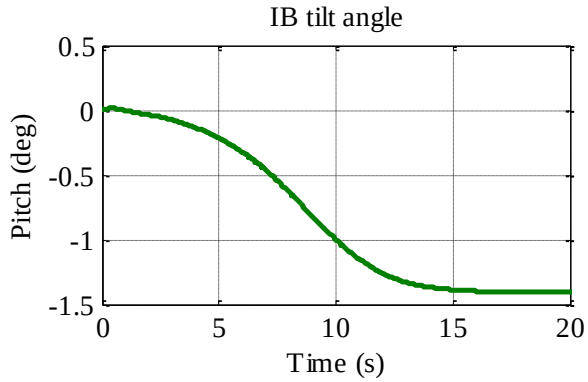
IB tilt angle
Pitch (deg)
0.5
0
-0.5
-1
-1.5
0
5
10
15
20
Time (s)

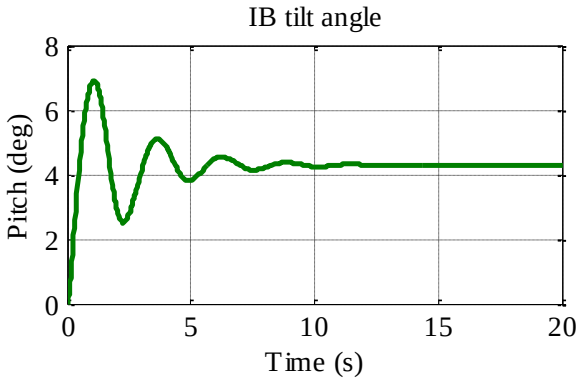
IB tilt angle
Pitch (deg)
8
6
4
2
0
0
5
10
15
20
Time (s)

(c)

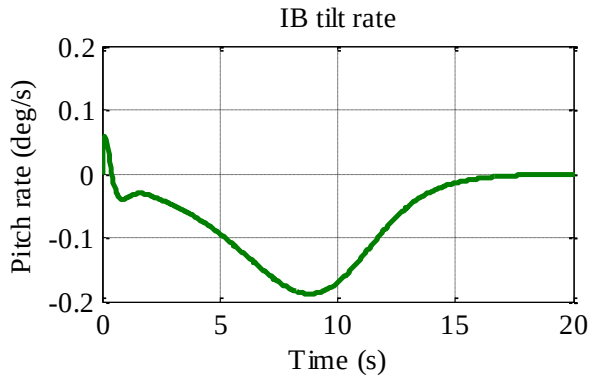
IB tilt rate
Pitch rate (deg/s)
0.2
0.1
0
-0.1
-0.2
0
5
10
15
20
Time (s)

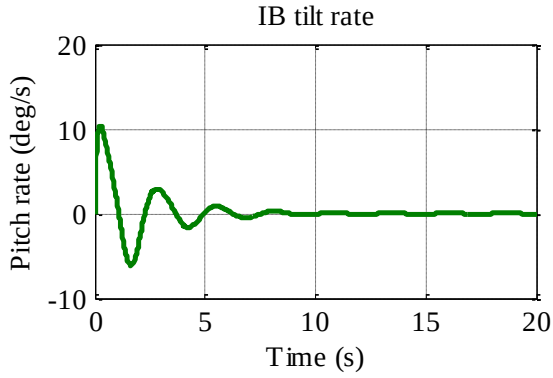
IB tilt rate
Pitch rate (deg/s)
20
10
0
-10
0
5
10
15
20
Time (s)

(d)

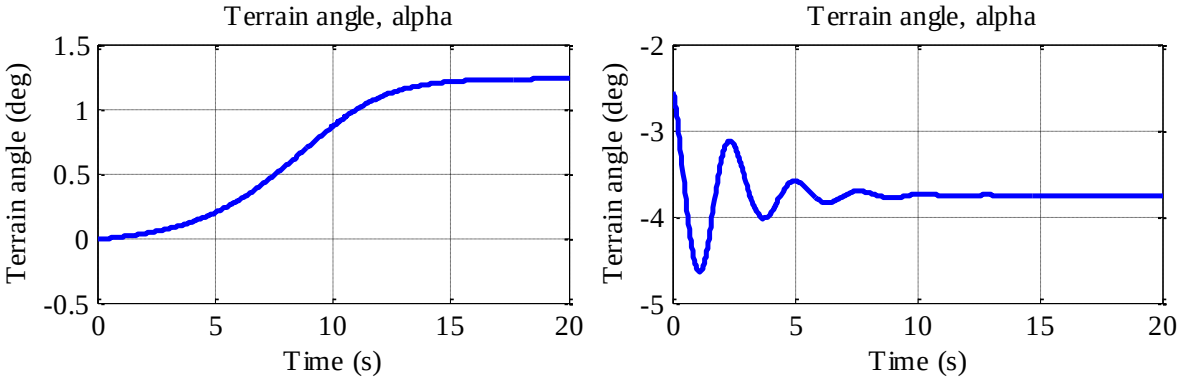

(e)

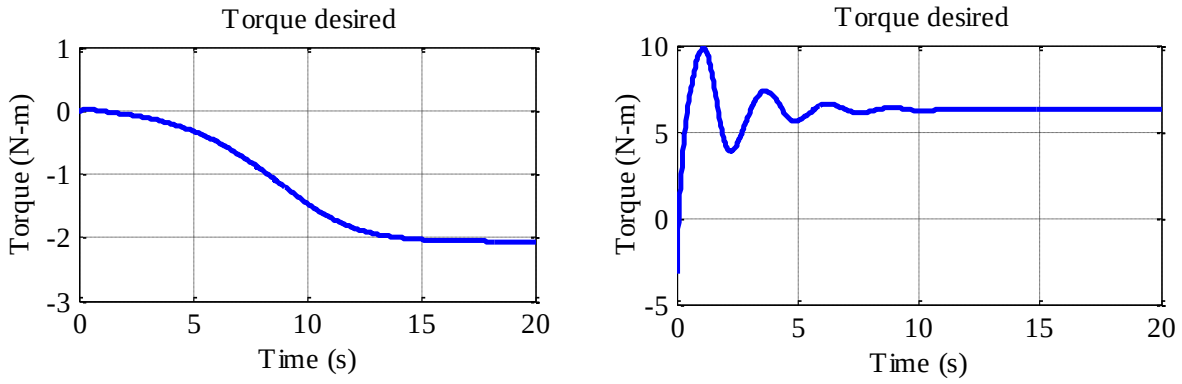

(f)

Figure 6-4: Transient response of states to regulate balanced position of the IB and keep the TWR stationary at different positions on a bump: (a) Position (b) Velocity (c) Pitch (d) Pitch rate (e) Wheel-Terrain contact angle (f) Torque.

Ten tests were carried for a range of the reference velocities. This range varied from 0-1 m/s with gaps of 0.1. In these tests the TWR starts motion from the starting point of the designed terrain, for example, the horizontal terrain, goes over the bump and finishes the run at horizontal terrain. Although the GS controller gains are smoothly interpolated for the range of wheel-terrain contact angle variation the increase in the rate and in the variation of the slope of the terrain affects the control negatively. The control is lost at a high variation rate. This is due to a limitation of the GS controller applied to the TWR. The pitch has to be corrected at every time step, due to the change in terrain slope which increases the integrated energy or power required for the motion over the bump. This also increases the integrated squared error in pitch shown in Figure 6-5. This suggests the use of high power motors in TWRs to traverse on the high inclination bumps and other kinds of uneven terrain.

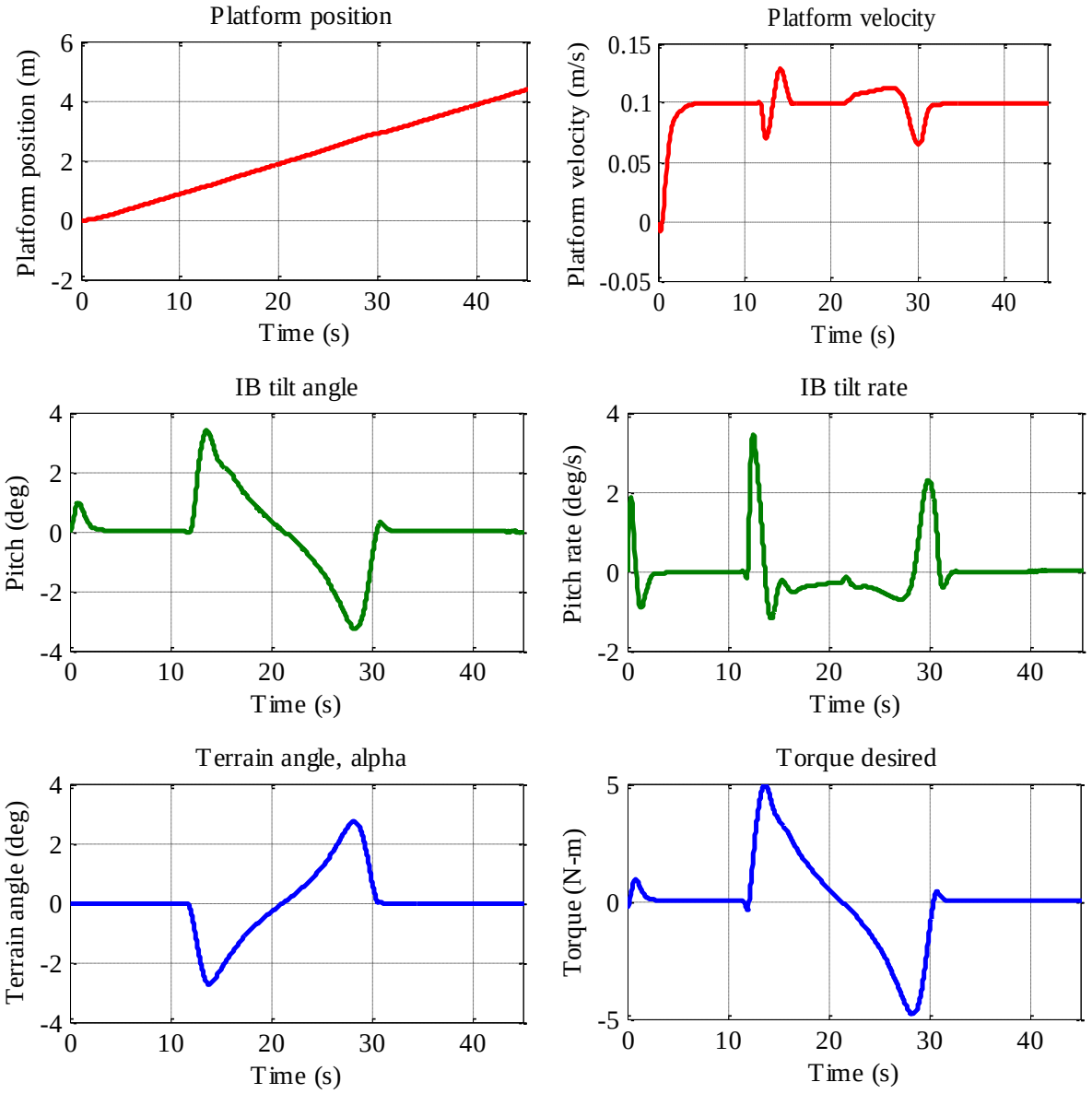

Figure 6-5: Transient response of states at different desired velocities on a bump: (a) Position (b) Velocity (c) Pitch (d) Pitch rate (e) Wheel-Terrain contact angle (f) Torque.

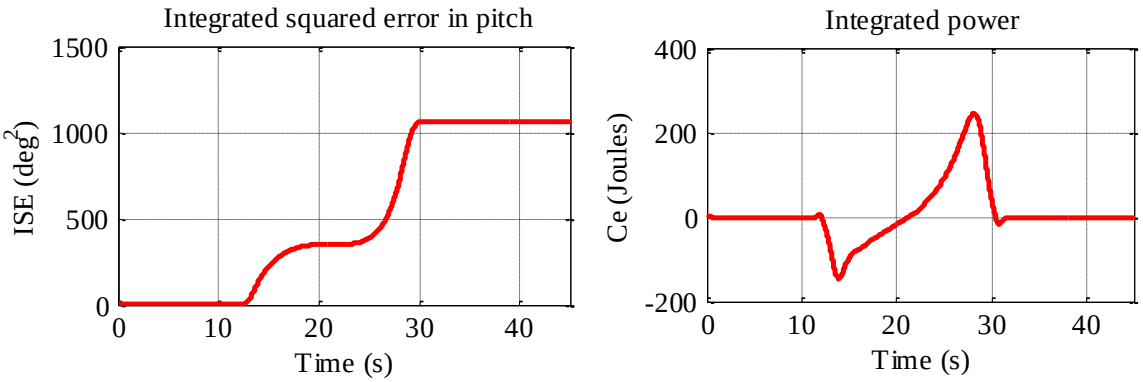

Figure 6-6 : Integrated metrics at different desired velocities on a bump: (a) Squared error of pitch (b) power consumption.

6.4. Control Lyapunov Function Based Controller

The results mentioned in the previous section, obtained from GS controller, concluded that at a high terrain slope variation rate the controller limits the stability of the system. The stability range is also limited to the very near vicinity of the equilibrium IB position. This is because GS controller which guarantees the stability of the local controllers does not guarantee the same stability at intermediate operating points where the gains were interpolated. We attempted to solve this problem designing a nonlinear Lyapunov function based controller, in this section. The objective of LFBC is to guarantee the stability of the control on uneven terrain and increase the stability region. The LFBC is developed for two wheeled robots motion on uneven terrain in chapter 3. The controller was synthesised for a domain of attraction. A partial feedback linearization was used to transform the dynamic model into an affine (3.11) form which was used to develop the control law (3.29). In the following sections, stability of the closed loop TWR system with LFBC and the stability region are computed.

6.4.1. Stability Analysis

Since the stability of the TWR exists in the sense of Lyapunov, the asymptotic stability of the system with the proposed controller is analysed. The LaSalle theorem (defined in chapter 3) is applied to prove the asymptotic stability of the equilibrium point of the TWR. The equilibrium point was considered at $\theta = \theta' = 0 \,\&\, q' = constant$. A compact set D is defined for TWRs as (6.3).

$$D = \left\{ \boldsymbol{x} \in \Omega_{i1} : \left(k_d\, \theta' cose_\theta + \frac{k_1 \cos e_\theta}{1+a_1} (\dot{\theta} - \dot{q} \sin\theta \tan\alpha) \right)^2 = \dot{W}^2 = 0 \right\} \tag{6.3}$$

It is clear that on D, $\dot{W} = 0$. So the auxiliary variable is constant on set D and $\ddot{W} = 0$. Hence,

$$W \text{ is constant}$$
$$\dot{W} = 0$$
$$\ddot{W} = 0$$

Since, $\dot{W} = k_d\, \dot{\theta} cose_\theta + \frac{k_1 \cos e_\theta}{1+a_1} \left(\dot{\theta} - \dot{q} \sin\theta \tan\alpha \right) = 0$, the time derivative is :

$$\ddot{W} = \left(\left(k_d + \frac{k_1}{1+a_1} \right) \left(\ddot{\theta} cose_\theta - \dot{\theta}^2 sine_\theta \right) - \frac{k_1}{1+a_1} [\ddot{q} \sin e_\theta \cos e_\theta] \right) = 0$$

Replacement of $\ddot{\theta}$ and $\ddot{q}$and manipulation of the resulting equation gives an equality for β given below. Substitution of this expression of β in the control law provided a relationship for v on the set D such that control law equates to zero in the set D. This relationship is used to analyse the stability conditions in a later paragraph.

$$\ddot{W} = \left(\begin{array}{c} \left(k_d + \frac{k_1}{1+a_1} \right) \left(\frac{\sin\theta - v.[\cos\theta + \sin\theta \tan\alpha]}{1+a_1} \cos e_\theta - \dot{\theta}^2 sine_\theta \right) \\ - \frac{k_1}{1+a_1} [v \sin e_\theta \cos e_\theta] \end{array} \right) = 0 \tag{6.4}$$

$$\Rightarrow \qquad \beta = \frac{\frac{k_1 v}{1+a_1}(\gamma - 1)}{\left(\frac{k_1}{1+a_1} + k_d \right)} \tag{6.5}$$

Since, $v\gamma + k_1\beta = -\dot{W}$ $\Rightarrow$ $v\gamma + k_1\beta = 0$ (6.6)

$$\Rightarrow \qquad v \left[\gamma + \frac{\frac{l}{1+a_1}(k_1 + k_1\gamma)}{\left(\frac{k_1}{1+a_1} + k_d \right)} \right] = 0$$

As $k_1 > 0$ => $(k_1 + k_1\gamma) > 0$, then $v = 0$ on set D which shows the system is stable. When control input is zero, $\ddot{q} = 0$ and $\dot{q}$ is a constant on set D. Also, $\dot{W} = \left[\frac{k_1}{(1+a)^2} + k_d \right] \dot{\theta} cos\theta = 0$ leads to $\dot{\theta} = 0$ and $\ddot{\theta} = 0$ for $\theta < \frac{\pi}{2}$. Substitution of $\ddot{\theta} = 0$ and $v = 0$ leads to $\theta = 0$ on

set D. Therefore, the largest invariant set M contained in the set D is the single unstable equilibrium point ($\theta = \dot{\theta} = 0$ & $\dot{q} = constant$). LaSalle's theorem, hence, proves that all the closed loop solutions starting in Ω_{i1} asymptotically converge to the largest invariant set M which is the unstable equilibrium point ($\theta = \dot{\theta} = 0$ & $\dot{q} = constant$).

6.4.2. Stability Region

Computation of the stability region of closed loop TWRs with LFBC is performed using a methodology presented in [141]. They have implemented the method to an inverted pendulum system. An inverted pendulum is a classic example of the implementation of control problems. The stability region of TWRs on uneven terrain with two controlled states (θ & $\dot{\theta}$) is defined as a compact set (6.7).

$$\Omega_0 = \left\{\left(\theta, \dot{\theta}\right) \epsilon\, R^2 :\ V_0 < 1 - \cos e_{\tilde{\theta}}\right\} \tag{6.7}$$

This is a compact set at or during which time initial conditions $\left(\theta_0, \dot{\theta_0}\right)$ satisfy that $V_0 < 1 - \cos e_{\tilde{\theta}}$ and $|\theta| < \tilde{\theta}$ with $|\theta_0| < \frac{\pi}{2}$.

Similarly, the stability region of the system with three controlled states $\theta, \dot{\theta}, \dot{q}$ is defined as (6.8):

$$\Omega_1 = \left\{\left(\theta, \dot{\theta}, \dot{q}\right), |\theta| < \tilde{\theta} : V_1 < K\right\} \tag{6.8}$$

This stability region was derived finding a condition when the TWR system has a singularity at$|\theta| = \pm\tilde{\theta}$. Equation (6.8) suggested the system has no singularity if $|\theta| < \tilde{\theta} < \frac{\pi}{2}$. the constraints suggested $|\theta_0|$ should be less than $\frac{\pi}{2}$ and $V_1 < K = k_d(1 - \cos e_{\tilde{\theta}})$. To avoid singularity at $|\theta| = \pm\tilde{\theta}$, $|\theta_0|$ should also belong to the neighbourhood of the origin. In other words states are bounded with $|\theta| < \tilde{\theta}$ if $|\theta(t)| < \tilde{\theta}$ and $V_1 < K$. $V_1 < K$, is an outcome from the fact that V_1 is a non- increasing function ($\dot{V}_1 = -\dot{W}^2\left(\dot{q}, \theta, \dot{\theta}\right)$).

Therefore the stability region of the TWR on uneven terrain is defined as the set of all initial values of $\theta, \dot{\theta}, \dot{q}$ such that $|\theta| < \tilde{\theta}$ and $V_1 < K$, which with the proposed controller stabilize the unstable equilibrium point of the closed loop TWR. This stability accords with Lyapunov as it fulfils the Lyapunov stability conditions i.e. $V_1(\boldsymbol{x})$ is a positive definite function for all $\boldsymbol{x}\, \epsilon\, \Omega_1$ and $\dot{V}_1(\boldsymbol{x})$ is negative semi definite for $\boldsymbol{x}$.

Chapter 7. Experimental Evaluation of Controllers

An experimental evaluation of the designed control algorithms is important to illustrate their application on a real time TWR and to confirm simulation results. In this chapter the baseline, GS and the LFBC (presented in previous chapters 4-6) are implemented on a real time TWR platform to evaluate the performance of three controllers. The two wheeled robot platform and experimental setup is portrayed in the following sections. The platform which has sensors to measure the states and a differential drive for the wheel actuation was designed at a full scale. The TWR was operated on three terrains: flat MDF ground, a ramp and a bump. These three terrains represent a horizontal, inclined and uneven terrain respectively. The performance of the controllers was quantified for the TWR stabilization control and velocity tracking. The experimental results show an increase in stability of the TWR with nonlinear or semi-nonlinear control. This encourages the design of nonlinear control and their implementation for TWRs.

7.1. Physical TWR Platform

7.1.1. Background

The TWR used in this work was developed in the Dynamics and Control Lab. of the University of Auckland. In 2006, a Segway p133 HT was obtained to serve as the basis of the testing platform. In order to convert the Segway into an autonomous TWR and prepare it for testing of different control algorithms developments were made over several years. To start with the base and motors of the Segway were kept and all other parts and control circuits were removed from the Segway. Kalra et al. [51] made these structural modifications, including adding a reaction wheel actuator. They also developed a controller to achieve IB balance. In 2008, Coelho et al. [52] added two computers to the platform to split the low-level and high-level tasks. The objective was to extend the operation of the platform to autonomous applications. They developed a linear state-space controller to track robot motion to the desired velocity and turn-rate. In 2010, the platform was made modular [142] through some structural and electrical changes. Later, the centre of gravity of the platform was raised for three reasons: to craft it into a significant statically unstable TWR, to ensure that the platform will achieve equilibrium positions of the IB on an inclined terrain of wheel-terrain

contact angle of at least 30 degrees and to provide an adequate clearance under the platform base. With these modifications, the overall system operation remained unchanged.

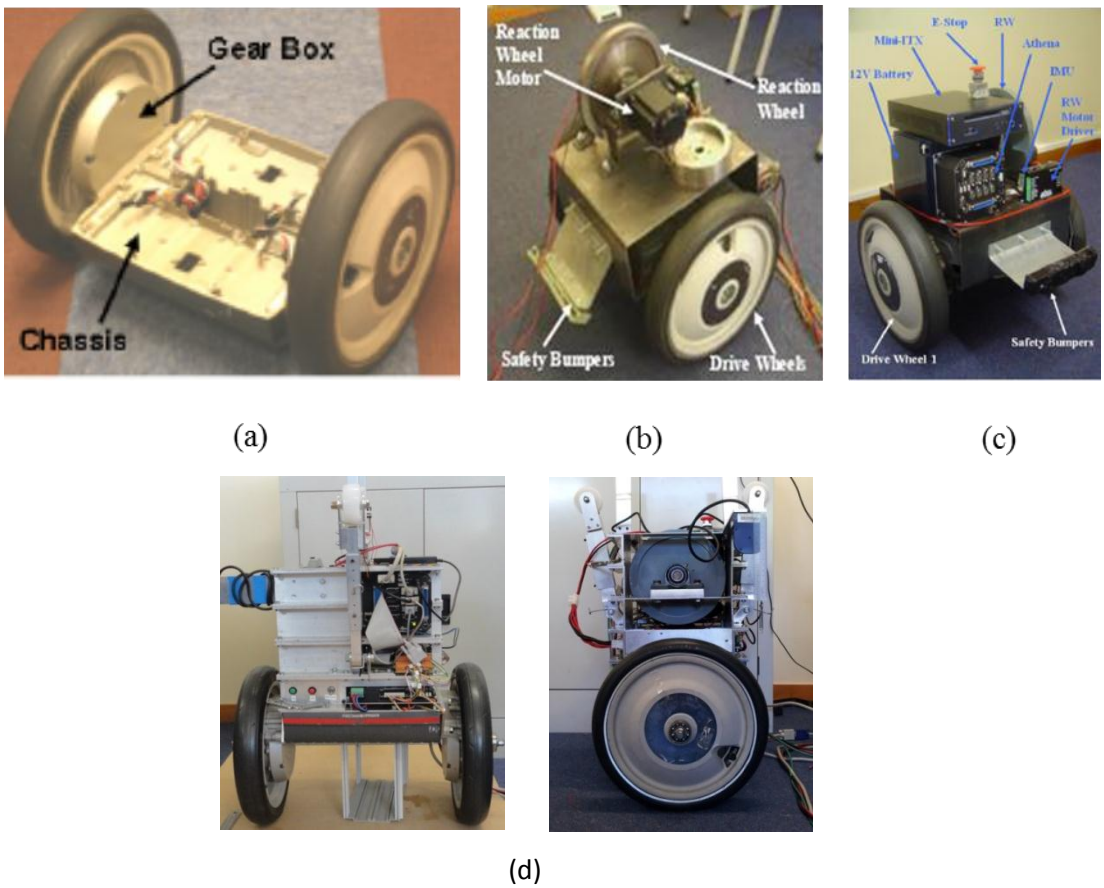

Figure 7-1: The developing stages of the TWR in Dynamics and Control lab, UoA.

7.1.2. Platform Description

The two-wheeled platform, shown in Figure 7-1(d) comprises of two main parts: Drive wheels and the IB. The drive wheels are integrated with the gears system. The key components of the drive wheel system also include two BLDC (Brushless DC) motors, motor drivers and digital encoder which are placed on the first module of chassis. The chassis, made of three modules, is one of the major components which combine to produce the IB section. The gears, wheels and chassis were retrieved from the Segway HT p133 because of their good construction quality. Another benefit was that the chassis and motors had been selected to ensure best possible fitting of components. The gears selected were to minimise the noise, backlash and has a great load capacity. The BLDC motors are powerful Segway's custom made which contain analogue hall sensors to provide a feedback to the motor drivers. The motor drivers control the drive wheel motors.

The platform is empowered with both the batteries and direct power supply with a selection switch. A power distribution board and a signal distribution board are placed at second module of the IB. The third module of IB consists of an Athena to control the signals and send commands to actuate the TWR. Athena is a small portable embedded PC that is able to run real-time applications. It has four RS232 connection ports, four USB connection ports, one keyboard and mouse connection port, one Ethernet port and one VGA connection port. Two sensors are mounted on the TWR platform: an IMU (VN-100) (Figure 7-2) to measure the pitch and pitch rate; a digital encoder to measure the absolute position and velocity of the TWR. Due to heavy weight, safety measures were taken which includes installation of E-stop, LEDs, separate motor ON/OFF switch, software limit switches and safety bumpers.

Figure 7-2: IMU used in the TWR

7.1.3. Hardware-in-Loop Implementation

A real-time program was used to provide testing on the platform. The program used is xPC Target. It is able to use standard PC hardware to enable prototyping and real-time testing of the controller algorithms used in MATLAB's Simulink. It requires the usage of two PCs, a host PC and a target PC to run real-time systems. The host PC is used to implement the controller algorithm in Simulink. The host PC used is a desktop computer that runs a Pentium 4 where the controller is designed. The host must have MATLAB, Simulink and Xpc target installed. The controller is converted to embedded C and sent through ethernet cable to the Target.

The target PC is used to run the implemented controller. The host PC converts Simulink blocks into C code. This C code is then downloaded onto the target PC and is run separately to the host PC to provide easy testing of the mobile balancing platform. Two download options have been set up to allow direct copying of the C code onto a USB drive or via a null modem cable onto the target PC. The target PC is capable of running in a Standalone mode, which means no connection between the host PC and target PC is required. The Host PC is the desktop computer changes certain values in real-time for the target PC. If the target PC and the host PC are linked, controller gains on the balancing platform can be changed and observed instantaneously. A monitor is connected to the target PC to enable visual feedback of the readings. The use of target scopes enables numerical or graphical readings to be displayed on the monitor. The plant is the TWR that is desired to be controlled.

The Athena (Figure 7-3) has been set up to send a desired speed to the motors. The Athena obtains voltage readings from the analog input to calculate the actual speed or turn-rate based on the wheel encoders. The desired speeds are analog output channels that output a voltage value to the DC brushless motors.

Figure 7-3: Athena (embedded PC)

7.2. Test Terrain

In addition to a flat terrain, a 2m long ramp and another 2m long bump were built to be used as test terrain. All the three terrain are wooden made out of MDF as shown in Figure 7-4. The ramp inclination angles can be changed with a variation of 5 degrees. The bump was prepared following the same dimensions used in simulation, Figure 6-1.

Figure 7-4: Setup of terrains with hardware-in-loop.

7.3. Terrain angle measurement

There was no sensor available to measure the inclination of the terrain. An alternative method was devised using the wheel encoders. A lookup table was created using the functions and scripts of MATLAB. This lookup table returns the terrain angle when given the distance driven along the bump.

7.4. Test on Horizontal Terrain

The experimental data was obtained for baseline and the LFBC on the flat horizontal terrain. The experiments were designed to verify the simulation results and validate the controllers. The performance is measured as a transient response, stability, stability region and velocity tracking of the physical TWR.

7.4.1. Baseline Controller

The following experiments were conducted.

1: This experiment was reproduced 11 times for an initial pitch of 5 degrees. The TWR showed rapid small amplitude oscillations with that initial pitch. The TWR failed to stabilize when the initial pitch was set to 10 degrees, so bigger initial pitch were not tested. The data collected during the failure was recorded.

2: The experiment was conducted 5 times for reference velocities of 0.1 and 0.3 m/s. The robot was placed on one end of a 2.7 m long wooden board and was released. It was stopped when it reached the other end. When given a reference velocity of 0.1 m/s, the TWR would stabilise really quickly. When given a reference velocity of 0.3 m/s, the TWR would oscillate a lot for a short period of time before stabilising. The TWR failed to stabilise when given a reference velocity of 0.5 m/s. The data for this failure was recorded.

7.4.2. LFBC

The LFBC designed for the TWR (chapter 3) is implemented on the flat MDF terrain. Two tests were conducted:

1: First experiment was reproduced 10 times for an initial pitch between 5 to 10 degrees approximately. The TWR showed rapid balancing of the IB with small amplitude oscillations.

2: The second experiment was conducted for different initial pitch. This varied from 5 deg to 60 degrees. The robot was placed on wooden board and was released with an initial pitch 5 deg. It was bent down at different angles to test whether it comes back to the upright position of the IB. The TWR stabilised really quickly but oscillated after short intervals of time. The TWR showed high region of stability for the pitch.

7.5. Tests on Inclined Terrain

The baseline controller is the only controller for which experimental data was obtained. The LFBC was tested, but the gains given did not make system stable. The data collected is stored in 4 different folders. Their content is detailed below:

7.5.1. Baseline Controller

To test the baseline controller on an incline the experiments were performed on a wooden inclined ramp. The baseline controller implemented on a horizontal terrain was tried to implement on the ramp of 5 deg of wheel-terrain contact angle.

7.5.2. Gain-Scheduled Controller

To schedule gains on inclined terrain the robot was run on 5, 10, 15 and 20 degrees sloped terrain. The terrain was set up and reference position and position gain were added to the controller. The position gain was setup as 0.29. The reference positions were set as shown in the Table 7-1. For example, 1.6 m for 5 degree inclined terrain. The robot was started on the flat part of the terrain close to where inclined terrain starts. The robot moved a little backward and then forward trying to get on the slope. Once it is on the slope, it tries to go forward as well as trying to get balanced slowly, shown in Figure 7-5.

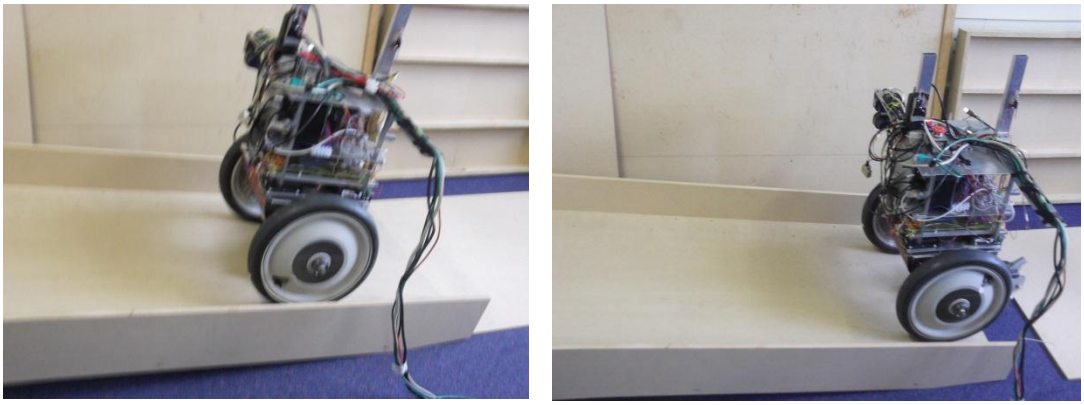

Figure 7-5: TWR balanced on inclined terrain.

The reference positions and the total torque demand recorded at the balancing position with respect to the terrain angle are shown in table 7-1.

Once we found the equilibrium torques and angles for 5 and 10 degrees slopes. The reference position was increased progressively until the TWR started climbing the incline and stabilised

itself. The TWR was then left alone for a period of time. The reference position had to be increased to very large values (16m and 29m respectively) in order for the TWR to stabilise itself on the incline. The robot didn't manage to stabilise itself on a 15 degree slope, as its wheels would constantly slip. If the surface of the slope and/or the wheels were made rougher the TWR should be able to stabilise itself on a 15 degree incline. The approximate equilibrium tilt angles and torques were estimated from the graphs by looking at the periods in time where the TWR was stable. These equilibrium torques and tilt angles were recorded in an excel file.

7.6. Tests on Uneven Terrain

The lineLength function was written in order to replace the laser sensors for gain scheduling over a bump: given an equation characterising the bump, it returns three vectors: a vector x of positions along the ground, a vector of displacement along the bump and a vector of instantaneous slopes of the bump. This data is stored in a lookup table.

The GS controller was modified to take in the displacement of the TWR, translate it to an instantaneous slope using the lookup tables generated by the lineLength function. This instantaneous slope is then used to choose the appropriate gains. The gain scheduling controller was tested over a range of reference velocities. We found that operating the robot with reference speeds larger than 0.40 m/s was too hazardous for safe operations. Therefore data was recorded over the range 0.05 m/s to 0.40 m/s. The experiment was repeated 5 times for each of the following reference velocities: 0.05, 0.10, 0.20 and 0.40 m/s.

7.6.1. Setup

A track was constructed using material available in the laboratory (MDF). Planks of wood were laid on the ground, as shown in the picture at Figure 7.6. The robot was positioned on the red lines (1m away from the start of the bump). It was then allowed to balance for about 10 seconds. The target distance was chosen to be 3.2m, in order to account for the 1m run-up and the 2.07m length of the bump. The target speed was set to be equal to the desired reference velocity. In order to be able to perform this experiment safely blocks of foam were attached onto the robot using red duct tape.

Figure 7-6: A bump used for testing.

Figure 7-7: Snapshots of testing GS controller on the bump at a reference velocity of 0.4 m/s.

7.6.2. Baseline Controller

To test the baseline controller on an uneven terrain the experiments were performed on a wooden bump. The baseline controller implemented on a horizontal terrain was tried to implement on the bump which failed.

7.6.3. Gain-scheduled Controller

The gain scheduling controller was tested over a range of reference velocities. We found that operating the robot with reference speeds larger than 0.40 m/s was too hazardous for safe operations. Therefore data was recorded over the range 0.05 m/s to 0.40 m/s. The experiment, shown in Figure 7-7, was repeated 5 times for each of the following reference velocities: 0.05, 0.10, 0.20 and 0.40 m/s.

7.7. Experimental Results

The results from the data collected during above described experiments, is plotted in the following Figures 7-8 to 7-20. The captions of these figures show the objective and limitations of these results.

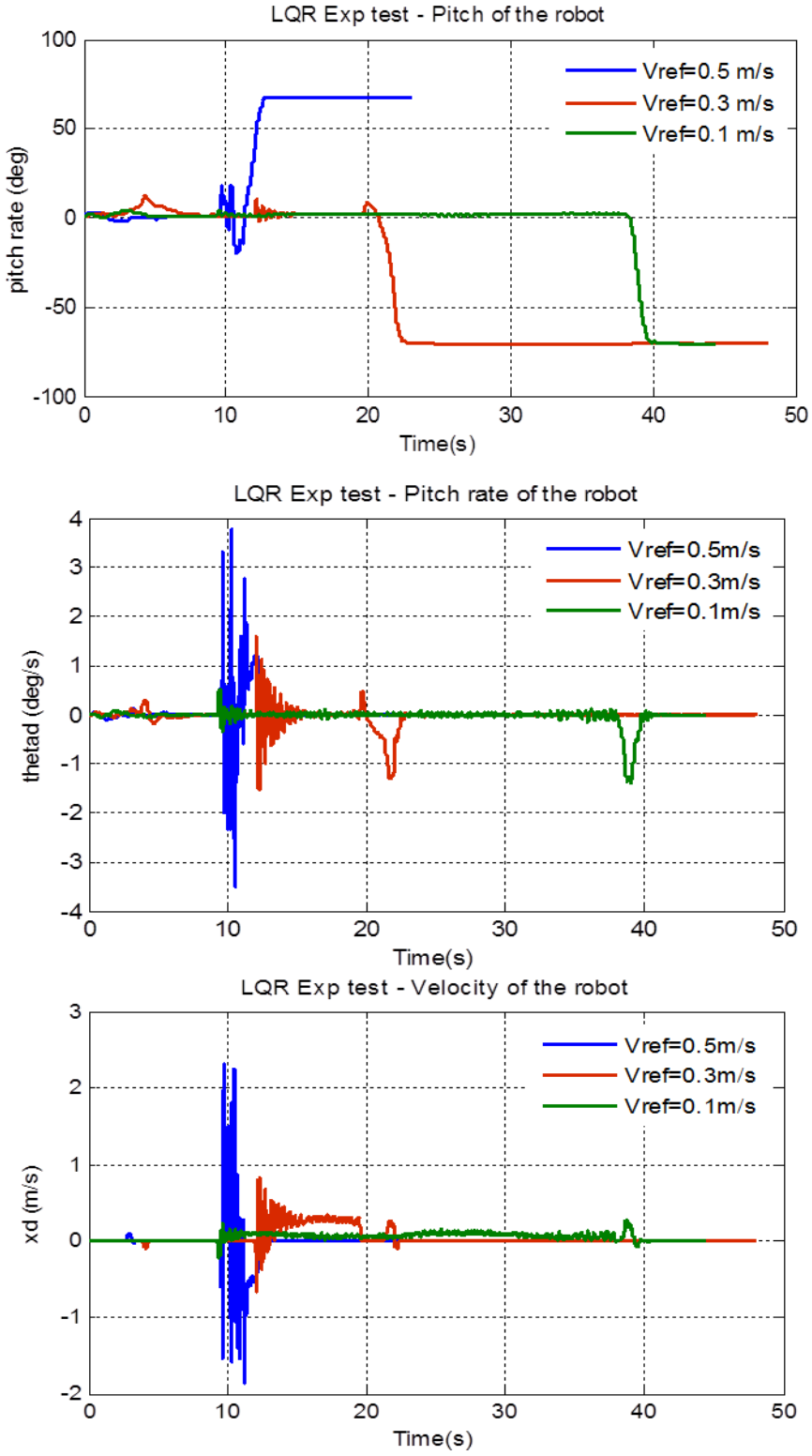

Figure 7-8: Response of TWR on horizontal terrain with baseline controller. The tests repeated for different desired velocities of the robot. TWR fails at and above a velocity of 50 cm/s.

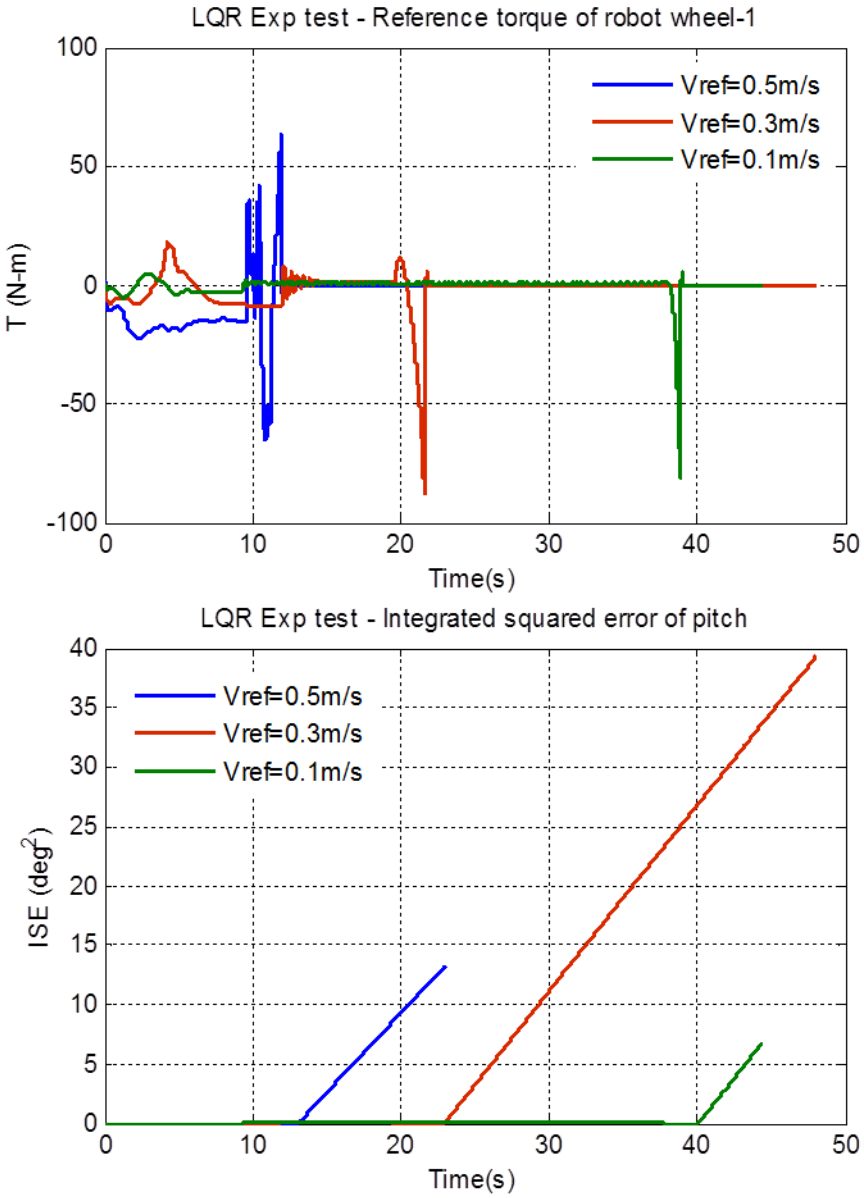

Figure 7-9: Response of TWR on horizontal terrain with baseline controller. The tests repeated for different desired velocities of the robot. TWR fails at and above a velocity of 50 cm/s.

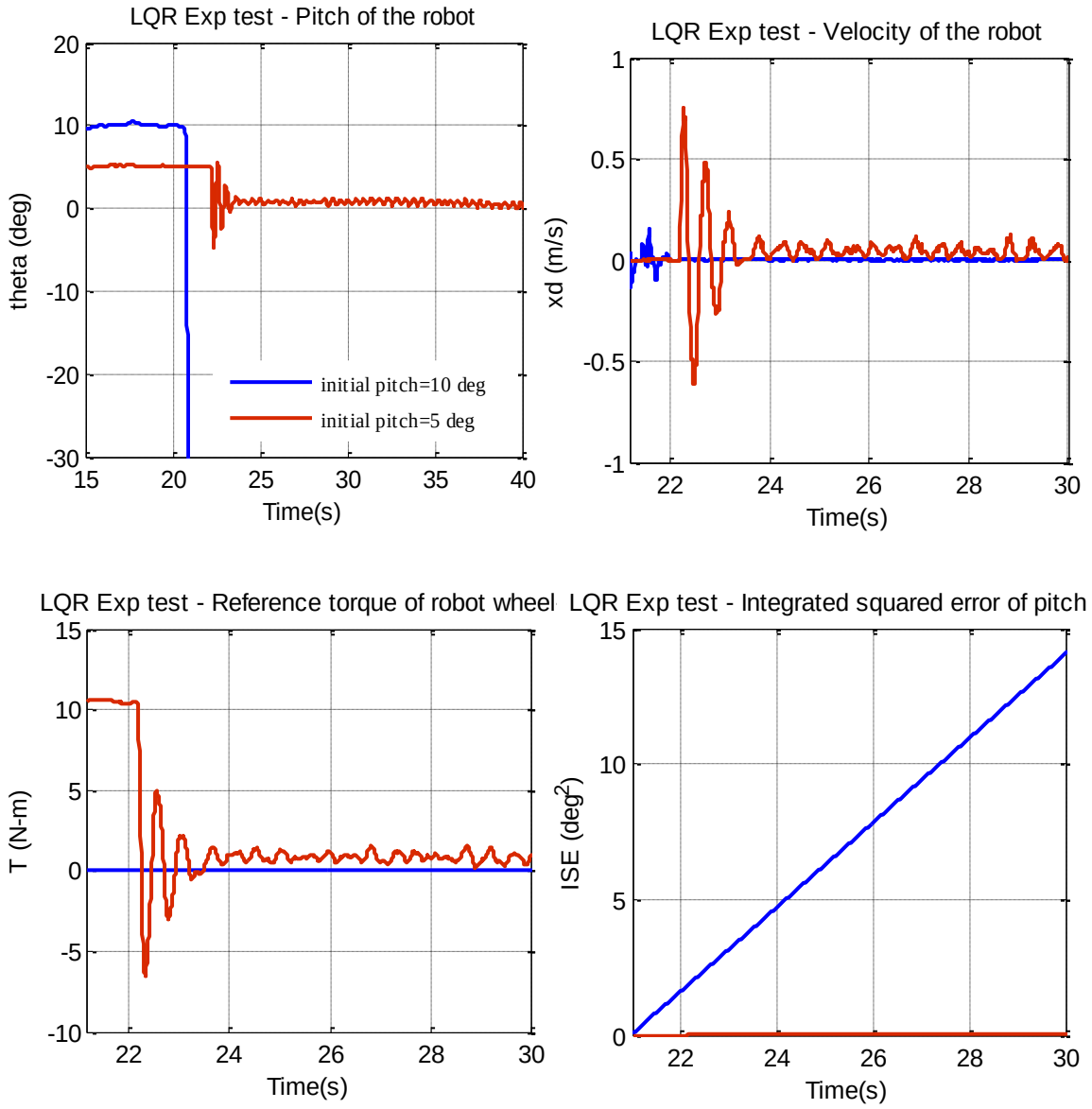

Figure 7-10: Response of TWR on horizontal terrain with baseline controller. The tests repeated for different initial pitch values of the robot. The TWR fails at an initial pitch more than 5 deg. This shows the linear controller has very limited stability region.

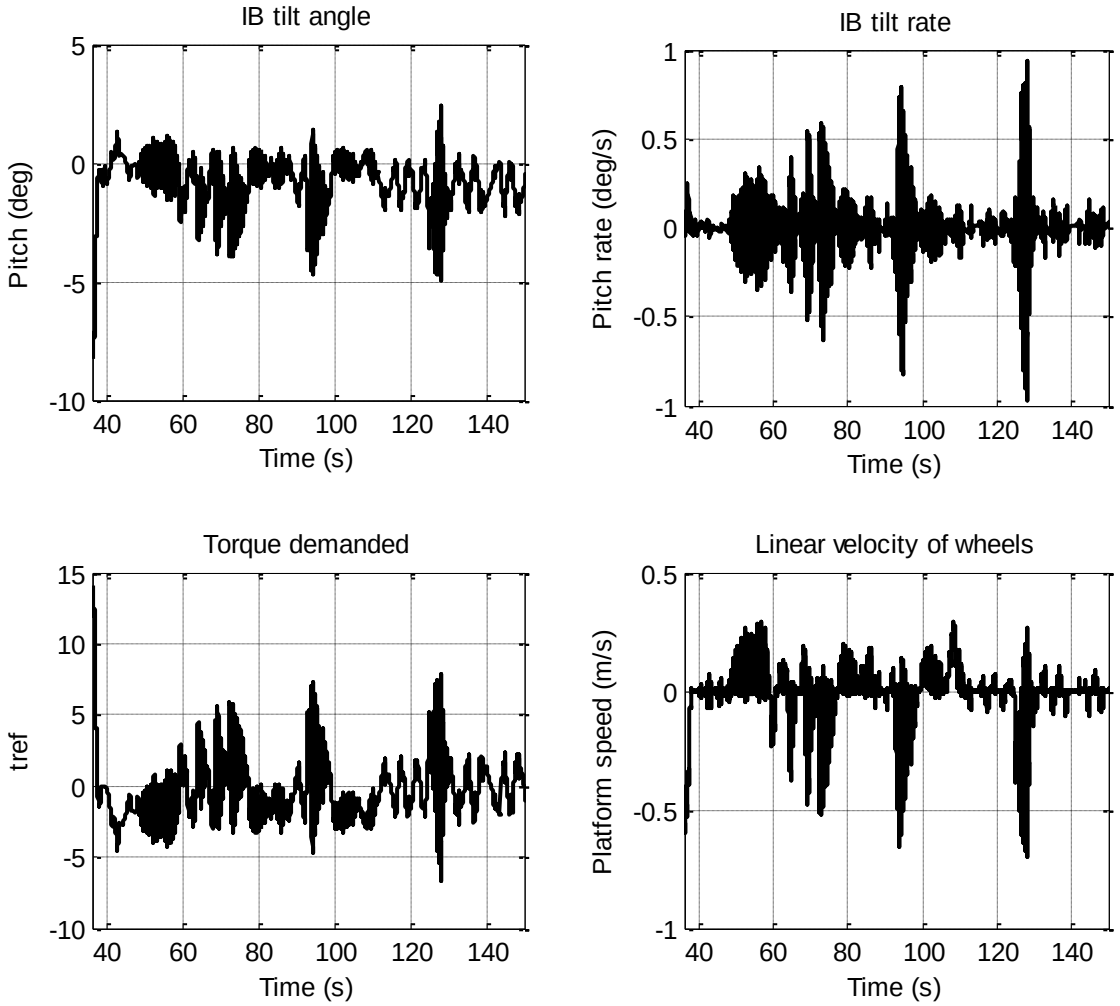

Figure 7-11: Response of TWR on horizontal terrain with the LFBC. The test was conducted with an initial pitch of 10 degrees. The TWR balanced very quickly.

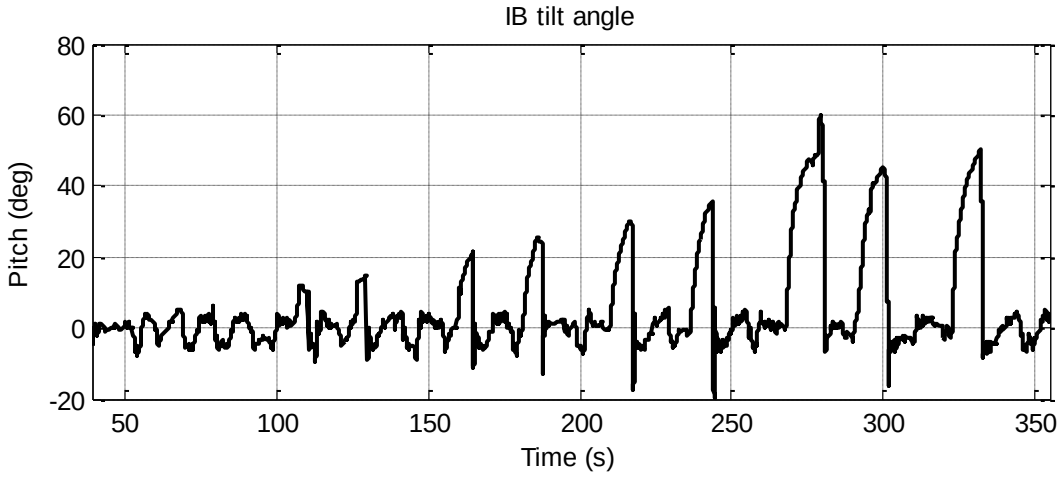

Figure 7-12: A chain of continuing tests conducted with increasing disturbance in pitch upto 60 degrees. The aim is to show high stability region.

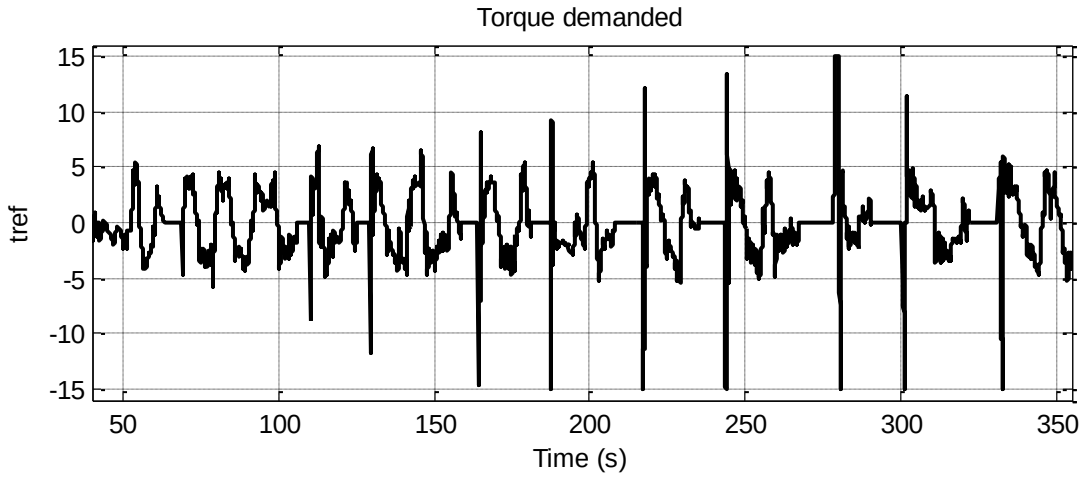

Figure 7-13: A chain of continuing tests conducted with increasing disturbance in pitch up to 60 degrees. The aim is to show low torque demand with high stability region.

7.7.1. Results on ramp

Table 7-1: Results of gains scheduled.

Test #	Slope angle (deg)	Gains				x_{ref}	xd_{ref}	Equilib-rium tilt angle	Uncertai-nty	Net equilib-rium torque	Uncert-ainty
		x (position)	xd (velocity)	Theta (tilt angle)	thetaD (tilt rate)						
1	5	1	30	150	250	16	0	8.5	0.2	2	0.5
2	10	1	30	150	250	29	0	14	0.2	4	0.2
3	15	1	30	150	250	60	0	19.5	0.2	8	0.5

Following are the results from experimentation on a ramp of 5 degrees inclination with different desired velocities. Figure 7-13 is for a desired velocity of zero, that is, to bring the TWR to its balanced stationary position on the ramp. The results shown in Figure 7-14 were plotted for the tests conducted to run the TWR at 0.1 m/s (10 cm/s).

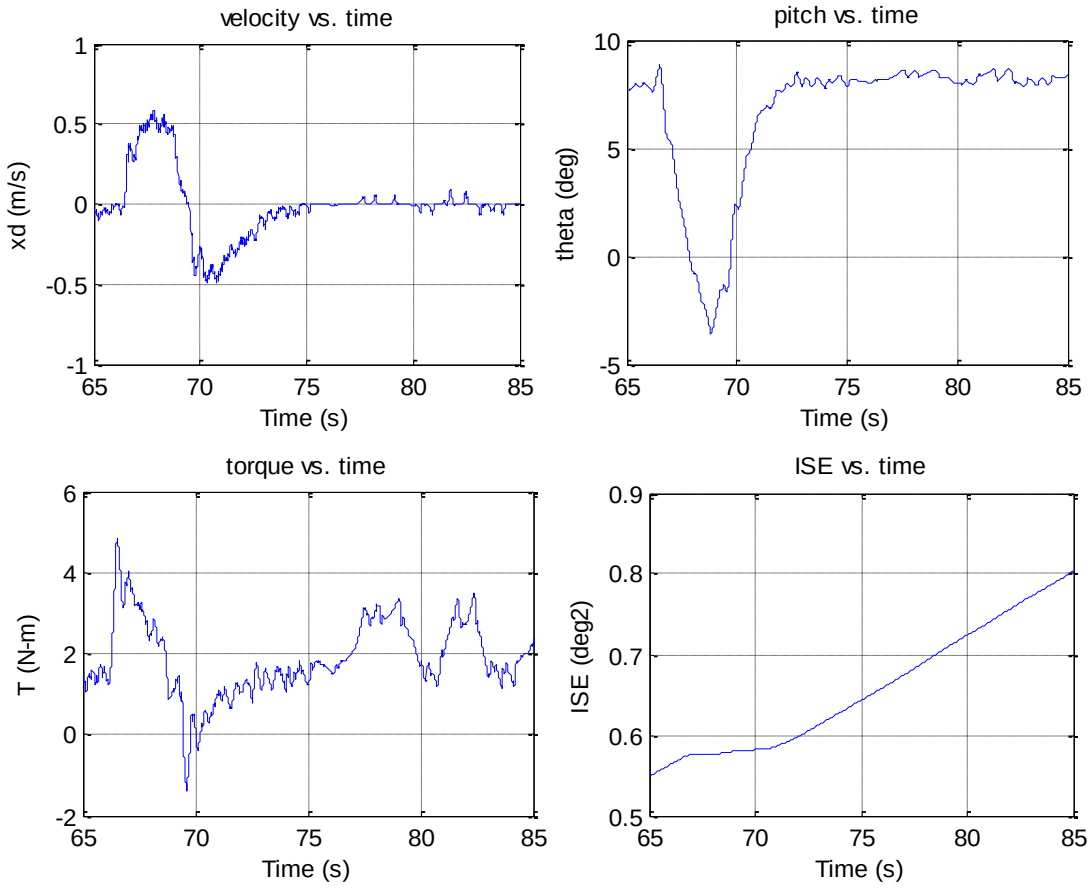

Figure 7-14: Balancing results on the ramp with a terrain inclination angle of 5 degrees.

The results show that GS controller settles the system within 10 seconds at an equilibrium IB position. These results are in accordance to the simulation results and verify the controller validity in real situations. The results with a nonzero desired velocity showed a stabilized behaviour but with short oscillations.

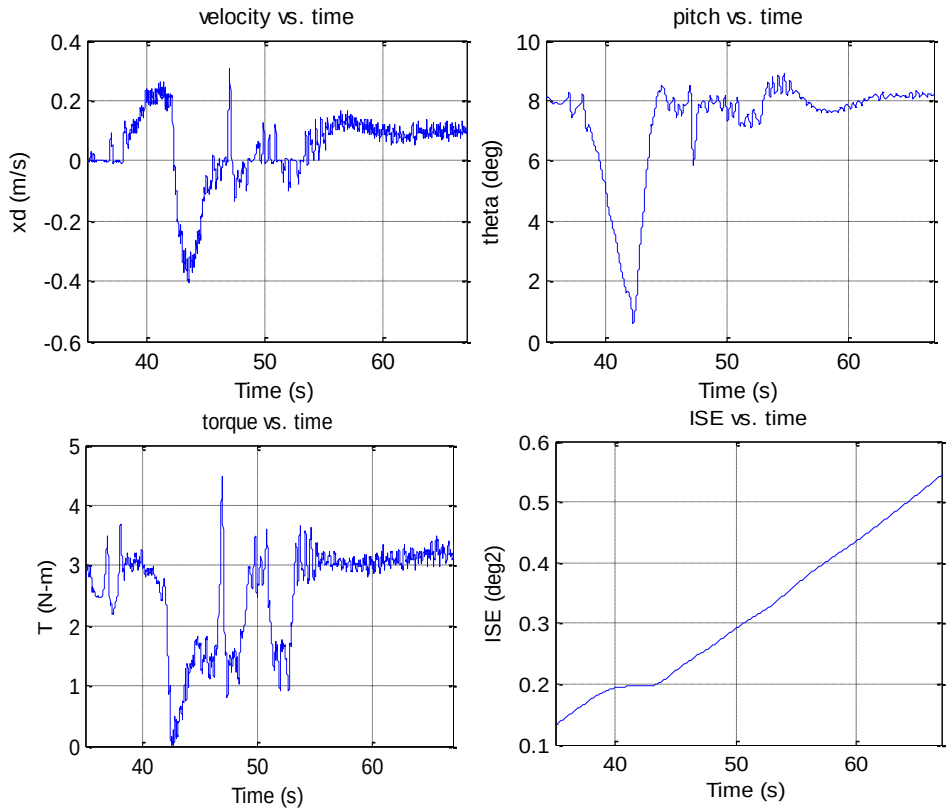

Figure 7-15: Results on the ramp of 5 degrees with desired velocity of 10 cm/s.

7.7.1. Results on bump

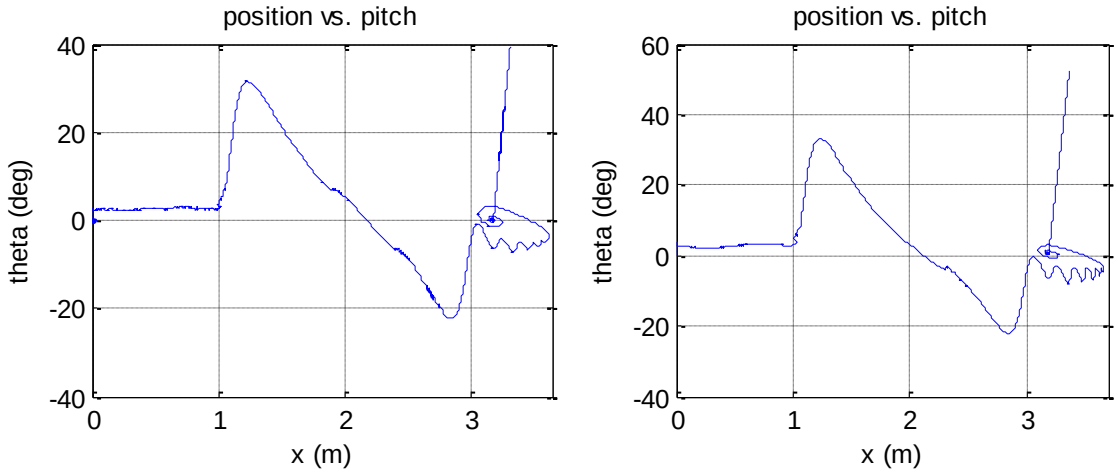

Figure 7-16: Pitch variation over the bump plotted against the position along the terrain in longitudinal direction with a desired velocity of 5cm/s (left) and 40cm/s (right). The ending loop in plots shows the return of TWR as a stopping wall was placed at 0.5 m.

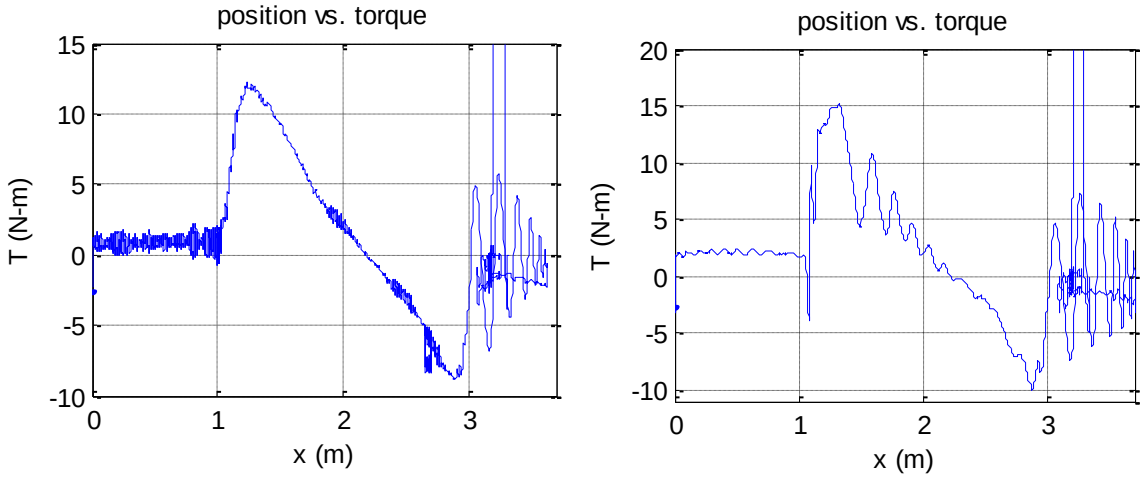

Figure 7-17: Torque demand over the bump plotted against the position along the terrain in longitudinal direction with a desired velocity of 5cm/s (left) and 40cm/s (right).

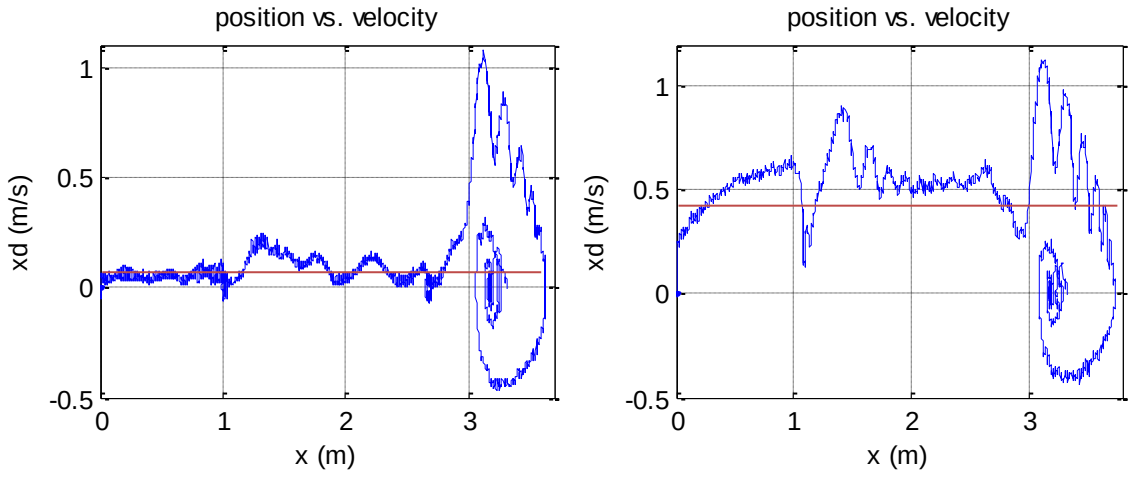

Figure 7-18: The reference (red) and actual velocity (blue) on the bump plotted against the position along the terrain in longitudinal direction with a desired velocity of 5cm/s (left) and 40cm/s (right).

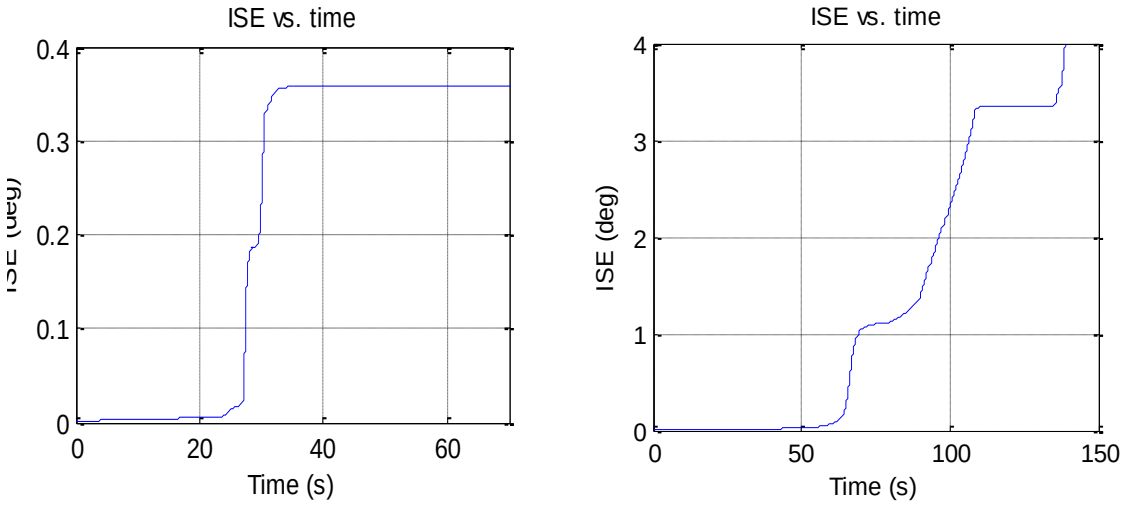

Figure 7-19: The integrated squared error in pitch on the bump plotted against the position along the terrain in longitudinal direction with a desired velocity of 5cm/s (left) and 40cm/s (right).

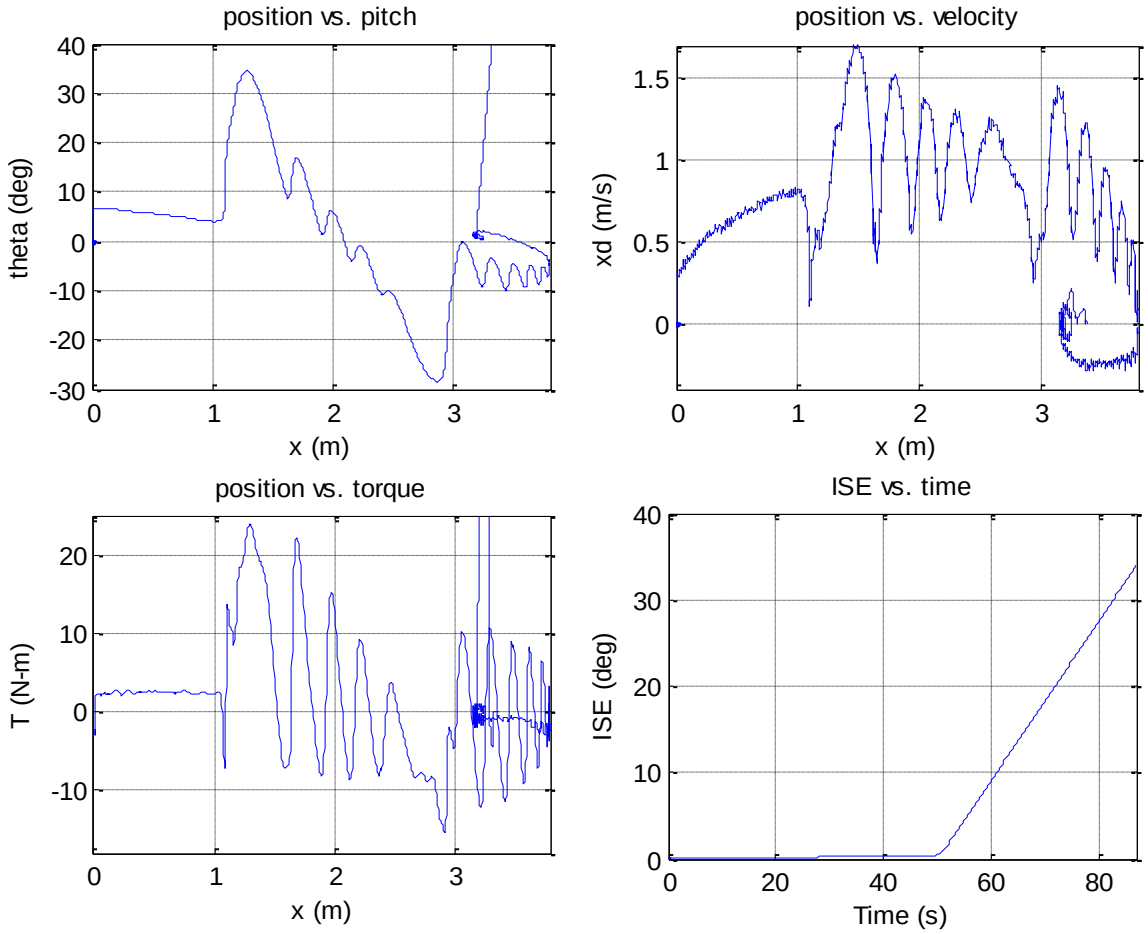

Figure 7-20: The pitch, velocity, torque and integrated squared error on the bump plotted against the position along the terrain in longitudinal direction with a desired velocity of 70cm/s. The performance of the controller is deteriorated at such a high velocity.

The results show that a GS controller is able to balance the TWR on the bump. It controlled the desired velocity as well but the stability region is very limited. It strengthens our hypothesis that the LFBC is necessary for large stability regions.

Chapter 8. Conclusions and Future Work

This thesis has focused on modelling, simulation, control and real time implementation of statically unstable two-wheeled robots. More specifically, we have considered how we can augment the stability of TWRs on ramps and bumps by designing and implementing linear and nonlinear control algorithms. The main conclusion from this study is that it may be possible to enhance the stability and track the velocity of the TWRs on horizontal as well as non-horizontal terrain using nonlinear control algorithms. This chapter seeks to summarize the main outcomes and conclusions of this research, as well as highlight the contributions made in this work. Lastly, this chapter provides a discussion of future directions.

8.1. Contributions

A couple of new control algorithms were developed in this research with the aim of increasing the stability of two-wheeled mobile robots in pedestrian environment. The major works carried out in this research are identified as: derivation of a new dynamics model of two-wheeled robot motion on uneven and inclined terrain; Testing a baseline controller; Design of a GS controller for TWR stability control; Synthesizing of a LFBC for TWR stability control and velocity tracking; Implementation of the three controllers in simulation as well as in real time on three types of terrain a flat ground, ramp and a bump. The outcomes, contributions and conclusions relating to the works conducted in this research are summarized in this section.

8.1.1. TWR Dynamic Modelling

In chapter 2 the mathematical model of statically unstable TWRs moving on uneven terrain was formulated by means of Lagrangian. The kinematics was derived to find accelerations at wheel-terrain contact point, wheel centre and at the centre of mass of the IB. The geometry of the terrain entered the dynamics via time rates of change of height of wheel-terrain contact point which is function of wheel-terrain contact angle. A constraint on the terrain radius of curvature was described to ensure a single contact point of the wheels and equilibrium position of the IB relative to terrain inclination was derived. We studied particular cases of motion on an inclined and horizontal terrain and derived linearized and state space models. We verified the model and validated through experiments on a real-time TWR.

8.1.2. Baseline Control

The LQR based full state feedback linear controller was formulated for the TWR in Chapter 3 and used as a baseline controller to realize the benefits of semi linear and nonlinear controllers over a linear controller. In Chapter 5 Baseline controller was implemented to comprehend the effects of terrain inclination on performance and stability region of TWRs. As per knowledge of the author this approach has not been reported in literature before. In Chapter 4 we under took a rigorous study of the Baseline controller in comparison to the nonlinear controller designed for stability control of the TWR which is another addition to the literature. It was concluded that baseline controller which is an optimal linear controller, needs a new set of control parameters for each inclination of the inclined terrain and it does not respond to the rate of change of inclination on bumps.

8.1.3. Gain-Scheduled Control

The gain-scheduled controller was proposed based on the conclusion derived from the implementation of the baseline controller on inclined and uneven terrain. The gains were scheduled relative to the wheel-terrain contact angle as described in Chapter 3. In Chapter 5 the GS controller was designed for the TWR motion on inclined terrain. The controller gains were calculated using LQR algorithm for stabilization and velocity tracking on different terrain inclinations. Then, scheduling of the gains was proposed using linear interpolation. Interpolation allows the controller to output a torque demand for those terrain inclinations for which the controller gains were not calculated. The GS controller design for TWRs stability on inclined and uneven terrain is one of the contributions of this thesis and was recognized in the literature [RAM paper]. We concluded that the GS controller enhances the stability of TWRs on pedestrian terrain but limits the stability region.

8.1.4. Lyapunov Function Based Control

The GS controller is a semi nonlinear control algorithm based on linear controller gains implemented on nonlinear dynamic system using a gain interpolation method. This controller showed a good performance but very short stability region. To increase the stability region with an equivalent performance a nonlinear LFBC was proposed. Chapters 3 presents the synthesis design procedure of a control Lyapunov function based controller for the stability of TWRs on uneven terrain. The same LFBC is reduced for stability of the TWR on horizontal and inclined terrain in chapter 4 and chapter 5 respectively. The novelty of the

proposed control algorithm is that it guarantees the asymptotic stability with computable stability region. We analysed the stability of LFBC and computed the stability regions in chapters 4-6. The simulation results on horizontal and inclined terrain (chapter 4&5) shows the augmentation of stability and stability region using nonlinear controller.

8.1.5. Performance Quantification

An evaluation of the performance of TWRs on horizontal terrain has been studied in literature in the form of transient responses. This research proposed some additional performance quantification metrics and presented in chapter 3. The energy consumption evaluation was proposed considering it a major issue for real systems and the integrated squared error was proposed to have an overview of the IB position control. In addition the stability region was considered as important performance quantification metric for the TWR motion on non-horizontal terrain.

8.1.6. Implementation of Controllers in Real-Time

The proposed control algorithms for TWRs in this research (baseline, GS and LFBC) were tested in simulation in different test scenarios (chapter 4-6). The objective was to examine the stability regulation and the velocity tracking of the TWR on pedestrian terrain. The real time implementation of the proposed control algorithms is presented in Chapter 7. Implementation of these control laws on the real system is one of the major contributions of this research. The baseline controller was implemented on horizontal terrain for model verification in closed loop (chapter 2), to evaluate stability region with different Lyapunov functions (chapter 3), evaluate performance in the form of transient response and velocity tracking on horizontal terrain; inclined terrain and uneven terrain (chapter 7). The GS controller was implemented on inclined and uneven terrain. The LFBC was implemented on horizontal terrain. The results showed an agreement with the simulation results and a stability region equivalent to the one computed in 4.2.3. Based on these observations it is expected the LFBC will be equally beneficial for augmented stability control of two wheeled robots on inclined as well as uneven terrain. It was, therefore, concluded the linear and nonlinear controllers are implementable on real time systems and they enhanced the stability of a full scale TWR on inclined and uneven terrain.

8.2. Avenues for Future Research

In general, control of TWR systems still remain to be an open area since lots of research works are required. The following areas are a few of the avenues which could be directed as a further research work:

1. As for the modelling, in the work reported here both the TWR and the terrain were modelled as rigid bodies. The wheels are not necessarily to be rigid in real vehicles; however tire compliance should be included in the model. The reported research work was limited to the pedestrian terrain in cities and towns. The pedestrian terrain in other areas could be made of partial stones or purely of soil. The terrain modeling can, therefore, be extended towards considering the properties of soft soil.
2. The controllers presented in this research were designed based on an assumption that the wheel-terrain contact angle was known. For real time implementation we used a terrain prepared for a known function. The wheel-terrain contact angle was estimated using the function from measured absolute position. In future it is proposed to deploy a sensor to measure and calculate the wheel-terrain contact angle online. This will widen TWR application in far and unknown sloped terrain.
3. From the control point of view, it would be useful to design controllers for yaw control as well.
4. Furthermore, this research work implemented the LFBC on real time TWR platform for its motion on a horizontal terrain only. It would be interesting to extend the experimental work for stability control of TWRs on inclined and uneven terrain using LFBC algorithm.
5. A topic for further research is to generalize the control approaches proposed in this study to other dynamic systems with similar properties.
6. The control of a TWR on a wavy or continuous bumpy footpath, using the results obtained for the motion on a bump as a first step, should be investigated.

Appendix A. Modeling

Coefficients for Uneven Terrain Model

$$h = -(Ml^2 + I_p)Ig^{'}(x) + (Mlr)^2\cos(\theta+\alpha)(\cos(\theta) - f^{'}(x)\sin(\theta)) + M_o(Ml^2r^2 + I_pr^2)(f^{'}(x)\sin(\alpha) - \cos(\alpha))$$

$$h_1 = Mrl\left(l + r\cos(\theta+\alpha)\right) + I_pr \quad ; \quad h_3 = Mlr^2(Ml^2 + I_p)\sin(\theta-\alpha)$$

$$h_2 = M_o(Ml^2r^2 + I_pr^2)\sin(\alpha)f^{''}(x) - (Ml^2 + I_p)Ig^{''}(x) - (Mlr)^2\sin(\theta)\cos(\theta+\alpha)f^{''}(x)$$

$$h_4 = M_o(Ml^2r^2 + I_pr^2)\sin(\alpha) - (Mlr)^2\sin(\theta)\cos(\theta+\alpha)$$

$$h_5 = -M_o(Ml^2r^3 + I_pr^3)\sin(2\alpha) + (Mlr)^2r\sin(\theta+\alpha)\cos(\theta+\alpha)$$

$$h_6 = -M_o(Ml^2r^3 + I_pr^3)\cos(2\alpha) - (Mlr)^2r\cos(\theta-\alpha)\cos(\theta+\alpha)$$

$$h_7 = Mrl\left(\sin(\theta)f^{'}(x) - \cos(\theta)\right) - Ig^{'}(x) + M_or^2(\sin(\alpha)f^{'}(x) - \cos(\alpha))$$

$$h_8 = M_oMlr^2\sin(\theta-\alpha)f^{''}(x) + MlI\cos(\theta)g^{''}(x) - MlI\sin(\theta)(f^{'}(x)g^{''}(x) + f^{''}(x)g^{'}(x))$$

$$h_9 = (Mlr)^2\sin(\theta-\alpha)(f^{'}(x)\sin(\theta) - \cos(\theta)) \quad ; \quad h_{10} = M_oMlr^2\sin(\theta-\alpha) + MlI\sin(\theta)g^{'}(x)$$

$$h_{11} = M_oMlr^3\sin(\theta+\alpha)(f^{'}(x)\sin(\alpha) - \cos(\alpha)) - MlrI\sin(\theta+\alpha)g^{'}(x) + M_oMlr^3\sin(2\alpha)(\cos(\theta) - f^{'}(x)\sin(\theta))$$
$$h_{12} = M_oMlr^3\cos(\theta-\alpha)(-f^{'}(x)\sin(\alpha) + \cos(\alpha)) + M_oMlr^3\cos(2\alpha)(\cos(\theta) - f^{'}(x)\sin(\theta)) + MlrI\cos(\theta-\alpha)g^{'}(x)$$

In above expressions

$g^{'}(x) = \frac{dg(x)}{dx}$ and $g^{''}(x) = \frac{d^2g(x)}{dx^2}$ with $g(x) = \int_{x_o}^{x_f}\sqrt{1+(\frac{dz}{dx})^2}.dx$

$f^{'}(x) = \frac{df(x)}{dx}$ and $f^{''}(x) = \frac{d^2f(x)}{dx^2}$ with $f(x) = a_2x^2 + a_1x + a_0$ defines the shape of unevenness of terrain.

Coefficients for Inclined Terrain Model

$$h = -(Ml^2 + I_p)Ig^{'}(x) + (Mlr)^2\cos(\theta+\alpha)(\cos(\theta) - f^{'}(x)\sin(\theta)) + M_o(Ml^2r^2 + I_pr^2)(f^{'}(x)\sin(\alpha) - \cos(\alpha))$$

$$h_1 = Mrl\left(l + r\cos(\theta+\alpha)\right) + I_pr \quad ; \quad h_3 = Mlr^2(Ml^2 + I_p)\sin(\theta-\alpha)$$

$$h_4 = M_o(Ml^2r^2 + I_pr^2)\sin(\alpha) - (Mlr)^2\sin(\theta)\cos(\theta+\alpha)$$

$$h_7 = Mrl\left(\sin(\theta)f^{'}(x) - \cos(\theta)\right) - Ig^{'}(x) + M_or^2(\sin(\alpha)f^{'}(x) - \cos(\alpha))$$

$$h_9 = (Mlr)^2\sin(\theta-\alpha)(f^{'}(x)\sin(\theta) - \cos(\theta)) \quad ; \quad h_{10} = M_oMlr^2\sin(\theta-\alpha) + MlI\sin(\theta)g^{'}(x)$$

Coefficients for Horizontal Terrain Model

$$h = -(Ml^2 + I_p)(I + M_o r^2) + (Mlr\cos(\theta))^2$$

$$h_1 = Mrl\left(l + r\cos(\theta)\right) + I_p r$$

$$h_3 = Mlr^2(Ml^2 + I_p)\sin(\theta)$$

$$h_4 = -(Mlr)^2\sin(\theta)\cos(\theta)$$

$$h_7 = Mrl\left(-\cos(\theta)\right) - I + M_o r^2$$

$$h_9 = (Mlr)^2\sin(\theta)(-\cos(\theta))$$

$$h_{10} = M_o Mlr^2\sin(\theta) + MlI\sin(\theta)$$

References

[1] S. W. Nawawi, M. N. Ahmad, and J. H. S. Osman, "Development of a Two-Wheeled Inverted Pendulum Mobile Robot," presented at the The 5th Student Conference on Research and Development -SCOReD 2007, Selangor, Malaysia, 2007, pp. 235-239.

[2] Hitachi. (2007, Retrieved on 30 May, 2008). *Hitachi's Robot Closer to Becoming Real-Life Assistant.* Available: http://www.foxnews.com/story/0,2933,312420,00.html

[3] K. Iagnemma and S. Dubowsky, "Mobile robot rough-terrain control (RTC) For planetary exploration," in *26th Biennial Mechanisms and Robotics Conference*, Baltimore, Maryland, 2000, pp. 1-8.

[4] K. Iagnemma and S. Dubowsky, "Traction Control of Wheeled Robotic Vehicles in Rough Terrain with Application to Planetary Rovers," *The International Journal of Robotics Research*, vol. 23, pp. 1029-1040, October–November 2004.

[5] N. Chakraborty and A. Ghosal, "Dynamic modeling and simulation of a wheeled mobile robot for traversing uneven terrain without slip," *Journal of Mechanical Design, Transactions of the ASME*, vol. 127, pp. 901-909, 2005.

[6] A. Patla, J. Frank, and D. Winter, "Assessment of balance control in the elderly: Major issues. ," *Canadian Physiotherapy*, vol. 42, pp. 89–97, 1990.

[7] C. L. Shih, "The dynamics and control of a biped walking robot with seven degrees of freedom." *ASME J. Dyn. Sys. Meas. Control*, vol. 118, pp. 683–690, Dec. 1996 1996.

[8] Y. Fujimoto and A. Kawamura, "Proposal of biped walking control based on robust hybrid position/force control. ," in *Proc. of the IEEE Conf. on Robotics and Automation*, Minneapolis, Minnesota, April 1996, pp. 2724–2740.

[9] K. Hirai, M. Hirose, Y. Haikawa, and T. Takenaka, "The development of the Honda humanoid robot." in *Proc. of the IEEE Conf. on Robotics and Automation*, Leuvin, Belgium, May, 1998, pp. 1321-1326.

[10] Q. Li, A. Takanishi, and I. Kato, "Learning control of compensative trunk motion for a biped walking robot based on ZMP stability criterion." in *Proc. of the IEEE/RSJ Intl. Conf. on Intelligent Robots and System*, Raleigh, NC, 1992, pp. 597-603.

[11] Q. Li, A. Takanishi, and I. Kato, "Learning control for a biped walking robot with a trunk. ," in *Proc. of the IEEE/RSJ Intl. Conf. on Intell. Robot. and Sys*, Los Alamitos, CA, 1993 pp. 1771–1777.

References

[12] A. Takanishi, M. Ishida, Y. Yamazaki, and I. Kato, "The realization of dynamic walking by the biped robot WL-10RD. ," in *Proc. of the Intl. Conf. on Adv. Robot.* , Tokyo, 1985, pp. 459–466.

[13] A. Takanishi, T. Takeya, H. Karaki, and I. Kato, "A control method for dynamic bipedwalking under unknown external force." in *Proc. of the IEEE/RSJ Intl. Conf. on Intell. Robot. and Sys. (IROS).* Los Alamitos, CA, 1990. , pp. 795–801.

[14] M. Vukobratovic, "How to control artificial anthropomorphic systems. ," *IEEE Transactions on System, Man and Cybernetics*, vol. 3(5), pp. 497–507, September, 1973.

[15] M. Vukobratovic, A. A. Frank, and D. Juricic, "On the stability of biped locomotion " *IEEE Transactions on Biomedical Engineering*, vol. 17(1), pp. 25–36, January, 1970.

[16] M. Vukobratovic and O. Timcenko, "Experiments with nontraditional hybrid control of biped locomotion robots." *Journal of intelligent and Robotic Systems* vol. 16, pp. 25–43, 1996.

[17] S. K. W. Au, Y. Xu, and W. W. K. Yu, "Control of tilt-up motion of a single wheel robot via model-based and human-based controllers," *Mechatronics*, vol. 11, pp. 451-473, 2001.

[18] S. Miao and Q. Cao, "Modeling of self-tilt-up motion for a two-wheeled inverted pendulum," *Industrial Robot: An International Journal*, vol. 38(1), pp. 76-85, 2011.

[19] H. P. Oliveira, A. J. Sousa, A. P. Moreira, and P. J. Costa, "Modeling and assessing of Omni-directional Robots with Three and Four Wheels," *Journal of Contemporary Robotics - Challenges and Solutions*, pp. 207-229, 2003.

[20] P. Muir and C. Neuman, "Kinematic Modeling for Feedback Control of an Omnidirectional Wheeled Mobile Robot," in *Autonomous Robot Vehicles*, I. Cox and G. Wilfong, Eds., ed: Springer New York, 1990, pp. 25-31.

[21] K. J. Waldron, "Terrain adaptive vehicles," *Journal of Mechanical Design, Transactions of the ASME*, vol. 117 B, pp. 107-112, 1995.

[22] G. Dudek and M. Jenkin, *Computational Principles of Mobile Robotics*. Cambridge, UK: Cambridge University Press, 2000.

[23] S. C. Peters and K. Iagnemma, "An Analysis of Rollover Stability Measurement for High-Speed Mobile Robots," in *Proceedings of the 2006 IEEE International Conference on Robotics and Automation*, Orlando, Florida, May, 2006, pp. 3711-3716.

References

[24] G. Klein, B. Cooper, and K. J. Waldron, "Mars Rover," *Unmanned Systems*, vol. 5(2), pp. 28-39, 1988.

[25] H. TAI and T. MURAKAMI, "A Control of Two Wheels Driven Redundant Mobile Manipulator Using A Monocular Camera System," presented at the M2VIP'8, Auckland, New Zealand, 2008.

[26] J. A. Alessio Salerno, "A New Family of Two-Wheeled Mobile Robots: Modeling and Controllability," *IEEE TRANSACTIONS ON ROBOTICS*, vol. 23, pp. 169-173, February, 2007 2007.

[27] J. F. K. Pathak, and S. K. Agrawal, "Velocity and position control of a wheeled inverted pendulum by partial feedback linearization," *IEEE Trans. Robot*, vol. 21, pp. 505-513, Jun. 2005 2005.

[28] A. D. a. Felix Grasser, Silvio Colombi and Alfred Ruffer, "JOE: A Mobile, Inverted Pendulum," *IEEE Trans. Indusrriol Elecrmnics*, vol. 49, pp. 107-114, 2002.

[29] H. Abe and T. Murakami, "A Realization of Stable Attitude Control in Two Wheels Driven Mobile Manipulator," *Papers of Technical Meeting on Industrial Instrumentation and Control*, vol. IIC-06, pp. 105-108, 2006.

[30] F. He, L. Sun, and Z. Du, "Intelligent Detection of Bumps in a Mobile Robot," in *Proceedings of the 2006 IEEE International Conference on Robotics and Biomimetics*, Kunming, China, 2006, pp. 136-141.

[31] Segway. (june 2013). *Segway PT*. Available: http://www.segway.com/individual/models/

[32] A. Salerno and J. Angeles, "A New Family of Two-Wheeled Mobile Robots: Modeling and Controllability," *IEEE TRANSACTIONS ON ROBOTICS*, vol. 23, pp. 169-173, 2007.

[33] Y. Kim, S. H. Kim, and Y. K. Kwak, "Dynamic Analysis of a Nonholonomic Two-Wheeled Inverted Pendulum Robot," *Journal of Intelligent and Robotic Systems* vol. 44, pp. 25-46, 2005.

[34] H. G. Nguyen, J. Morrell, K. D. Mullens, A. B. Burmeister, S. Miles, N. Farrington, K. M. Thomas, and D. W. Gage, "Segway Robotic Mobility Platform," in *Proceedings of SPIE (Mobile Robots XVII)*, Philadelphia, PA, 2004, pp. 1-14.

[35] Segway. (2009, June). *Segway Advanced Development*. Available: http://www.segway.com/puma/

References

[36] K. Yamafuji and Q. Feng, "Study on the Postural Control of a Twin Cycle (1st Report) –Design and Simulation of a Nonlinear Control System of an Inverted Pendulum Model," *Journal of JSPE,* vol. 53, pp. 1622-1625, 1987.

[37] D. Voth, "Segway to the Future," in *IEEE intelligent systems* vol. 20, ed, 2005, pp. 5-8.

[38] F. Grasser, A. D'arrigo, S. Colombi, and A. Ruffer, "JOE: A Mobile, Inverted Pendulum," *IEEE Transactions on Industrial Electronics,* vol. 49(1), pp. 107-114, 2002.

[39] A. Salerno, S. Ostrovskaya, and J. Angeles, "The Development of Quasiholonomic Wheeled Robots," in *Proceedings of the 2002 IEEE International Conference on Robotics & Automation*, Washington DC, 2002, pp. 3514-3520.

[40] A. Salerno and J. Angeles, "The Robust Design Of A Two-Wheeled QuasiHolonomic Mobile Robot," in *Proceedings of DETC' 03 , ASME 2003 Design Engineering Technical Conferences and Computers and Information in Engineering Conference*, Chicago, Illinois, USA, 2003, pp. 1-7.

[41] D. P. Anderson. (2003, May 19th , 2003). nBot Balancing Robot. Available: http://www.geology.smu.edu/~dpa-www/robo/nbot/

[42] P. Deegan and R. Grupen. (2004, Retrieved on April 29, 2011). *UMass Amherst uBot*. Available: www-robotics.cs.umass.edu/Research/Distributed_Control/uBot/uBot.html

[43] Hitachi. (2008). *Emiew2*. Available: Hitachi Research & Development Emiew2. Retrieved September 21, 2008 from http://hitachie.com/rd/research/robotics/emiew2_01.html

[44] Hitachi. (2008). *Emiew*. Available: Hitachi Research & Development Emiew. Retrieved September 21, 2008 from http://www.hitachi.com/rd/research/robotics/emiew1_01.html

[45] E. Fraquelli, "Gyro-wheel car zooms along on giant tires at 116 mph Gyrauto," *Modern Mech. Inventions,* vol. 14, pp. 43-44, 1935.

[46] S. Shoval, I. Ulrich, and J. Borenstein, "NavBelt and the GuideCane," *IEEE Robotics and Automation Magazine,* vol. 10, pp. 9-20, 2003.

[47] K. Yamafuji. (1986). *two wheeled inverted pendulum robot*. Available: www.japantimes.co.jp/cgi-bin/getarticle.pl5?nn20011231a9.htm

References

[48] P. H. Batavia and I. Nourbakhsh, "Path Planning for the Cye Personal Robot," in *Proceedings of the 2000 IEEE/RSJ International Conference on Intelligent Robots and Systems*, 2000.

[49] S. A. Stoeter, P. E. Rybski, M. Gini, and N. Papanikolopoulos, "Autonomous stair-hopping with scout robots," in *IEEE International Conference on Intelligent Robots and Systems*, Lausanne, 2002, pp. 721-726.

[50] J. Åkesson, A. Blomdell, and R. Braun, "Design and Control of YAIP – an Inverted Pendulum on Two Wheels Robot," in *International Conference on Control Applications*, Munich, Germany, 2006, pp. 2178-2183.

[51] S. Kalra, D. Patel, and D. K. Stol, "Design and Hybrid Control of a Two Wheeled Robotic Platform," in *Australian Conference on Robotics and Automation (ACRA)*, Australia, 2007.

[52] V. Coelho, S. Liew, K. Stol, and G. Liu, "Development of a Mobile Two Wheel Balancing Platform for Autonomous Applications," in *15th International Conference on Mechatronics and Machine Vision in Practice (M2VIP08)*, Auckland, 2008.

[53] C. Samson and K. Ait-Abderrahim, "Feedback control of a nonholonomic wheeled cart in cartesian space," in *Proceedings of the International Conference on Robotics and Automation*, sacramento, California, 1991, pp. 1136-1141.

[54] Y. Zhao and S. L. BeMent, "Kinematics, Dynamics and Control of Wheeled Mobile Robots," in *Proceedings of 1992 IEEE international Conference on Robotics and Automation*, Nice, France, 1992, pp. 91-96.

[55] T. Nomura, Y. Kitsuka, H. Suemitsu, and T. Matsuo, "Adaptive Backstepping Control for a Two-Wheeled Autonomous Robot," presented at the ICROS-SICE International Joint Conference, Fukuoka International Congress Center, Japan, 2009.

[56] V. A. Brusin, "Adaptive stabilization of the two mass inverted pendulum on a vehicle system," *Soviet Journal of Computer and Systems Sciences*, vol. 30, pp. 53-61, 1992.

[57] V. Williams and V. Matsuoka, "Learning to balance the inverted pendulum using neural networks," in *Proc. IEEE International Joint Conference on Neural Networks*, USA, 1992, pp. 214-219.

[58] M. J. Anderson and W. J. Grantham, "Lypunov Optimal feedback control of a nonlinear inverted pendulum," *Journal of Dynamics Systems, Measurement and Control, Transactions of ASME*, vol. 111, pp. 554-558, 1989.

References

[59] Liu and Kojima, "Optimal Design Method Of Nonlinear Stabilizing Control System Of Inverted Pendulum By Genetic Algorithms," *Trans. Japan Society of Mechanical Engineers*, vol. 60, pp. 3124-3129, 1994.

[60] H. M. Tai and S. Shenoi, "Robust Fuzzy Controllers," in *Proc. IEEE International Conference on Systems, Man and Cybernetics*, 1994, pp. 85-90.

[61] J. S. a. W. Li, *Applied Nonlinear Control*. Englewood Cliffs, NJ: Prentice Hall, 1991.

[62] A. Salerno and J. Angeles, "On the Nonlinear Controllability of a Quasiholonomic Mobile Robot," in *Proceedings of the 2003 IEEE International Conference On Robotics &Automation*, Taipei, Taiwan, 2003, pp. 3379-3384.

[63] O. Y. Chee and M. S. B. Abidin, "Design And Development of Two Wheeled Autonomous Balancing Robot," in *Research and Development, 2006. SCOReD 2006. 4th Student Conference on*, 2006, pp. 169-172.

[64] F. Grasser, A. D'arrigo, S. Colombi, and A. Ruffer, "JOE: A Mobile, Inverted Pendulum," *IEEE Trans. Indusrriol Elecrmnics,* vol. 49, pp. 107-114, 2002.

[65] D. J. Kamen, R. R. Ambrogi, R. J. Duggan, D. J. Field, R. K. Heinzmann, B. Amsbury, and C. C. Langenfeld, "Personal Mobility Vehicles and Methods. U.S. Patent PCT/USOO/15144," 2000.

[66] T. Willingham. (2002). *Guide to building a RC robot*. Available: http://dc.cen.uiuc.edu/.

[67] J. Borenstein and I. Ulrich, "The GuideCane — A Computerized Travel Aid for the Active Guidance of Blind Pedestrians," in *Proceedings of the IEEE International Conference on Robotics and Automation*, Albuquerque, NM, 1997, pp. 1283-1288.

[68] A. Drenner, I. Burt, T. Dahlin, B. Kratochvil, C. McMillen, B. Nelson, N. Papanikolopoulos, P. E. Rybski, K. Stubbs, D. Waletzko, and K. B. Yesin, "Mobility Enhancements to the Scout Robot Platform," in *Proc. IEEE Int. Conf. Robot. Autom,* Washington, DC, 2002, pp. 1069–1074.

[69] Z. Kausar, K. Stol, and N. Patel, " The Effect of Terrain Inclination on Performance and the Stability Region of Two-Wheeled Mobile Robots. ," *Int J Adv Robot Syst,* vol. 9, pp. 1-11, 2012.

[70] R. P. M. Chan, K. A. Stol, and C. R. Halkyard, "Review of modelling and control of two-wheeled robots," *Annual Reviews in Control,* vol. 37, pp. 89-103, 2013.

[71] Y. Ha and S. i. Yuta, "Trajectory Tracking Control for Navigation of Self-contained Mobile Inverse Pendulum," in *Proceedings of the IEEE/RSJ/GI International*

Conference on Intelligent Robots and Systems '94. 'Advanced Robotic Systems and the Real World', 1994, pp. 1875-1882.

[72] R. C. Ooi, "Balancing a Two-Wheeled Autonomous Robot," Degree in Mechatronics Engineering Final year report, School of Mechanical Engineering, The University of Western Australia, CRAWLEY 2003.

[73] Y. Kim, S.-H. Lee, and D. H. Kim, "Dynamic equations of a Wheeled Inverted Pendulum with changing its center of gravity," in *Control, Automation and Systems (ICCAS), 2011 11th International Conference on*, 2011, pp. 853-854.

[74] X. Ruan and J. Cai, "Fuzzy Backstepping Controllers for Two-Wheeled Self-Balancing Robot," in *Informatics in Control, Automation and Robotics, 2009. CAR '09. International Asia Conference on*, 2009, pp. 166-169.

[75] J. Lien, L. Tu, W. Ross, and C. Burvill, "Implementation issues for an inexpensive inverted-pendulum mobile robot," in *Information and Automation, 2006. ICIA 2006. International Conference on*, 2006, pp. 372-377.

[76] L. Jingtao, G. Xueshan, H. Qiang, D. Qinjun, and D. Xingguang, "Mechanical design and dynamic modeling of a two-wheeled inverted pendulum mobile robot," in *Proceedings of the IEEE International Conference on Automation and Logistics, ICAL 2007*, Jinan, 2007, pp. 1614-1619.

[77] J. H. Han, S. S. Zhao, J. S. Li, and H. Li, "Research on developed parallel two-wheeled robot and its control system," in *Proceedings of the IEEE International Conference on Automation and Logistics (ICAL)*, Qingdao, 2008, pp. 2471-2475.

[78] K. Pathak, J. Franch, and S. K. Agrawal, "Velocity and position control of a wheeled inverted pendulum by partial feedback linearization," *IEEE Trans. Robot*, vol. 21(3), pp. 505-513, 2005.

[79] T. Takei, R. Imamura, and S. Yuta, "Baggage Transportation and Navigation by a Wheeled Inverted Pendulum Mobile Robot," *Industrial Electronics, IEEE Transactions on*, vol. 56, pp. 3985-3994, 2009.

[80] J. S. Hu and M. C. Tsai, "Design of robust stabilization and fault diagnosis for an auto-balancing two-wheeled cart," *Advanced Robotics*, vol. 22, pp. 319-338, 2008.

[81] M.-C. Tsai and J.-S. Hu, "Pilot control of an auto-balancing two-wheeled cart," *Advanced Robotics*, vol. 21, pp. 817-827, 2007.

[82] J. Wu, Y. Liang, and Z. Wang, "A robust control method of two-wheeled self-balancing robot," in *Strategic Technology (IFOST), 2011 6th International Forum on*, 2011, pp. 1031-1035.

References

[83] K. M. K. Goher and M. O. Tokhi, "Modeling Simulation and Balance Control of a Two-Wheeled Robotic Machine with Static Variation in Load Position," presented at the Proc. 22nd European Conference on Modeling and Simulation, Nicosia, Cyprus, 2008.

[84] A. Shimada and N. Hatakeyama, "Movement control of two-wheeled inverted pendulum robots considering robustness," in *Proceedings of the SICE Annual Conference*, Tokyo, 2008, pp. 3361-3365.

[85] Z. Kausar, K. Stol, and N. Patel, "Performance Enhancement of a Statically Unstable Two Wheeled Mobile Robot Traversing on an Uneven Surface," presented at the Robotics Automation and Mechatronics (RAM), 2010 IEEE Conference on 2010.

[86] D. S. Nasrallah, J. Angeles, and H. Michalska, "Velocity and orientation control of an anti-tilting mobile robot moving on an inclined plane," in *IEEE Proc. Int. Conf. Robot. Autom*, Orlando, FL, 2006, pp. 3717–3723.

[87] A. N. K. Nasir, M. A. Ahmad, R. Ghazali, and N. S. Pakheri, "Performance Comparison between Fuzzy Logic Controller (FLC) and PID Controller for a Highly Nonlinear Two-Wheels Balancing Robot," in *Informatics and Computational Intelligence (ICI), 2011 First International Conference on*, 2011, pp. 176-181.

[88] S. W. Nawawi, M. N. Ahmad, and J. H. S. Osman., "Real-Time Control of Two-Wheeled Inverted Pendulum Mobile Robot," *World Academy of Science, Engineering and Technology,* vol. 29, pp. 214-220, 2008.

[89] F. Grasser, A. D'Arrigo, S. Colombi, and A. C. Rufer, "JOE: A mobile, inverted pendulum," *IEEE Transactions on Industrial Electronics,* vol. 49, pp. 107-114, 2002.

[90] S. W. Nawawi, M. N. Ahmad, and J. H. S. Osman, "Development of a Two-Wheeled Inverted Pendulum Mobile Robot," in *Research and Development, 2007. SCOReD 2007. 5th Student Conference on*, 2007, pp. 1-5.

[91] Y. Kim, S. H. Kim, and Y. K. Kwak, "Dynamic analysis of a nonholonomic two-wheeled inverted pendulum robot," *Journal of Intelligent and Robotic Systems: Theory and Applications,* vol. 44, pp. 25-46, 2005.

[92] C. H. Chiu, "The design and implementation of a wheeled inverted pendulum using an adaptive output recurrent cerebellar model articulation controller," *IEEE Transactions on Industrial Electronics,* vol. 57, pp. 1814-1822, 2010.

[93] C.-C. Tsai, H.-C. Huang, and S.-C. Lin, "Adaptive Neural Network Control of a Self-Balancing Two-Wheeled Scooter," *IEEE TRANSACTIONS ON INDUSTRIAL ELECTRONICS,* vol. 57, pp. 1420-1428, April 2010.

References

[94] A. Shimada and N. Hatakeyama, "High-Speed Motion Control of Wheeled Inverted Pendulum Robots," in *Mechatronics, ICM2007 4th IEEE International Conference on*, 2007, pp. 1-6.

[95] Y.-K. Chin, W. C. Lin, D. M. Sidlosky, D. S. Rule, and M. S. Sparschu, "Sliding-Mode ABS Wheel-Slip Control," in *American Control Conference*, 1992, pp. 1-8.

[96] H. Chang and J. Chang, "An algorithm for constructing Lyapunov functions based on the variable gradient method," *Automatic Control, IEEE Transactions on*, vol. 15, pp. 510-512, 1970.

[97] H. D. Chiang and J. S. Thorp, "Stability regions of nonlinear dynamical systems: a constructive methodology," *Automatic Control, IEEE Transactions on*, vol. 34, pp. 1229-1241, 1989.

[98] R. Genesio, M. Tartaglia, and A. Vicino, "On the estimation of asymptotic stability regions: State of the art and new proposals," *Automatic Control, IEEE Transactions on*, vol. 30, pp. 747-755, 1985.

[99] R. Genesio and A. Vicino, "Some results on the asymptotic stability of second-order nonlinear systems," *Automatic Control, IEEE Transactions on*, vol. 29, pp. 857-861, 1984.

[100] R. Genesio and A. Vicino, "New techniques for constructing asymptotic stability regions for nonlinear systems," *Circuits and Systems, IEEE Transactions on*, vol. 31, pp. 574-581, 1984.

[101] J. Hewit and C. Storey, "Numerical application of Szego's method for constructing Liapunov functions," *Automatic Control, IEEE Transactions on*, vol. 14, pp. 106-108, 1969.

[102] A. Michel and R. Miller, "Stability analysis of discrete- time interconnected systems via computer-generated Lyapunov functions with applications to digital filters," *Circuits and Systems, IEEE Transactions on*, vol. 32, pp. 737-753, 1985.

[103] A. Michel, R. Miller, and N. Boo, "Stability analysis of interconnected systems using computer generated Lyapunov functions," *Circuits and Systems, IEEE Transactions on*, vol. 29, pp. 431-440, 1982.

[104] P. Varaiya, F. F. Wu, and C. Rong-Liang, "Direct methods for transient stability analysis of power systems: Recent results," *Proceedings of the IEEE*, vol. 73, pp. 1703-1715, 1985.

References

[105] H. D. Chiang and L. Fekih-Ahmed, "A constructive methodology for estimating the stability regions of interconnected nonlinear systems," *Circuits and Systems, IEEE Transactions on,* vol. 37, pp. 577-588, 1990.

[106] L. Jaewook, "Dynamic gradient approaches to compute the closest unstable equilibrium point for stability region estimate and their computational limitations," *Automatic Control, IEEE Transactions on,* vol. 48, pp. 321-324, 2003.

[107] L. Jaewook and C. Hsiao-Dong, "Theory of stability regions for a class of nonhyperbolic dynamical systems and its application to constraint satisfaction problems," *Circuits and Systems I: Fundamental Theory and Applications, IEEE Transactions on,* vol. 49, pp. 196-209, 2002.

[108] C. Hsiao-Dong and L. Fekih-Ahmed, "Quasi-stability regions of nonlinear dynamical systems: optimal estimations," *Circuits and Systems I: Fundamental Theory and Applications, IEEE Transactions on,* vol. 43, pp. 636-643, 1996.

[109] C. Hsiao-Dong and L. Fekih-Ahmed, "Quasi-stability regions of nonlinear dynamical systems: theory," *Circuits and Systems I: Fundamental Theory and Applications, IEEE Transactions on,* vol. 43, pp. 627-635, 1996.

[110] G. Chesi, "Estimating the domain of attraction for uncertain polynomial systems," *Automatica,* vol. 40, pp. 1981-1986, 2004.

[111] G. Chesi, "Establishing stability and instability of matrix hypercubes," *Systems & Control Letters,* vol. 54, pp. 381-388, 2005.

[112] G. Chesi, A. Garulli, A. Tesi, and A. Vicino, "LMI-based computation of optimal quadratic Lyapunov functions for odd polynomial systems," *International Journal of Robust and Nonlinear Control,* vol. 15, pp. 35-49, 2005.

[113] E. J. Davison and E. M. Kurak, "A computational method for determining quadratic lyapunov functions for non-linear systems," *Automatica,* vol. 7, pp. 627-636, 1971.

[114] J. J. E. Slotine and W. Li, *Applied Nonlinear Control System*. Englewood Cliffs: Prentice Hall Inc., 1991.

[115] T. Weehong and A. Packard, "Stability region analysis using sum of squares programming," in *Proceedings of the American Control Conference*, Minneapolis, MN, 2006, pp. 2297-2302.

[116] G. Golub, S. Nash, and C. Van Loan, "A Hessenberg-Schur method for the problem AX + XB= C," *Automatic Control, IEEE Transactions on,* vol. 24, pp. 909-913, 1979.

References

[117] X. A. Wang and W. Dayawansa, "On global Lyapunov functions of nonlinear autonomous systems," in *Decision and Control, 1999. Proceedings of the 38th IEEE Conference on*, 1999, pp. 1635-1639 vol.2.

[118] D. C. Sorensen and Y. Zhou, "Direct methods for matrix Sylvester and Lyapunov equations," *Journal of Applied Mathematics*, vol. 2003, pp. 277-303, 2003.

[119] Z. Tian and C. Gu, "A numerical algorithm for Lyapunov equations," *Applied Mathematics and Computation*, vol. 202, pp. 44-53, 2008.

[120] R. Lozano and D. Dimogianopoulos, "Stabilization of a chain of integrators with nonlinear perturbations: Application to the inverted pendulum," in *Proceedings of the IEEE Conference on Decision and Control*, Maui, HI, 2003, pp. 5191-5196.

[121] K. Kyoungchul, M. Hyosang, J. Doyoung, and M. Tomizuka, "Control of an Exoskeleton for Realization of Aquatic Therapy Effects," *Mechatronics, IEEE/ASME Transactions on*, vol. 15, pp. 191-200, 2010.

[122] A. Kelly and A. Stentz, "Rough terrain autonomous mobility part 2: An active vision, predictive control approach. ," *Autonomous Robots*, vol. 5, pp. 163-198, 1998.

[123] Z. Kausar, K. Stol, and N. Patel, "Nonlinear control design using Lyapunov function for two-wheeled mobile robots " in *19th International Conference on Mechatronics and Machine Vision in Practice (M2VIP), 2012* Auckland, New Zealand 2012, pp. 123 - 128.

[124] Z. Kausar, K. Stol, and N. Patel, "Stability region estimation of statically unstable two wheeled mobile robots," in *Robotics and Biomimetics (ROBIO), 2011 IEEE International Conference on*, 2011, pp. 1379-1384.

[125] Q. Wu and J.Chen, "effects of ramp angle and mass distributions on passive dynamic gait — an experimental study " *Int J Human Robot*, vol. 7, pp. 55-72, 2010.

[126] N. Chakraborty and A. Ghosal, "Kinematics of wheeled mobile robots with toroidal wheels on uneven terrain," in *Proceedings of the ASME Design Engineering Technical Conference*, Chicago, IL, 2003, pp. 1331-1341.

[127] B. J. Choi, S. V. Sreenivasan, and P. W. Davis, "Two wheels connected by an unactuated variable length axle on uneven ground: Kinematic modeling and experiments," *Journal of Mechanical Design, Transactions of the ASME*, vol. 121, pp. 235-240, 1999.

[128] D. S. Nasrallah, "Contributions to the Modeling and Control of Two-Wheeled Mobile Robots," PhD, Department of Mechanical Engineering, McGill University, Montreal, Quebec, 2007.

References

[129] J. S. Shamma and M. Athans, "Gain scheduling: potential hazards and possible remedies," *Control Systems Magazine, IEEE,* vol. 12, pp. 101-107, 1992.

[130] M. F. and P. L., "Adding integrators, saturated controls and stabilization for feedforward systems," *IEEE Transactions on Automatic Control,* vol. 41, pp. 1559-1577, November 1996.

[131] D. R. Jones and K. A. Stol, "Modelling and Stability Control of Two-Wheeled Robots in Low-Traction Environments," in *Australasian Conference on Robotics and Automation (ACRA),* Brisbane, 2010.

[132] M. A. Hassan and C. Storey, "Numerical determination of domains of attraction for electrical power systems using the method of Zubov," *International Journal of Control,* vol. 34, pp. 371-381, 1981.

[133] J. Willems, "Direct method for transient stability studies in power system analysis," *Automatic Control, IEEE Transactions on,* vol. 16, pp. 332-341, 1971.

[134] A. S. Shiriaev, A. Friesel, J. Perram, and A. Pogromsky, "On stabilization of rotational modes of an inverted pendulum," in *Decision and Control, 2000. Proceedings of the 39th IEEE Conference on*, 2000, pp. 5047-5052 vol.5.

[135] M. W. Spong, "Partial feedback linearization of underactuated mechanical systems," in *Intelligent Robots and Systems' 94.'Advanced Robotic Systems and the Real World', IROS'94. Proceedings of the IEEE/RSJ/GI International Conference on*, 1994, pp. 314-321.

[136] M. J. Whatley and D. C. Pott, "Adaptive gain improves reactor control," *Hydrocarbon processing,* pp. 75-78, May, 1984 1984.

[137] G. Stein, *Adaptive flight control – A pragmatic view.* New York: Academic Press, 1980.

[138] H. Jian, G. Zhi-Hong, T. Matsuno, T. Fukuda, and K. Sekiyama, "Sliding-Mode Velocity Control of Mobile-Wheeled Inverted-Pendulum Systems," *Robotics, IEEE Transactions on,* vol. 26, pp. 750-758, 2010.

[139] W. J. Rugh and J. S. Shamma, "Research on gain scheduling - survey paper," *Automatica,* vol. 36, pp. 1401-1425, 2000.

[140] C. R. Knopse, "Treating non-linearity as linearity: gain scheduling, LPV's and frozen linear methods," in *Minicourse in Proceedings ACC* 2004.

[141] C. Aguilar-Ibanez, M. S., and Suarez-Castanon, "Stabilization of the inverted pendulum via a constructive Lyapunov function," *Acta Applied Math,* vol. 111, pp. 15-26, 2010.

References

[142] D. Jones, "Control of Two-Wheeled Robots in Low-Traction Environments," Masters of Engineering, Mechanical Engineering, University of Auckland, Auckland, 2011.

List of Author's Publications

- Peer-reviewed Journal Papers

    1. Zareena Kausar, Karl Stol, Nitish Patel, "The Effect of Terrain Inclination on Performance and the Stability Region of Two-Wheeled Mobile Robots," *Int J Adv Robot Syst,* vol. 9, pp. 1-11, 2012.

    2. Zareena Kausar, Karl Stol, Nitish Patel, "Lyapunov Function Based Nonlinear Control for Two-Wheeled Mobile Robots," International journal of Bio-mechatronics and Biomedical Robotics. (To appear: Accepted for publication on 12th July 2013)

- Peer-reviewed Papers in Conference Proceedings

    1. Zareena Kausar, Karl Stol, Nitish Patel, "Performance enhancement of a statically unstable two wheeled mobile robots traversing on an uneven surface," Proceedings of IEEE international conference on Robotics, automation and mechatronics (RAM), Singapore; pp.156-162, June 28-30, 2010.

    2. Zareena Kausar, Karl Stol, Nitish Patel, "Stability region estimation of statically unstable two wheeled mobile robots," Proceedings of IEEE international conference on Robotics and Biomimetics (ROBIO) Phuket, Thailand; pp.1379, Dec 7-11, 2011.

    3. Zareena Kausar, Karl Stol, Nitish Patel, "Nonlinear control design using Lyapunov function for two-wheeled mobile robots," Proceedings of 19th International Conference on Mechatronics and Machine Vision in Practice (M2VIP'12) Auckland, New Zealand; pp.123-128, Nov 28-30, 2012.